

# UC Irvine

## UC Irvine Previously Published Works

### Title

A Broad-Spectrum Multi-Antigen mRNA/LNP-Based Pan-Coronavirus Vaccine Induced Potent Cross-Protective Immunity Against Infection and Disease Caused by Highly Pathogenic and Heavily Spike-Mutated SARS-CoV-2 Variants of Concern in the Syrian Hamster Mo...

### Permalink

<https://escholarship.org/uc/item/6jh6r7q8>

### Journal

bioRxiv, 5(02-23)

### ISSN

2692-8205

### Authors

Prakash, Swayam  
Dhanushkodi, Nisha R  
Singer, Mahmoud  
[et al.](#)

### Publication Date

2024-02-15

### DOI

10.1101/2024.02.14.580225

Peer reviewed

1 A Broad-Spectrum Multi-Antigen mRNA/LNP-Based Pan-Coronavirus Vaccine Induced Potent  
2 Cross-Protective Immunity Against Infection and Disease Caused by Highly Pathogenic and Heavily  
3 Spike-Mutated SARS-CoV-2 Variants of Concern in the Syrian Hamster Model

4 Swayam Prakash<sup>1, #</sup>; Nisha R. Dhanushkodi<sup>1, #</sup>; Mahmoud Singer<sup>1</sup>; Afshana Quadiri<sup>1</sup>, Latifa Zayou<sup>1</sup>,  
5 Hawa Vahed<sup>1, 7</sup>, Pierre-Gregoire Coulon<sup>1</sup>; Izabela Coimbra Ibraim<sup>4</sup>; Christine Tafoya<sup>4</sup>; Lauren  
6 Hitchcock<sup>4</sup>; Gary Landucci<sup>4</sup>, Donald N. Forthal<sup>4, 5</sup>, Assia El Babsiri<sup>1</sup>, Delia F. Tifrea<sup>2</sup>, Cesar, J.  
7 Figueroa<sup>3</sup>, Anthony B. Nesburn<sup>1</sup>, Baruch D. Kuppermann<sup>1</sup>, Daniel Gil<sup>7</sup>, Trevor M. Jones<sup>7</sup>, Jeffrey B.  
8 Ulmer<sup>7</sup> & Lbachir BenMohamed<sup>1, 6, 7, \*</sup>

9 <sup>1</sup>Laboratory of Cellular and Molecular Immunology, Gavin Herbert Eye Institute, University of  
10 California Irvine, School of Medicine, Irvine, CA 92697; <sup>2</sup>Department of Pathology and Laboratory  
11 Medicine, School of Medicine, Irvine, CA 92697; <sup>3</sup>Department of Surgery, Divisions of Trauma,  
12 Burns & Critical Care, School of Medicine, Irvine, CA 92697; <sup>4</sup>BSL-3 Laboratories, High Containment  
13 Core Facility, School of Medicine, University of California, Irvine; <sup>5</sup>Division of Infectious Diseases,  
14 Department of Medicine, University of California, Irvine School of Medicine, Irvine, CA, USA  
15 <sup>6</sup>Institute for Immunology; University of California Irvine, School of Medicine, Irvine, CA 92697; and  
16 <sup>7</sup>Department of Vaccines and Immunotherapies, TechImmune, LLC, University Lab Partners, Irvine,  
17 CA 92660, USA.

18 Running Title: A Combined B- and T-cell-Based mRNA/LNP pan-Coronavirus Vaccine.

19 <sup>#</sup>Authors have contributed equally to this study.

20 \*Corresponding Author: Professor Lbachir BenMohamed, Laboratory of Cellular and Molecular  
21 Immunology, Gavin Herbert Eye Institute, University of California Irvine, School of Medicine, Hewitt  
22 Hall, Room 2032; 843 Health Sciences Road; Irvine, CA 92697-4390; Phone: 949-824-8937. Fax:  
23 949-824-9626. E-mail: Lbenmoha@uci.edu.

24 Support and Conflict of Interest: Studies of this report were supported by Public Health Service  
25 Research grants AI158060, AI150091, AI143348, AI147499, AI143326, AI138764, AI124911, and  
26 AI110902 from the National Institutes of Allergy and Infectious Diseases (NIAID) to LBM. LBM has  
27 an equity interest in TechImmune, LLC., a company that may potentially benefit from the research  
28 results and serves on the company's Scientific Advisory Board. LBM's relationship with  
29 TechImmune, LLC., has been reviewed and approved by the University of California, Irvine by its  
30 conflict-of-interest policies.

31 Keywords: pan-Coronavirus vaccine, SARS-CoV-2, COVID-19, Variants of concern, Cross-  
32 protective, CD4<sup>+</sup> T cells, CD8<sup>+</sup> T cells.

33

34

35

## ABSTRACT

36 The first-generation Spike-alone-based COVID-19 vaccines have successfully contributed to  
37 reducing the risk of hospitalization, serious illness, and death caused by SARS-CoV-2 infections.  
38 However, waning immunity induced by these vaccines failed to prevent immune escape by many  
39 variants of concern (VOCs) that emerged from 2020 to 2024, resulting in a prolonged COVID-19  
40 pandemic. We hypothesize that a next-generation Coronavirus (CoV) vaccine incorporating highly  
41 conserved non-Spike SARS-CoV-2 antigens would confer stronger and broader cross-protective  
42 immunity against multiple VOCs. In the present study, we identified ten non-Spike antigens that are  
43 highly conserved in 8.7 million SARS-CoV-2 strains, twenty-one VOCs, SARS-CoV, MERS-CoV,  
44 Common Cold CoVs, and animal CoVs. Seven of the 10 antigens were preferentially recognized by  
45 CD8<sup>+</sup> and CD4<sup>+</sup> T-cells from unvaccinated asymptomatic COVID-19 patients, irrespective of VOC  
46 infection. Three out of the seven conserved non-Spike T cell antigens belong to the early expressed  
47 Replication and Transcription Complex (RTC) region, when administered to the golden Syrian  
48 hamsters, in combination with Spike, as nucleoside-modified mRNA encapsulated in lipid  
49 nanoparticles (LNP) (i.e., combined mRNA/LNP-based pan-CoV vaccine): (i) Induced high  
50 frequencies of lung-resident antigen-specific CXCR5<sup>+</sup>CD4<sup>+</sup> T follicular helper (T<sub>FH</sub>) cells,  
51 GzmB<sup>+</sup>CD4<sup>+</sup> and GzmB<sup>+</sup>CD8<sup>+</sup> cytotoxic T cells (T<sub>CYT</sub>), and CD69<sup>+</sup>IFN- $\gamma$ <sup>+</sup>TNF $\alpha$ <sup>+</sup>CD4<sup>+</sup> and CD69<sup>+</sup>IFN-  
52  $\gamma$ <sup>+</sup>TNF $\alpha$ <sup>+</sup>CD8<sup>+</sup> effector T cells (T<sub>EFF</sub>); and (ii) Reduced viral load and COVID-19-like symptoms  
53 caused by various VOCs, including the highly pathogenic B.1.617.2 Delta variant and the highly  
54 transmittable heavily Spike-mutated XBB1.5 Omicron sub-variant. The combined mRNA/LNP-based  
55 pan-CoV vaccine could be rapidly adapted for clinical use to confer broader cross-protective  
56 immunity against emerging highly mutated and pathogenic VOCs.

57

58

59

60

## IMPORTANCE

61

62

63

64

65

66

67

68

69

70

71

72

73

74

75

76

77

78

79

As of January 2024, over 1500 individuals in the United States alone are still dying from COVID-19 each week despite the implementation of first-generation Spike-alone-based COVID-19 vaccines. The emergence of highly transmissible SARS-CoV-2 variants of concern (VOCs), such as the currently circulating highly mutated BA.2.86 and JN.1 Omicron sub-variants, constantly overrode immunity induced by the first-generation Spike-alone-based COVID-19 vaccines. Here we report a next generation broad spectrum combined multi-antigen mRNA/LNP-based pan-CoV vaccine that consists of nucleoside-modified mRNA encapsulated in lipid nanoparticles (LNP) that delivers three highly conserved non-Spike viral T cell protein antigens together with the Spike protein B-cell antigen. Compared side-by-side to the clinically proven first-generation Spike-alone mRNA/LNP-based vaccine, the combined multi-antigen mRNA/LNP-based pan-CoV vaccine-induced higher frequencies of lung-resident non-Spike antigen-specific T follicular helper ( $T_{FH}$ ) cells, cytotoxic T cells ( $T_{CYT}$ ), effector T cells ( $T_{EFF}$ ) and Spike specific-neutralizing antibodies. This was associated to a potent cross-reactive protection against various VOCs, including the highly pathogenic Delta variant and the highly transmittable heavily Spike-mutated Omicron sub-variants. Our findings suggest an alternative broad-spectrum pan-Coronavirus vaccine capable of (i) disrupting the current COVID-19 booster paradigm; (ii) outpacing the bivalent variant-adapted COVID-19 vaccines; and (iii) ending an apparent prolonged COVID-19 pandemic.

80

## INTRODUCTION

81 The Coronavirus disease 2019 (COVID-19) pandemic has created one of the largest global  
82 health crises in nearly a century<sup>1, 2, 3, 4, 5, 6</sup>. As of January 2024, the number of confirmed SARS-CoV-  
83 2 cases has reached over 770 million, and COVID-19 disease caused nearly 7 million deaths<sup>1, 5, 6</sup>.  
84 Since early 2020, the world has continued to contend with successive waves of COVID-19, fueled by  
85 the emergence of over 20 variants of concern (VOCs) with continued enhanced transmissibility<sup>7</sup>.  
86 While the Wuhan strain Hu1 is the ancestral variant of SARS-CoV-2 that emerged in late 2019 in  
87 China, Alpha (B.1.1.7), Beta (B.1.351), and Gamma (B.1.1.28) VOCs subsequently emerged  
88 between 2020 to 2021 in the United Kingdom, South Africa, and Brazil, respectively<sup>7</sup>. The most  
89 pathogenic Delta variant (B. 1.617. 2) was identified in India in mid-2021 where it led to a deadly  
90 wave of infections<sup>7</sup>. The fast and heavily Spike-mutated Omicron variants and sub-variants (i.e.,  
91 B.1.1.529, XBB1.5, EG.5, HV.1, BA.2.86, and JN.1) that emerged from 2021-2023 are less  
92 pathogenic but are more immune-evasive<sup>8, 9</sup>. Over the last 4 years, breakthrough infections by  
93 these VOCs contributed to repetitive seasonal surges that often strain the world's healthcare  
94 systems, sustained hospitalizations, illnesses, and deaths<sup>8, 9</sup>.

95 While the first-generation Spike-based COVID-19 vaccines have contributed to reducing the  
96 burden of COVID-19, vaccine-waning immunity against heavily Spike-mutating emerging variants  
97 and sub-variants contributed to a prolonged COVID-19 pandemic<sup>10, 11, 12</sup>. The first-generation  
98 COVID-19 vaccines were subject to regular updates to incorporate the Spike mutations of the new  
99 VOCs that emerged throughout the pandemic<sup>13</sup>. This “copy-passed” vaccine strategy that “chased”  
100 the emerged VOC into a new batch of “improved” bivalent COVID-19 vaccines was often surpassed  
101 by fast-emerging and rapidly mutating Omicron lineages<sup>13</sup>. The sequences of Spike protein in the  
102 recently circulating EG.5, HV.1, and JN.1 Omicron subvariants have already undergone over 100  
103 accumulated mutations, away from the recent XBB1.5-adapted bivalent vaccine<sup>14, 15, 16</sup>. The  
104 “improved” bivalent vaccine was only effective 4 to 29% against the Omicron subvariants, circulating  
105 in Winter 2022<sup>14, 15, 16</sup>, and its effectiveness decreased even further against the more recent  
106 divergent and highly transmissible EG.5, HV.1, and JN.1 Omicron subvariants, circulating in Winter  
107 2023<sup>14, 15, 16</sup>. These observations highlight the need for an alternative and superior next-generation

108 pan-CoV vaccine strategy that incorporates highly conserved non-Spike antigens to induce broad,  
109 cross-protective immunity against past, present, and future VOCs<sup>10, 17, 18</sup>. Such a pan-Coronavirus  
110 vaccine may put an end to, and eradicate, an apparent prolonged COVID-19 pandemic<sup>19</sup>.

111 Recently, our group and others have: (i) Identified specific sets of highly conserved SARS-  
112 CoV-2 non-Spike antigens targeted by frequent cross-reactive functional CD4<sup>+</sup> and CD8<sup>+</sup> T cells from  
113 asymptomatic COVID-19 patients (i.e., unvaccinated individuals who never develop any COVID-19  
114 symptoms despite being infected with SARS-CoV-2)<sup>3, 5, 20, 21, 22, 23, 24, 25, 26</sup>; (ii) Discovered that  
115 increased frequencies of lung-resident CD4<sup>+</sup> and CD8<sup>+</sup> T cells specific to common antigens  
116 protected against multiple SARS-CoV-2 VOCs in mouse models<sup>1, 3, 27</sup>; and (iii) Demonstrated that  
117 enriched cross-reactive lung-resident memory CD4<sup>+</sup> and CD8<sup>+</sup> T cells that selectively target early-  
118 transcribed SARS-CoV-2 antigens, from the replication and transcription complex (RTC) region, are  
119 associated with a rapid clearance of infection in so-called “SARS-CoV-2 aborters” (i.e., unvaccinated  
120 SARS-CoV-2 exposed seronegative individuals who rapidly abort the virus replication)<sup>28, 29, 30, 31, 32</sup>.  
121 We hypothesize that a next-generation Coronavirus vaccine that incorporates highly conserved and  
122 early expressed RTC antigens selectively targeted by CD4<sup>+</sup> and CD8<sup>+</sup> T cells from asymptomatic  
123 COVID-19 patients and “SARS-CoV-2 aborters”, would confer a strong and broader protective  
124 immunity against rapidly transmissible and highly pathogenic VOCs.

125 In the present study, using *in-silico* bioinformatic techniques, we identified non-Spike RTC  
126 antigens highly conserved in 8.7 million genome sequences of SARS-CoV-2 strains that circulate  
127 worldwide, 21 VOCs; SARS-CoV; MERS-CoV; common cold Coronaviruses; and animal CoV (i.e.,  
128 Bats, Civet Cats, Pangolin and Camels). Seven non-Spike highly conserved antigens were  
129 selectively recognized by cross-reactive CD4<sup>+</sup> and CD8<sup>+</sup> T cells from unvaccinated asymptomatic  
130 COVID-19 patients. Three of seven T cell antigens, when combined with Spike, and delivered as  
131 mRNA/LNP vaccine, safely induced strong, rapid, broad, B- and airway-resident polyfunctional cross-  
132 protective T cell immunity against several pathogenic and heavily mutated SARS-CoV-2 variants and  
133 sub-variants in the hamster model. These findings provide critical insights into developing multi-  
134 antigen broad-spectrum pan-Coronavirus vaccines capable of conferring cross-variants and cross-  
135 strain protective immunity.

## RESULTS

136

137 **1. Five highly conserved regions, that encode ten common structural, non-structural,**  
138 **and accessory protein antigens, were identified in the SARS-CoV-2 single-stranded RNA**  
139 **genome:** The SARS-CoV-2 single-stranded genome is comprised of 29903 bp that encodes 29  
140 proteins, including 4 structural, 16 nonstructural, and 9 accessory regulatory proteins <sup>33</sup>. Using  
141 several *in-silico* bioinformatic approaches and alignments of 8.7 million genome sequences of SARS-  
142 CoV-2 strains that circulated worldwide throughout the pandemic, including twenty-one VOCs /  
143 Variants of Interest (VOI) /Variants being Monitored (VBM); SARS-CoV; MERS-CoV; Common Cold  
144 Coronaviruses (i.e.,  $\alpha$ -CCC-229E,  $\alpha$ -CCC-NL63,  $\beta$ -CCC-HKU1, and  $\beta$ -CCC-OC43 strains); and  
145 twenty-five animal's SARS-like Coronaviruses (SL-CoVs) genome sequences isolated from bats,  
146 pangolins, civet cats, and camels, we identified 5 highly conserved regions in the SARS-CoV-2  
147 single-stranded RNA genome (1-1580bp, 3547-12830bp, 1772-21156bp, 22585-24682bp, and  
148 26660-27421bp, **Fig. 1A**). Further Sequence Homology Analysis confirmed that the five SARS-CoV-  
149 2 genome regions encode for ten highly conserved non-Spike T cell antigens (NSP-2 (Size: 1914 bp,  
150 Nucleotide Range: 540 bp - 2454 bp), NSP-3 (Size: 4485 bp, Nucleotide Range: 3804 bp - 8289 bp),  
151 NSP-4 (Size: 1500 bp, Nucleotide Range: 8290 bp - 9790 bp), NSP-5-10 (Size: 3378 bp, Nucleotide  
152 Range: 9791 bp - 13169 bp), NSP-12 (Size: 2796 bp, Nucleotide Range: 13170 bp - 15966 bp),  
153 NSP-14 (Size: 1581 bp, Nucleotide Range: 17766 bp - 19347 bp), ORF7a/b (Size: 492 bp,  
154 Nucleotide Range: 27327 bp - 27819 bp), Membrane (Size: 666 bp, Nucleotide Range: 26455 bp -  
155 27121 bp), Envelope (Size: 225 bp, Nucleotide Range: 26177 bp - 26402 bp), and Nucleoprotein  
156 (Size: 1248 bp, Nucleotide Range: 28206 bp - 29454 bp) (**Fig. 1B**). The sequences of the ten highly  
157 conserved antigens were then used to design and construct N1-methylpseudouridine (m<sup>1</sup> $\psi$ ) -  
158 modified mRNAs encapsulated in lipid nanoparticles (mRNA/LNP vaccines) that are subsequently  
159 preclinically tested for safety, immunogenicity, and protective efficacy against several SARS-CoV-2  
160 variants and sub-variants of concern in the golden Syrian hamster model (**Fig. 1C**).

161 Mutations screened against twelve major SARS-CoV-2 variants of concern and sequence  
162 homology analysis confirmed the sequences representing the 10 non-Spike antigens are highly

163 conserved in the currently highly mutated BA.2.86 and JN.1 Omicron sub-variants (**Table 1**). As  
164 expected, with 346 cumulative mutations, the sequence of the Spike is heavily mutated in the latest  
165 Omicron sub-variants compared to the non-Spike antigens. The sequences of Spike protein have 42  
166 and 43 new mutations in the current highly transmissible and most immune-evasive Omicron sub-  
167 variants, BA.2.86 and JN.1 (**Table 1**). In contrast, compared to Spike, the sequences of the three  
168 non-Spike antigens (NSP-2, NSP-14, and Nucleoprotein) remain relatively conserved in these sub-  
169 variants BA.2.86 and JN.1 (21, 0, 57 mutations respectively). Of significant interest, the sequence of  
170 NSP-12 and NSP-14 antigens are fully conserved (100%) in all variants and sub-variants, including  
171 the recent BA.2.86 and JN.1, supporting the vital role of these two antigens in the life cycle of SARS-  
172 CoV-2. Of the ten non-Spike antigens, NSP3 (58 cumulative mutations) and nucleoprotein (57  
173 cumulative mutations) are the less conserved in all variants and sub-variants. Nevertheless, the  
174 nucleoprotein was considered in our combined vaccine since it is the most abundant viral protein,  
175 and one of the most predominantly targeted antigens by T cells in individuals with less severe  
176 COVID-19 disease<sup>34, 35</sup>.

177 **2. Enriched cross-reactive memory CD4<sup>+</sup> and CD8<sup>+</sup> T cells, preferentially target seven**  
178 **of the ten highly conserved SARS-CoV-2 antigens and correlated with improved disease**  
179 **outcome in unvaccinated asymptomatic COVID-19 patients:** We next determined whether the  
180 ten highly conserved non-Spike antigens are targeted by CD4<sup>+</sup> and CD8<sup>+</sup> T cells from “naturally  
181 protected” unvaccinated COVID-19 patients. We used peripheral blood-derived T cells from  
182 unvaccinated COVID-19 patients who were enrolled throughout the COVID-19 pandemic,  
183 irrespective of which SARS-CoV-2 variants of concern they were exposed to (**Supplemental Fig.**  
184 **S1A**).

185 CD4<sup>+</sup> and CD8<sup>+</sup> T cell responses specific to highly conserved epitopes, selected from these  
186 non-Spike antigens, were compared in unvaccinated asymptomatic individuals (those individuals  
187 who never develop any COVID-19 symptoms despite being infected with SARS-CoV-2) versus  
188 unvaccinated symptomatic COVID-19 patients (those patients who developed severe to fatal COVID-  
189 19 symptoms) (**Fig. 2A**). Unvaccinated HLA-DRB1\*01:01<sup>+</sup> and HLA-A\*0201 COVID-19 patients ( $n =$



190 71) enrolled throughout the COVID-19 pandemic (January 2020 to December 2023), irrespective of  
191 variants of concern infection, and divided into six groups, based on the level of severity of their  
192 COVID-19 symptoms (from severity 5 to severity 0, assessed at discharge – **Fig. 2A**). The clinical,  
193 and demographic characteristics of this cohort of COVID-19 patients are detailed in **Table 1**. Fresh  
194 PBMCs were isolated from these COVID-19 patients, on average within 5 days after reporting a first  
195 COVID-19 symptom or a first PCR-positive test. PBMCs were then stimulated *in vitro* for 72 hours  
196 using recently identified highly conserved 13 HLA-DR-restricted CD4<sup>+</sup> or 16 HLA-A\*0201-restricted  
197 CD8<sup>+</sup> T cell peptide epitopes derived from the non-structural proteins (NSPs), the ORF7a//b,  
198 Membrane, and Envelop, and Nucleoprotein, as detailed in *Materials & Methods*. The number of  
199 responding IFN- $\gamma$ -producing CD4<sup>+</sup> T cells and IFN- $\gamma$ -producing CD4<sup>+</sup> and CD8<sup>+</sup> T cells specific to  
200 epitopes from all the ten selected conserved antigens (**Fig. 2B**), 13 individual cross-reactive CD4<sup>+</sup> T  
201 cell epitopes (**Fig. 2C**); and 16 individual cross-reactive CD8<sup>+</sup> T cell epitopes (**Fig. 2D**) from the  
202 selected 10 highly conserved antigens were quantified, in each of the six groups of COVID-19  
203 patients, using ELISpot assay (i.e., number of IFN- $\gamma$ -spot forming T cells or “SFCs”). We then  
204 performed the Pearson correlation analysis to determine the linear correlation between the  
205 magnitude of CD4<sup>+</sup> and CD8<sup>+</sup> T cell responses directed toward each of the conserved SARS-CoV-2  
206 epitopes, and the severity of COVID-19 symptoms. A negative correlation is considered strong when  
207 the coefficient R-value is between -0.7 and -1.

208 Overall, the highest frequencies of cross-reactive epitopes-specific IFN- $\gamma$ -producing CD4<sup>+</sup> and  
209 CD8<sup>+</sup> T cells (determined as mean SFCs > 50 per 0.5 x 10<sup>6</sup> PBMCs fixed as threshold) were  
210 detected in the unvaccinated COVID-19 patients with less severe disease (i.e., severity 0, 1, and 2,  
211 **Figs. 2B, 2C** and **2D**). In contrast, the lowest frequencies of cross-reactive IFN- $\gamma$ -producing CD4<sup>+</sup>  
212 and CD8<sup>+</sup> T cells were detected in unvaccinated severely ill COVID-19 patients (severity scores 3  
213 and 4, mean SFCs < 50) and in unvaccinated COVID-19 patients with fatal outcomes (severity score  
214 5, mean SFCs < 25). We found a strong positive linear correlation between the high magnitude of  
215 IFN- $\gamma$ -producing CD4<sup>+</sup> and CD8<sup>+</sup> T cells specific to seven out of ten common T cell antigens and the  
216 “natural protection” observed in unvaccinated asymptomatic COVID-19 patients (**Figs. 2B, 2C** and

217 **2D)**. This positive correlation existed regardless of whether CD4<sup>+</sup> and CD8<sup>+</sup> T cells target structural,  
218 non-structural, or accessory regulatory SARS-CoV-2 antigens.

219 Taken together, these results: (i) Demonstrate an overall higher magnitude of CD4<sup>+</sup> and CD8<sup>+</sup>  
220 T cell responses specific to seven out of ten highly conserved non-Spike antigens present in  
221 unvaccinated asymptomatic COVID-19 patients irrespective of SARS-CoV-2 variants of concern they  
222 were exposed to; (ii) Suggest a crucial role of these seven highly conserved structural, non-  
223 structural, and accessory regulatory T cell antigens, in protection from symptomatic and fatal  
224 Infections caused by multiple variants; and (iii) Validates the conserved non-Spike Coronavirus  
225 antigens as potential targets for a pan-Coronavirus vaccine.

226 **3. Conserved SARS-CoV-2 NSP-2, NSP-14 and Nucleoprotein-based mRNA/LNP**  
227 **vaccines confer protection against the highly pathogenic Delta variants (B.1.617.2):** We  
228 constructed methyl-pseudouridine–modified (m1Ψ) mRNA that encodes each of the ten highly  
229 conserved T cell antigens (i.e., NSP-2, NSP-3, NSP-4, NSP-5-10, NSP-12, NSP-14, ORF7a/b,  
230 Membrane, Envelope, and Nucleoprotein), based on the Omicron sub-variant BA.2.75, that are  
231 capped using CleanCap technology<sup>36</sup> (i.e., ten T cell antigen mRNA vaccines). The modified mRNA  
232 vaccines expressing the prefusion Spike proteins, stabilized by either two (Spike 2P) or six (Spike  
233 6P) prolines, were constructed as B cell antigen mRNA vaccines<sup>37, 38</sup>. The 12 B- and T-cell mRNA  
234 vaccines were then encapsulated in the lipid nanoparticles (LNPs) as the delivery system<sup>39</sup> (**Figs.**  
235 **1B, 1C, and 3A**). The “plug-and-play” mRNA/LNP platform, was selected as an antigen delivery  
236 technology over other platforms, as over one billion doses of the clinically proven Spike mRNA/LNP-  
237 based vaccines being already distributed around the world showed a high level of safety. The  
238 mRNA/LNP platform responds to current goals of the next-generation pan-CoV vaccines: (i) the  
239 ability to safely confer durable, cross-protective T cell responses; and (ii) the ability to be  
240 manufactured at a large scale to support a rapid and a global mass vaccination.

241 To downselect the 10 T-cell antigens mRNA/LNP-based vaccines, the protective efficacy of  
242 each T-cell antigen mRNA/LNP-based vaccine, delivered individually by intramuscular route, was  
243 compared against the highly pathogenic Delta variant (B.1.617.2) in the outbred golden Syrian

244 hamster model (**Fig. 3B**). The Golden Syrian hamsters are naturally susceptible to SARS-CoV-2  
245 infection, owing to the high degree of similarity between hamster ACE2 and human ACE2 (hACE2),  
246 and develop symptoms of COVID-19-like disease that closely mimic the COVID-19 pathogenesis in  
247 humans <sup>40, 41, 42, 43, 44</sup>. Female golden Syrian hamsters ( $n = 5$  per group) were immunized  
248 intramuscularly twice on day 0 (prime) and day 21 (boost) with individual mRNA/LNP based vaccine  
249 expressing each of the 10 highly conserved non-Spike T-cell antigens and delivered using 2 doses (1  
250  $\mu\text{g}/\text{dose}$  ( $n = 5$ ) and 10  $\mu\text{g}/\text{dose}$  ( $n = 5$ ), **Fig. 3B**). The initial 1  $\mu\text{g}$  and 10  $\mu\text{g}$  doses were selected  
251 based of previous similar mRNA-LNP vaccine studies in mice and hamsters <sup>35, 45</sup>. Hamsters that  
252 received phosphate-buffered saline alone were used as mock-immunized controls (*Saline, Mock, n =*  
253 *5*). Power analysis demonstrated 5 hamsters per group was enough to produce significant results  
254 with a power > 80%. Three weeks after the second immunization, all animals were challenged  
255 intranasally with the SARS-CoV-2 Delta variant (B.1.617.2) ( $1 \times 10^5$  pfu total in both nostrils). In early  
256 LD<sub>50</sub> experiments, we compared 3 different doses of the delta B.1.617.2 variant,  $5 \times 10^4$  pfu,  $1 \times 10^5$   
257 pfu, and  $5 \times 10^5$  pfu, and determined the middle dose of  $1 \times 10^5$  pfu as the optimal LD<sub>50</sub> in hamsters  
258 (data *not shown*).

259       Following intranasal inoculation of hamsters with  $1 \times 10^5$  pfu of the highly pathogenic Delta  
260 variant B.1.617.2, hamsters progressively lose up to 10% of their body weight within the first week  
261 after infection, before gradually returning to their original weight by about 10 days after infection.  
262 Hamsters that received the mRNA/LNP vaccine expressing Spike 2P or Spike 6P were both  
263 protected against weight loss following the challenge with the highly pathogenic Delta variant  
264 B.1.617.2. ( $P \leq 0.001$ , **Fig. 3C**). At a low dose of  $1\mu\text{g}/\text{dose}$ , the Spike 6P mRNA/LNP was slightly  
265 better in preventing weight loss compared to Spike 2P mRNA/LNP. Three out of ten highly  
266 conserved T-cell antigens mRNA/LNP-based vaccines, NSP-2, NSP-14, and Nucleoprotein  
267 prevented weight loss of the hamsters at a dose of as low as  $1 \mu\text{g}/\text{dose}$  ( $P < 0.05$ , **Fig. 3D**). At the  
268  $1\mu\text{g}/\text{dose}$ , following intranasal inoculation with  $1 \times 10^5$  pfu of the highly pathogenic Delta variant  
269 B.1.617.2, the NSP-2 antigen was the most protective antigen with only 2% of body weight loss,  
270 followed by 4% of body weight loss for the nucleoprotein and 6% of body weight loss for the NSP-14

271 (*Black arrows*). The hamsters that were vaccinated with NSP-2, NSP-14, or Nucleoprotein  
272 mRNA/LNP vaccine gradually reversed their lost body weight as early as 4-5 days after challenge  
273 (*Black arrows, Fig. 3D*). In contrast, the mock-vaccinated hamsters gradually reversed their lost body  
274 weight late starting 6 to 9 days after being challenged (*Red arrows, Fig. 3D*). At the high 10 µg/dose,  
275 two conserved T-cell antigens mRNA/LNP-based vaccines (i.e., NSP-3 and, ORF-7a/b) produced  
276 moderate protection against weight loss starting 6 days post-challenge. The remaining 5 T-cell  
277 antigens mRNA/LNP-based vaccines (i.e., NSP-4, NSP-5-10, NSP-12, Membrane, and Envelope)  
278 did not produce any significant protection against weight loss ( $P > 0.05$ , **Fig. 3D**). As expected, the  
279 mock-vaccinated hamsters were not protected and started losing weight as early as two days  
280 following challenge with the highly pathogenic Delta variant B.1.617.2.

281 Infectious virus titers are retrieved from the respiratory tract of infected hamsters and are  
282 approximately 1–2 logs higher in the nasal turbinate than in the lung, peaking at 2–4 days after  
283 infection. The modified mRNA/LNP vaccine expressing T cell NSP-2, NSP-14, and Nucleoprotein, at  
284 a dose as low as 1 µg/dose, produced a strong 20- to 40-fold reduction in median nasal viral titer  
285 two- and six-days following challenge with the highly pathogenic Delta variant B.1.617.2 ( $P < 0.05$ ).

286 We next tested the protective efficacy of NSP-2, NSP-14, and Nucleoprotein mRNA/LNP-  
287 based vaccines (**Figs. 4A** and **4B**) delivered at an intermediate dose of 5 µg/dose against lung  
288 pathology (**Fig. 4C**) and weight loss (**Fig. 4D**), viral replication (**Fig. 4E**) caused by highly pathogenic  
289 Delta variant (B.1.617.2) in the golden Syrian hamster model.

290 Sars-CoV-2 infected hamsters developed lung pathologies, including alveolar destruction,  
291 proteinaceous exudation, hyaline membrane formation, marked mononuclear cell infiltration, cell  
292 debris-filled bronchiolar lumen, alveolar collapse, lung consolidation, and pulmonary hemorrhage.  
293 These lung pathologies are largely resolved by day 14 after infection, with air-exchange structures  
294 being restored to normal. In contrast, vaccination with individual NSP-2, NSP-14, and Nucleoprotein  
295 mRNA/LNP-based vaccines significantly reduced lung pathology ( $P < 0.05$ , **Fig. 4C**), following  
296 challenge with the highly pathogenic Delta variant B.1.617.2. The lungs of hamsters vaccinated with  
297 NSP-14 mRNA/LNP show peri bronchiolitis (*arrow*), perivasculitis (*asterisk*), and multifocal interstitial

298 pneumonia (arrowhead). Lungs of hamsters that received NSP-2 or Nucleoprotein mRNA/LNP  
299 vaccine demonstrate normal bronchial, bronchiolar (*arrows*), and alveolar architecture (**Fig. 4C**). In  
300 contrast, the lungs of mock-vaccinated hamsters demonstrated bronchi with bronchiolitis (*arrows*)  
301 and adjacent marked interstitial pneumonia (*asterisks*). No serious local or systemic unwanted side  
302 effects were noticed in the mRNA/LNP vaccinated hamsters confirming the safety mRNA/LNP  
303 delivery system.

304 At an intermediate dose of 5  $\mu\text{g}/\text{dose}$ , the NSP-2, NSP-14, and Nucleoprotein mRNA/LNP-  
305 based vaccines prevented weight loss of the hamsters, gradually reversing the lost body weight as  
306 early as 4-5 days after the challenge (*Black arrows*, **Fig. 4D**). At 5  $\mu\text{g}/\text{dose}$ , the nucleoprotein was  
307 the most protective antigen when it comes to prevention of body weight, followed by NSP-14 and  
308 NSP-2, respectively. Following intranasal inoculation of mock-vaccinated hamsters with  $1 \times 10^5$  pfu  
309 of the highly pathogenic Delta variant B.1.617.2, the Nucleoprotein-vaccinated hamsters  
310 progressively lose their body weight declining by only 2% within the first 4 days after infection, before  
311 gradually and reversing the lost body weight starting on day 4 after challenge (*black arrow*, **Fig. 4D**).  
312 The NSP14-vaccinated hamsters progressively lose their body weight declining by only 6% within the  
313 first 5 days after infection, before reversing the lost body weight starting on day 6 after challenge  
314 (*black arrow*, **Fig. 4D**). The NSP2-vaccinated hamsters progressively lose their body weight declining  
315 by only 3% within the first 4 days after infection, before gradually and reversing the lost body weight  
316 starting on day 4 after challenge (*black arrow*, **Fig. 4D**). In contrast, following intranasal inoculation of  
317 mock-vaccinated hamsters with  $1 \times 10^5$  pfu of the highly pathogenic Delta variant B.1.617.2, animals  
318 progressively lose their body weight declining by greater than 10% within the first week after  
319 infection, before gradually and spontaneously reversing the lost body weight starting on day 7 after  
320 challenge (*red arrows*, **Fig. 4D**).

321 Infectious virus titers retrieved on days 2 and 6 post-challenge from the nasal turbinate of  
322 mock-vaccinated hamsters are approximately 20- to 40-fold logs higher compared to hamsters that  
323 received modified mRNA/LNP vaccine expressing T cell NSP-2, NSP-14, and Nucleoprotein, at the  
324 dose of 5  $\mu\text{g}/\text{dose}$ , suggesting a fast and strong reduction in median nasal viral titer in the NSP-2,

325 NSP-14, and Nucleoprotein mRNA/LNP vaccinated animals following challenge with the highly  
326 pathogenic Delta variant B.1.617.2 ( $P < 0.05$ , **Fig. 4E**).

327 These results indicate that mRNA/LNP vaccines based on three out of ten highly conserved  
328 RTC T-cell antigens, NSP-2, NSP-14, and Nucleoprotein, safely confer protection against infection  
329 and COVID-19-like disease caused by the highly pathogenic Delta variant (B.1.617.2).

330 **4. A combined NSP-2, NSP-14, and Nucleoprotein-based mRNA/LNP vaccine confer**  
331 **robust and broad protection against multiple SARS-CoV-2 variants and sub-variants of**  
332 **concern:** We next determined the protective efficacy of a combined T cell antigens mRNA/LNP-  
333 based Coronavirus vaccine, that incorporate the highly conserved NSP-2, NSP-14 and Nucleoprotein  
334 T cell antigens (**Fig. 5A**), against VOCs with various characteristics, including the ancestral wild-type  
335 Washington variant (WA1/2020), the highly pathogenic Delta variant (B.1.617.2), and the heavily  
336 Spike-mutated and most immune-evasive Omicron sub-variant (XBB.1.5).

337 Female golden Syrian hamsters were immunized intramuscularly twice on day 0 and day 21  
338 with 2 doses of the combination T-cell antigens mRNA/LNP-based vaccine at either 1  $\mu\text{g}/\text{dose}$  ( $n =$   
339 20 per group) or 10  $\mu\text{g}/\text{dose}$  ( $n = 20$ ) or mock-immunized ( $n = 15$  per group) (**Fig. 5B**). Three-weeks  
340 after the second immunization, animals were divided into groups of 5 hamsters each and challenged  
341 intranasally, in both nostrils, with  $2 \times 10^5$  pfu of the wild-type Washington variant (WA1/2020) ( $n = 5$   
342 per group), the  $1 \times 10^5$  pfu of Delta variant (B.1.617.2) ( $n = 5$  per group) or  $2 \times 10^5$  pfu of Omicron  
343 sub-variant (XBB1.5) ( $n = 5$  per group). In an earlier experiment, we tested 3 different doses for each  
344 variant and sub-variant and determined the dose of  $2 \times 10^5$  pfu as the optimal  $\text{LD}_{50}$  for the wild-type  
345 Washington variant (WA1/2020),  $1 \times 10^5$  pfu as the optimal  $\text{LD}_{50}$  for the Delta variant (B.1.617.2), and  
346  $2 \times 10^5$  pfu as the optimal  $\text{LD}_{50}$  for the Omicron sub-variant (XBB1.5) in hamsters (data *not shown*).

347 Vaccination with the combined NSP-2, NSP-14, and Nucleoprotein-based mRNA/LNP  
348 vaccine, at 5  $\mu\text{g}/\text{dose}$ , significantly reduced lung pathology (**Fig. 5C**), fast prevented weight loss of  
349 the hamsters ( $P < 0.05$ ) (**Fig. 5D**), and elicited a 20- to 40-fold reduction in median lung viral titer  
350 two- and six-days (**Fig. 5E**) following wild-type Washington variant (WA1/2020), Delta variant

351 (B.1.617.2), and Omicron sub-variant (XBB1.5) in hamsters. Of interest, 5 out of 5 hamsters that  
352 received the combined NSP-2, NSP-14, and Nucleoprotein-based mRNA/LNP vaccine and  
353 challenged with the heavily Spike-mutated and most immune-evasive Omicron sub-variant (XBB.1.5)  
354 did not lose any weight (*Black arrow, Fig. 5D, right panel*). The combined mRNA/LNP vaccine fast  
355 prevented weight loss in 5 out of 5 five hamsters, starting as early as 2 days post-challenge with the  
356 ancestral wild-type Washington variant (WA1/2020) and the highly pathogenic Delta variant  
357 (B.1.617.2) (*Black arrow, Fig. 5D, right and middle panels*). As expected, the mock-vaccinated mice  
358 did not show a significant reduction in lung pathology, weight loss, and lung viral replication (**Figs.**  
359 **5C, 5D, and 5E**). The mock-vaccinated mice started losing weight as early as 1-2 days post-  
360 challenge and did not reverse the weight loss until late 7-8-days post-challenge with Washington,  
361 Delta, and Omicron variants (*red arrows, Figs. 5C, 5D, and 5E*).

362 Fourteen days post-challenge, lung tissues were collected and fixed, and 5- $\mu$ m sections were  
363 cut from hamsters and stained with hematoxylin and eosin. The lungs of hamsters that received the  
364 combined NSP-2, NSP-14, and Nucleoprotein-based mRNA/LNP vaccine demonstrated normal  
365 bronchial, bronchiolar (*arrows*), and alveolar architecture (**Fig. 5C**). In contrast, the lungs of mock-  
366 immunized hamsters acute bronchi with bronchiolitis (*arrows*) and adjacent marked interstitial  
367 pneumonia (*arrowheads*).

368 Altogether, these results demonstrate that compared to individual mRNA/LNP vaccines, the  
369 combined NSP-2, NSP-14, and Nucleoprotein-based mRNA/LNP vaccine provided a synergetic or  
370 additive beneficial effect by inducing fast, robust, and broad protection against infection and disease-  
371 caused multiple SARS-CoV-2 variants and sub-variants of concern.

372 **5. A combined Spike, NSP-2, NSP-14, and Nucleoprotein-based mRNA/LNP vaccine**  
373 **confers a more potent and rapid protection against the highly pathogenic Delta SARS-CoV-2**  
374 **variant (B.1.617.2).** We next investigated whether the combination of NSP-2, NSP-14, and  
375 Nucleoprotein-based mRNA/LNP vaccines with the clinically proven Spike-alone mRNA/LNP-based  
376 vaccine would result in a beneficial additive or synergetic effect that translate in increased level of  
377 protection (**Fig. 6A**). For this experiment, we chose the prefusion Spike proteins stabilized by two

378 (Spike 2P) over six (Spike 6P) prolines<sup>37, 38</sup>. Although the mRNA/LNP Spike 6P provided slightly  
379 better protection than the mRNA/LNP Spike 2P (**Fig. 3C**), the latter was selected as it is safe with  
380 over one billion doses of the clinically proven Spike-alone mRNA/LNP-based vaccines that were  
381 already administered around the world. Given that most of the human population already received  
382 one to four doses of the first generation of Spike 2P-based COVID-19 vaccine, given the combined  
383 Spike 2P, NSP-2, NSP-14, and Nucleoprotein-based mRNA/LNP vaccine as boosters in humans  
384 with pre-existing Spike 2P immunity may boost the protective efficacy<sup>46</sup>.

385 We first ascertained the expression of the four proteins, Spike, NSP-2, NSP-14, and  
386 Nucleoprotein, after *in vitro* mRNA transfection into human epithelial HEK293T cells. We detected  
387 the expression of each protein, with a slight increase of Spike, NSP-2, and Nucleoprotein expression  
388 over NSP-14 protein (*white arrows*, **Fig. 6B**). The co-transfection of the 4 mRNA together did not  
389 result in competition as all the four antigens were equally expressed *in vitro* in human epithelial  
390 HEK293T cells (*data not shown*).

391 The efficacy of the combined Spike, NSP-2, NSP-14, and Nucleoprotein-based mRNA/LNP  
392 vaccine was compared to the Spike-alone-based mRNA/LNP vaccine against the highly pathogenic  
393 Delta SARS-CoV-2 variant (B.1.617.2) at an equimolar low amount of 1 µg/dose (**Fig. 6C**). Three  
394 groups of hamsters ( $n = 5$ ) were then vaccinated with mRNA/LNP-S (1 µg), or mRNA/LNP-S +  
395 mRNA/LNP-T cell Ag (1 µg for each mRNA/LNP) or with empty LNP (*Mock*), at weeks 0 and 3 (**Fig.**  
396 **6C**). Three weeks after the booster (week 6), all hamsters were intranasally challenged with the  
397 SARS-CoV-2 Delta variant (B.1.617.2) ( $1 \times 10^5$  pfu).

398 The combined Spike, NSP-2, NSP-14, and Nucleoprotein-based mRNA/LNP vaccine  
399 significantly reversed the weight loss in hamsters as early as 2 days post-challenge with SARS-CoV-  
400 2 Delta variant (B.1.617.2) (*black arrow*, **Fig. 6D**). In contrast, the Spike-alone-based mRNA/LNP  
401 vaccine reversed the weight loss starting 5 days post-challenge with SARS-CoV-2 Delta variant  
402 (B.1.617.2) (*green arrow*, **Fig. 6D**). As expected, the mock-vaccinated hamsters lost weight as early  
403 as 2 days post-infection and did not reverse the weight loss until late 7 days post-challenge with  
404 SARS-CoV-2 Delta variant (B.1.617.2) (*red arrow*, **Fig. 6D**).



405 On day 4 post-challenge, protection was analyzed based on viral loads ( $n = 5$ ) (**Fig. 6E**).  
406 Compared to the mock-vaccinated control hamsters, the combined Spike, NSP-2, NSP-14, and  
407 Nucleoprotein-based mRNA/LNP vaccine significantly reduced the viral load (5-log reduction of viral  
408 RNA copies) (**Fig. 6E**). In contrast Spike-alone-based mRNA/LNP vaccine modestly reduced the  
409 viral load (3-log reduction of viral RNA copies) (**Fig. 6E**). These data indicate that at a low dose of 1  
410  $\mu\text{g}/\text{dose}$ , the combined Spike, NSP-2, NSP-14, and Nucleoprotein-based mRNA/LNP vaccine  
411 provided stronger protection against a highly pathogenic Delta variant (B.1.617.2) compared to an  
412 equimolar amount of the of Spike-alone-based mRNA/LNP vaccine.

413 These results indicate that, compared to the Spike-alone-based mRNA/LNP vaccine,  
414 combined Spike, NSP-2, NSP-14, and Nucleoprotein-based mRNA/LNP vaccine induced faster and  
415 stronger protection against the highly pathogenic Delta SARS-CoV-2 variant (B.1.617.2).

416

417 **6. The combined Spike, NSP-2, NSP-14, and Nucleoprotein-based mRNA/LNP vaccine**  
418 **induces stronger, faster, and broader protection against multiple variants and sub-variants**  
419 **compared to Spike-alone-based mRNA/LNP vaccine:** We next investigated whether a combined  
420 Spike, NSP-2, NSP-14, and Nucleoprotein-based mRNA/LNP vaccine (**Fig. 7A**), would induce  
421 broader and stronger protection against the wild-type Washington variant (WA1/2020) and the  
422 heavily Spike-mutated and most immune-evasive Omicron sub-variant (XBB.1.5) (in addition to the  
423 highly pathogenic Delta variant (B.1.617.2), shown above).

424 The hamsters that received the combined Spike, NSP-2, NSP-14, and Nucleoprotein-based  
425 mRNA/LNP vaccine significantly reversed the weight loss as early as 2 days post-challenge with the  
426 wild-type Washington variant (WA1/2020) (*black arrow*, **Fig. 7B**). In contrast, the hamsters that  
427 received the Spike-alone-based mRNA/LNP vaccine reversed the weight loss late 6 days post-  
428 challenge with the wild-type Washington variant (WA1/2020) (*green arrow*, **Fig. 7B**). Moreover, the  
429 hamsters that received the combined Spike, NSP-2, NSP-14, and Nucleoprotein-based mRNA/LNP  
430 vaccine significantly reversed the weight loss as early as the first day post-challenge with the heavily  
431 Spike-mutated and most immune-evasive Omicron sub-variant (XBB.1.5) (*black arrow*, **Fig. 7C**). In  
432 contrast, the hamsters that received the Spike-alone-based mRNA/LNP vaccine reversed the weight

433 loss late 6 days post-challenge with the Omicron sub-variant (XBB.1.5) (*green arrow*, **Fig. 7C**). As  
434 expected, the mock-vaccinated hamsters lost weight fast as early as the first day post-challenge and  
435 did not reverse the weight loss until late 7 to 8 days post-challenge with the wild-type Washington  
436 variant (WA1/2020) and the Omicron sub-variant (XBB.1.5) (*red arrow*, **Figs. 7B** and **7C**).

437 Histopathological analysis showed that compared to lungs of mock-vaccinated controls, the  
438 lungs of hamsters that received the combination of Spike, NSP-2, NSP-14, and Nucleoprotein-based  
439 mRNA/LNP vaccine were fully protected from all lesions with normal bronchial, bronchiolar, and  
440 alveolar architecture (**Fig. 7D**). In contrast, the lungs of hamsters that received the Spike-alone-  
441 based mRNA/LNP vaccine developed small lesions, including interstitial pneumonia and  
442 peribronchitis (**Fig. 7D**). As expected, considerable pathological changes, including bronchitis and  
443 interstitial pneumonia, are evident in the lungs of mock-immunized hamsters on 4 days post-  
444 challenge (**Fig. 7D**). The higher lung pathology and lower virus titers detected in the lungs of  
445 hamsters that received the Spike-alone-based mRNA/LNP vaccine suggest an immune escape by  
446 the highly pathogenic the heavily Spike-mutated and most immune-evasive Omicron sub-variant  
447 (XBB.1.5). In contrast, lack of lung pathology and higher virus titers detected in the lungs of hamsters  
448 that received the combined spike, NSP-2, NSP-14, and Nucleoprotein-based mRNA/LNP vaccines  
449 likely indicates a lack of immune escape by the heavily Spike-mutated and most immune-evasive  
450 Omicron sub-variant (XBB.1.5).

451 The virus titers determined on days 2 and 6 post-challenge, confirmed the significant  
452 reduction of the lung viral burden by up to 5 logs by the combined Spike, NSP-2, NSP-14, and  
453 Nucleoprotein-based mRNA/LNP vaccine following challenge by wild-type Washington variant  
454 (WA1/2020) or the Omicron sub-variant (XBB.1.5) (**Figs. 7E** and **7F**).

455 Together the results (*i*) demonstrated that the combined Spike, NSP-2, NSP-14, and  
456 Nucleoprotein-based mRNA/LNP vaccine induces stronger and broader protection against multiple  
457 variants and sub-variants; and (*ii*) suggest that the combined Spike, NSP-2, NSP-14, and  
458 Nucleoprotein-based mRNA/LNP vaccine that include T cell antigens likely induced stronger Spike-

459 specific neutralizing antibodies that prevented immune escape by the heavily Spike-mutated  
460 variants, compared to Spike-alone-based mRNA/LNP vaccine.

461 **7. Enriched lungs-resident Non-Spike antigen-specific CD4<sup>+</sup> and CD8<sup>+</sup> T cells and**  
462 **Spike-specific neutralizing antibodies induced by the combined Spike, NSP-2, NSP-14, and**  
463 **Nucleoprotein-based mRNA/LNP vaccine:** Finally, we determined whether the observed rapid and  
464 broad clearance of SARS-CoV-2 infections in hamsters vaccinated with the combined Spike, NSP-2,  
465 NSP-14, and Nucleoprotein-based mRNA/LNP vaccine would be associated with anti-viral lung-  
466 resident NSP-2, NSP-14, and Nucleoprotein-specific CD4<sup>+</sup> and CD8<sup>+</sup> T cell responses (**Fig. 8**). After  
467 all, the protective NSP-2 and NSP-14 and Nucleoprotein T cell antigens in the combined vaccine all  
468 belong to the early-transcribed RTC region and are selectively targeted by human lung-resident  
469 enriched memory CD4<sup>+</sup> and CD8<sup>+</sup> T cells from “SARS-CoV-2 aborters” (i.e., those SARS-CoV-2  
470 exposed seronegative healthcare workers and in household contacts who were able to rapidly abort  
471 the virus replication)<sup>28, 29, 30, 31, 32</sup>. Correlation of the frequencies of lung-enriched NSP-2, NSP-14,  
472 and Nucleoprotein-specific-specific CD4<sup>+</sup> and CD8<sup>+</sup> T cells with protection from virus load after  
473 challenge with various variants and sub-variants were compared in the hamsters that received the  
474 combined Spike, NSP-2, NSP-14, and Nucleoprotein-based mRNA/LNP vaccine vs. mock-vaccine.

475 Lungs from vaccinated and mock-vaccinated hamsters were collected 2 weeks after the  
476 SARS-CoV-2 challenge and cell suspensions were stimulated with pools of 15-mer overlapping NSP-  
477 2, NSP-14, or Nucleoprotein (**Fig. 6C**). The frequency and function of lung-resident NSP-2-, NSP-14-  
478 , and Nucleoprotein-specific CD8<sup>+</sup> and CD4<sup>+</sup> T cells were compared in vaccinated protected  
479 hamsters versus mock-vaccinated unprotected hamsters (**Fig. 8**).

480 The data showed that the combined Spike, NSP-2, NSP-14, and Nucleoprotein-based  
481 mRNA/LNP vaccines elicited robust NSP-2- (**Fig. 8A**), NSP-14- (**Fig. 8B**), Nucleoprotein-specific  
482 (**Fig. 8C**) and (**Fig. 8D**) Spike-specific CD4<sup>+</sup> and CD8<sup>+</sup> T cell responses. While there seem to be  
483 more CD4<sup>+</sup> T cell responses than CD8<sup>+</sup> T cell responses in the lungs, overall, NSP-2, NSP-14, and  
484 Nucleoprotein appeared to be targeted by the same frequencies of functional CD4<sup>+</sup> and CD8<sup>+</sup> T cells.

485 Among the cytokines examined, IFN- $\gamma$  and TNF- $\alpha$  were highly expressed by NSP-2-, NSP-  
486 14-, and Nucleoprotein-specific CD4<sup>+</sup> and CD8<sup>+</sup> T cells. The combined vaccine appeared to induce  
487 higher NSP-2- and Nucleoprotein-specific IFN- $\gamma$ <sup>+</sup>TNF- $\alpha$ <sup>+</sup>CD4<sup>+</sup> and IFN- $\gamma$ <sup>+</sup>TNF- $\alpha$ <sup>+</sup>CD8<sup>+</sup> T cell  
488 responses compared to NSP-14-specific IFN- $\gamma$ <sup>+</sup>TNF- $\alpha$ <sup>+</sup>CD4<sup>+</sup> and IFN- $\gamma$ <sup>+</sup>TNF- $\alpha$ <sup>+</sup>CD8<sup>+</sup> T cell responses  
489 ( $P < 0.001$  for IFN- $\gamma$ ). The analyses of T cell responses in the lungs of protected and non-protected  
490 hamsters indicate that the combined Spike, NSP-2, NSP-14, and Nucleoprotein-based mRNA/LNP  
491 vaccine induced high frequencies of NSP-2, NSP-14, and Nucleoprotein-specific lung-resident  
492 CXCR5<sup>+</sup>CD4<sup>+</sup> T follicular helper cells (T<sub>FH</sub> cells), compared to Spike-alone-based mRNA/LNP  
493 vaccine. This suggests that these CXCR5<sup>+</sup>CD4<sup>+</sup> T<sub>FH</sub> cells likely contribute to the augmentation in the  
494 Spike-specific neutralizing antibodies and protection observed in the combined Spike, NSP-2, NSP-  
495 14, and Nucleoprotein-based mRNA/LNP vaccine group compared to Spike-alone-based  
496 mRNA/LNP vaccine.

497 Analysis of CD4<sup>+</sup> and CD8<sup>+</sup> T cell responses in the peripheral blood of vaccinated hamsters  
498 after two doses of the combined mRNA vaccine, before challenge, and after challenge indicated the  
499 combined Spike, NSP-2, NSP-14, and Nucleoprotein-based mRNA/LNP vaccine-induced robust  
500 NSP-2-, NSP-14- and Nucleoprotein-specific CD4<sup>+</sup> and CD8<sup>+</sup> T cell responses subsequently boosted  
501 by the exposure to the virus after challenge with Washington variant (WA1/2020), Delta variant  
502 (B.1.617.2), and Omicron sub-variant (XBB.1.5). These results confirm the antigen specificity of the  
503 induced CD4<sup>+</sup> and CD8<sup>+</sup> T cell responses. Compared to SARS-CoV-2-specific T cells in peripheral  
504 blood and spleen, we found better correlations between protection and lung-resident SARS-CoV-2  
505 specific T cells (*not shown*), confirming the importance of airways-resident T cells in protection<sup>28, 29,</sup>  
506 <sup>30, 31</sup>.

507 Since the combined Spike, NSP-2, NSP-14, and Nucleoprotein-based mRNA/LNP vaccine  
508 induced strong NSP-2, NSP-14, and Nucleoprotein-specific CXCR5<sup>+</sup>CD4<sup>+</sup> T<sub>FH</sub> cells compared to the  
509 Spike mRNA/LNP vaccine alone, we next determined whether the combined vaccine would induce  
510 better Spike-specific neutralizing antibody titers. Serum samples were collected after vaccination and  
511 before the viral challenge and tested by ELISA and neutralization assays against Washington, Delta,

512 and Omicron. Higher titers of IgG-specific antibodies were detected in 5 out of 5 hamsters that  
513 received the combined vaccines compared to hamsters that received the Spike-alone vaccine (**Fig.**  
514 **8E**, *upper panel*). Moreover, compared to the Spike-alone-based mRNA/LNP vaccine, the combined  
515 Spike, NSP-2, NSP-14, and Nucleoprotein-based mRNA/LNP vaccine elicited stronger serum  
516 neutralizing activity against the wild-type virus ( $P < 0.005$ ) the Delta variant ( $P < 0.005$ ) and the  
517 Omicron variants ( $P < 0.005$ ) (**Fig. 8E**, *lower panel*). While serum from the mRNA/LNP-Spike alone  
518 vaccinated hamsters manifested strong neutralizing activity against the wild-type Washington for variant  
519 but markedly reduced neutralizing activity (a 5-fold reduction) against the heavily Spike-mutated  
520 Delta and Omicron variants (**Fig. 8E**). These results suggest that the combination of Spike, NSP-2,  
521 NSP-14, and Nucleoprotein-based mRNA/LNP vaccine induced stronger Spike-specific neutralizing  
522 antibodies that prevented immune escape by the heavily Spike-mutated variants.

523 All together, these results indicate that, at a dose as low as 1 $\mu$ g/dose, the combined Spike,  
524 NSP-2, NSP-14, and Nucleoprotein-based mRNA/LNP vaccine elicited Spike-specific neutralizing  
525 antibodies and airway-resident NSP-2-, NSP-14-, and Nucleoprotein-specific GzmB<sup>+</sup>CD4<sup>+</sup> T<sub>CYT</sub> and  
526 GzmB<sup>+</sup>CD8<sup>+</sup> T<sub>CYT</sub> cells, CD69<sup>+</sup>IFN- $\gamma$ <sup>+</sup>TNF $\alpha$ <sup>+</sup>CD4<sup>+</sup> T<sub>EFF</sub> cells, CD69<sup>+</sup>IFN- $\gamma$ <sup>+</sup>TNF $\alpha$ <sup>+</sup>CD8<sup>+</sup> T<sub>EFF</sub> cells, and  
527 CXCR5<sup>+</sup>CD4<sup>+</sup> T<sub>FH</sub> cells that correlated with protection against several VOCs, including the ancestral  
528 wild-type Washington variant (WA1/2020), the highly pathogenic Delta variant (B.1.617.2), and the  
529 heavily Spike-mutated and most immune-evasive Omicron sub-variant (XBB.1.5). Compared to  
530 animals that received the Spike alone, the high frequency of CXCR5<sup>+</sup>CD4<sup>+</sup> T<sub>FH</sub> cells in the lungs of  
531 hamsters that received the combined vaccine likely contributed to stronger Spike-specific neutralizing  
532 antibody activities that cleared the virus in the lungs. The airway-resident B- and T cell immunity  
533 induced by combined Spike, NSP-2, NSP-14, and Nucleoprotein-based mRNA/LNP vaccine likely  
534 contribute collectively to the enhanced protection capable of conferring broad cross-strain protective  
535 immunity against infection and disease caused by multiple variants and sub-variants.

## DISCUSSION

536

537 As of January 2024, the world is entering its fifth year of a persistent COVID-19 pandemic,  
538 fueled by the continuous emergence of heavily Spike-mutated and highly contagious SARS-CoV-2  
539 variants and sub-variants that: (i) Escaped immunity induced by the current clinically proven Spike-  
540 alone-based vaccines; (ii) Disrupt the efficacy of the COVID-19 booster paradigm<sup>8, 9, 11, 12, 47, 48</sup>; and  
541 (iii) Outpaced the development of variant-adapted bivalent Spike-alone vaccines<sup>1, 4, 5, 6, 19</sup>. This bleak  
542 outlook of a prolonged COVID-19 pandemic emphasizes the urgent need for developing a next-  
543 generation broad-spectrum pan-Coronavirus vaccine capable of conferring strong cross-variants and  
544 cross-strain protective immunity that would prevent, immune evasions and breakthrough infections<sup>4</sup>.

545 In the present pre-clinical vaccine study, using *in silico*, *in vitro*, and *in vivo* approaches, we  
546 demonstrate that a combined Spike, NSP-2, NSP-14, and Nucleoprotein-based mRNA/LNP vaccine  
547 induced a broad cross-protective immunity against several highly contagious and heavily Spike-  
548 mutated SARS-CoV-2 variants and subvariants. The three highly conserved NSP-2, NSP-14, and  
549 Nucleoprotein antigens incorporated in the combined mRNA/LNP vaccine are (i) Expressed by the  
550 early transcribed virus RTC region; (ii) Preferentially targeted by human cross-reactive memory CD4<sup>+</sup>  
551 and CD8<sup>+</sup> T cells associated with protection of asymptomatic COVID-19 patients (i.e., unvaccinated  
552 individuals who never develop any COVID-19 symptoms despite being infected with SARS-CoV-2);  
553 and (iii) selectively targeted by lung-resident enriched memory CD4<sup>+</sup> and CD8<sup>+</sup> T cells from SARS-  
554 CoV-2 exposed seronegative individuals who were able to rapidly abort the virus replication (i.e.,  
555 “SARS-CoV-2 aborters”)<sup>28, 29, 30, 31</sup>. Hamsters that received the combined mRNA/LNP vaccine,  
556 displayed lower virus load, improved lung pathology, and early reversion of weight loss caused by  
557 various VOCs including the ancestral wild-type Washington variant (WA1/2020), the highly  
558 pathogenic Delta variant (B.1.617.2), the heavily Spike-mutated Omicron sub-variants (B.1.1.529 and  
559 XBB1.5). The potent and broad cross-protection induced by the combined mRNA/LNP vaccine was  
560 associated with enhanced Spike-specific neutralizing antibodies, enriched lung-resident NSP-2-  
561 NSP-14- and Nucleoprotein-specific T follicular helper (T<sub>FH</sub>) cells, cytotoxic T cells (T<sub>CYT</sub>), effector T  
562 cells (T<sub>EFF</sub>). The findings in humans that were confirmed in the hamster model, suggest an alternative

563 broad-spectrum pan-Coronavirus vaccine capable of (i) disrupting the current COVID-19 booster  
564 paradigm; (ii) outpacing the bivalent variant-adapted COVID-19 vaccines; and (iii) ending an  
565 apparent prolonged COVID-19 pandemic.

566 SARS-CoV-2 remains a major global public health concern. Although the current rate of  
567 SARS-CoV-2 infections has decreased significantly; COVID-19 still ranks very high as a cause of  
568 death worldwide. As of January 2024, the weekly mortality rate is still at over 1500 deaths in the  
569 United States alone, which surpasses even the worst mortality rates recorded for influenza. The  
570 efficacy of the first-generation Spike-alone-based COVID-19 vaccines is threatened by the  
571 emergence of many immune-evasive SARS-CoV-2 variants and subvariants with the capacity to  
572 evade protective neutralizing antibody responses<sup>1, 4, 5, 6, 19</sup>. The waning immunity induced by Spike-  
573 alone vaccines as well as the antigenic drift of SARS-CoV-2 variants has diminished vaccine efficacy  
574 against many recent heavily mutated Spike VOCs<sup>4, 49</sup>. Emerging SARS-CoV-2 variants, particularly  
575 the Omicron lineages, with frequent mutations in the Spike protein, evade immunity induced by  
576 vaccination or by natural infection<sup>50, 51</sup>. Thus, the first-generation Spike-based COVID-19 vaccines  
577 must be regularly updated to fit new VOCs with high transmissibility that kept emerging throughout  
578 the pandemic. This “copy-passed” vaccine strategy that “chases” the VOCs by adapting the mutated  
579 Spike sequence of the emerged VOCs into a new batch of an “improved” vaccine is often surpassed  
580 by a next fast emerging variant or subvariant. These mutations have accounted for many  
581 breakthrough infections in recent COVID-19 surges<sup>1, 4, 5, 6, 19</sup>. Breakthrough infections by the most  
582 recent highly contagious, and heavily Spike-mutated Omicron sub-variants, XBB1.5, EG.5, HV.1,  
583 BA.2.86, and JN.1 contribute to a prolonged COVID-19 pandemic<sup>8, 9, 48</sup>. Thus, 4 years into the  
584 pandemic, the long-term outlook of COVID-19 is still a serious concern that threatens public health,  
585 outlining the need for a safe next-generation broad-spectrum pan-CoV vaccine, that could be quickly  
586 implemented in the clinic. Here, we describe an alternative multi-antigen B- and T-cell-based pan-  
587 CoV vaccine that utilized the mRNA/LNP platform, an antigen delivery technology that is “plug-and-  
588 play”. The strategy is readily scalable to produce a broad-spectrum, next-generation pan-CoV  
589 vaccine in case of a fast seasonal surge of yet another fast-spreading variant, such as the current  
590 highly transmissible and most immune-evasive Omicron sub-variants ‘Pirola’ BA.2.86 and JN.1 that

591 are currently spreading around the world. Several antigen delivery platforms can be theoretically  
592 used to administer the B- and T-cell antigens discovered in this study: Adenovirus <sup>52</sup>, poxvirus <sup>53</sup>, and  
593 modified vaccinia Ankara vectors <sup>54, 55, 56</sup>, self-assembling protein nanoparticle (SAPN) <sup>57</sup>, and  
594 mRNA/LNP technology platform <sup>35</sup>. In the present NIH-supported pan-CoV vaccine project, we  
595 originally proposed to use the SAPN platform as a delivery system. However, early in 2021, we  
596 abandoned the SAPN platform and switched to the mRNA/LNP technology platform as a safer, easy-  
597 to-produce, and readily scalable antigen delivery platform most adapted to mass vaccination. After  
598 extensive 4-year pre-clinical vaccine trials using the mRNA/LNP technology platform in both hamster  
599 and mouse models, we demonstrate safety, immunogenicity (including neutralizing antibodies), and  
600 protective efficacy of the combined pan-CoV mRNA/LNP-based vaccine. Throughout the COVID-19  
601 pandemic, unlike many of other antigen delivery platforms cited above, the mRNA/LNP technology  
602 platform showed superior clinical safety, clinical immunogenicity, including neutralizing antibodies,  
603 and clinical protective efficacy, with over one billion doses of the clinically proven Spike mRNA/LNP-  
604 based vaccines safely delivered worldwide with very mild side effects, since early 2021. Moreover,  
605 the present combined mRNA/LNP-based pan-CoV vaccine produced broader protection against  
606 multiple variants and sub-variants, including the highly pathogenic Delta variant (B.1.617.2), and the  
607 heavily Spike-mutated and most immune-evasive Omicron sub-variant (XBB.1.5). This contrasts  
608 most combined pan-CoV vaccine candidates that only protected against earlier circulating wild type  
609 or ancestral variants (i.e., Washington or Wuhan strains)<sup>35, 52, 53, 54, 55, 56</sup>. Given that the mRNA/LNP  
610 vaccine technology platform has been clinically proven with a good safety profile in large human  
611 populations, the present multivalent combined mRNA/LNP-based pan-CoV vaccine approach could  
612 be rapidly adapted to clinical use against emerging and re-emerging VOCs. Based on the results  
613 obtained from an extensive 4-year preclinical animal studies at the University of California, Irvine,  
614 this broad-spectrum multi-antigen mRNA/LNP-based pan-Coronavirus vaccine is being proposed by  
615 the pharmaceutical company, TechImmune LLC, to move into phase I/II clinical trial.

616 To the best of our knowledge, the present extensive pre-clinical study is the first to  
617 systematically characterize the safety, immunogenicity, and protective efficacy of genome-wide  
618 SARS-CoV-2-derived T-cell antigens delivered as mRNA/LNP-based vaccine candidates. These



619 include 3 structural (Membrane, Envelope, and Nucleoprotein), 6 non-structural (NSP-2, NSP-3,  
620 NSP-4, NSP-5-10, NSP-12, and NSP-14), and 1 accessory regulatory protein (ORF7a/b). A handful  
621 of studies have reported Spike and Nucleoprotein combined vaccine candidates using various  
622 antigen delivery systems, including mRNA/LNP<sup>35</sup>, adenovirus vector<sup>52</sup>, poxvirus vector<sup>53</sup>, and  
623 modified vaccinia Ankara vector<sup>54, 55, 56</sup>. Moreover, except for one study, these studies did not  
624 compare side-by-side the efficacy of the combined vaccine with the current, clinically proven Spike-  
625 alone vaccine. The present study is the first to demonstrate that, compared to a Spike-alone  
626 mRNA/LNP vaccine, three out of ten conserved individual non-Spike mRNA/LNP vaccines (NSP-2,  
627 NSP-14, and Nucleoprotein-based mRNA/LNP vaccines) induced robust protective immunity that  
628 control multiple variants and sub-variants with various characteristics, including the ancestral wild-  
629 type Washington variant (WA1/2020), the highly pathogenic Delta variant (B.1.617.2), and the  
630 heavily Spike-mutated and most immune-evasive Omicron sub-variant (XBB.1.5). Compared to the  
631 Spike-alone mRNA/LNP vaccine, the combined B- and T-cell Spike, NSP-2, NSP-14, and  
632 Nucleoprotein-based mRNA/LNP vaccine not only induces airway-resident antigen-specific  
633 CXCR5<sup>+</sup>CD4<sup>+</sup> T<sub>FH</sub> cells, GzmB<sup>+</sup>CD4<sup>+</sup> T<sub>CYT</sub> and GzmB<sup>+</sup>CD8<sup>+</sup> T<sub>CYT</sub>, CD69<sup>+</sup>IFN- $\gamma$ <sup>+</sup>TNF $\alpha$ <sup>+</sup>CD4<sup>+</sup> T<sub>EFF</sub> cells  
634 and CD69<sup>+</sup>IFN- $\gamma$ <sup>+</sup>TNF $\alpha$ <sup>+</sup>CD8<sup>+</sup> T<sub>EFF</sub> cells but also elicited stronger Spike-specific antibody responses  
635 and serum-neutralizing antibody activities when compared to the Spike-alone mRNA/LNP vaccine. A  
636 key feature of T<sub>FH</sub> cells is high expression of the chemokine receptor CXCR5, which binds the pro-  
637 inflammatory chemokine CXCL13 expressed in B cell follicles<sup>58</sup>. Thus, CXCL13, acting on CXCR5,  
638 promotes the migration of T<sub>FH</sub> cells to the B cell follicles and into the germinal centers. High levels of  
639 CXCL13 in COVID-19 patients directly correlated with a high frequency of Spike-specific B cells and  
640 the magnitude of Spike-specific IgG with neutralizing activity<sup>59</sup>. Thus, adding the NSP-2, NSP-14,  
641 and Nucleoprotein antigen to the Spike may have an additive or synergetic protective effect in the  
642 combined B- and T-cell Spike, NSP-2, NSP-14, and Nucleoprotein-based mRNA/LNP vaccine. One  
643 could not exclude cross-priming effects between NSP-2, NSP-14, and Nucleoprotein antigens on one  
644 hand and Spike antigen on the other hand in the combined vaccine group of hamsters. Thigh  
645 frequencies of NSP-2, NSP-14, and Nucleoprotein-specific CXCR5<sup>+</sup>CD4<sup>+</sup> T<sub>FH</sub> cells induced by the  
646 combined mRNA/LNP vaccine may helped the select Spike-specific B cells contributing development

647 of high-affinity neutralizing Abs to multiple VOCs<sup>60, 61</sup>. A detailed comparison of the early innate  
648 immunity events that occur after administration of the combined mRNA/LNP vaccine vs. the Spike-  
649 alone mRNA/LNP vaccine would help elucidate the underlying mechanism behind the strong  
650 protective immunity induced by the combined mRNA/LNP vaccine.

651 The antiviral B and T cell immune mechanisms reported in this study, are expected to inform  
652 the design of next-generation broad-spectrum pan-Coronavirus vaccines<sup>1, 4, 5, 6, 19</sup>. The present  
653 results from the hamster model confirm our and others recent reports in mouse models that  
654 increased frequencies of lung-resident IFN- $\gamma$ <sup>+</sup>TNF- $\alpha$ <sup>+</sup>CD4<sup>+</sup> and IFN- $\gamma$ <sup>+</sup> TNF- $\alpha$ <sup>+</sup>CD8<sup>+</sup> T<sub>EFF</sub> cells specific  
655 to common antigens protected against multiple SARS-CoV-2 VOCs<sup>1, 3, 27</sup>. Interferons restrict SARS-  
656 CoV-2 infection in human airway epithelial cells<sup>2, 62</sup>. TNF- $\alpha$  induces multiple antiviral mechanisms  
657 and synergizes with interferon IFN- $\gamma$  in promoting antiviral activities<sup>63</sup>. We demonstrated that high  
658 frequencies of lung-resident antigen-specific IFN- $\gamma$ <sup>+</sup>TNF- $\alpha$ <sup>+</sup>CD4<sup>+</sup> T cells and IFN- $\gamma$ <sup>+</sup>TNF- $\alpha$ <sup>+</sup>CD8<sup>+</sup> T  
659 cells correlated with protection induced by the combined mRNA/LNP vaccine in hamsters. Similarly,  
660 we found that compared to severely ill COVID-19 patients and patients with fatal COVID-19  
661 outcomes, the asymptomatic COVID-19 patients displayed significantly higher magnitude of SARS-  
662 CoV-2 specific IFN- $\gamma$ <sup>+</sup>CD4<sup>+</sup> and IFN- $\gamma$ <sup>+</sup>CD8<sup>+</sup> T cell responses. These results agree with previous  
663 reports that enriched SARS-CoV-2-specific IFN- $\gamma$ -producing T cells in COVID-19 patients are  
664 associated with moderate COVID-19 disease<sup>60, 61, 64</sup>. Additionally, our findings suggest that induction  
665 of antigen-specific lung-resident antiviral IFN- $\gamma$ <sup>+</sup>TNF- $\alpha$ <sup>+</sup>CD4<sup>+</sup> T cells and IFN- $\gamma$ <sup>+</sup>TNF- $\alpha$ <sup>+</sup>CD8<sup>+</sup> T cells  
666 likely cleared lung-epithelial infected cells contributing to the observed reduction of viral load and  
667 lung pathology in the hamsters vaccinated with the combined mRNA/LNP vaccine. Moreover,  
668 increased frequencies of airway-resident SARS-CoV-2-specific cytotoxic CD4<sup>+</sup> and CD8<sup>+</sup> T<sub>CYT</sub> cells  
669 by the combined mRNA/LNP vaccine may have also contributed to the clearance of infected  
670 epithelial cells of the upper respiratory tract, as suggested by our and other reports<sup>1, 3, 27, 3, 60, 61, 64</sup>.

671 Viral transcription is an essential step in SARS-CoV-2 infection and immunity after invasion  
672 into the target cells. In the present study, we found early-transcribed non-structural proteins,  
673 including NSP-2, NSP-7, NSP-12, NSP-13, and NSP-14, from the RTC region, and the structural

674 Nucleoprotein are selectively targeted: (i) by peripheral blood cross-reactive memory CD4<sup>+</sup> and CD8<sup>+</sup>  
675 T cells from asymptomatic COVID-19 patients. This is in agreement with our and others reports that  
676 detected high frequencies of cross-reactive functional CD4<sup>+</sup> and CD8<sup>+</sup> T cells, directed toward  
677 specific sets of conserved SARS-CoV-2 non-Spike antigens, including NSP-2, NSP-7, NSP-12, NSP-  
678 13, NSP-14, and Nucleoprotein, in the unvaccinated asymptomatic COVID-19 patients<sup>5, 20, 21, 22, 23, 24,</sup>  
679 <sup>25, 26</sup>; and (ii) by lung-resident cross-reactive memory CD4<sup>+</sup> and CD8<sup>+</sup> T cells associated with rapid  
680 clearance of infection in so-called “SARS-CoV-2 aborters”<sup>28, 29, 30, 31, 32</sup>. The vigorous and enriched  
681 cross-reactive RTC-specific CD4<sup>+</sup> and CD8<sup>+</sup> T-cells mounted by “SARS-CoV-2 aborters”  
682 spontaneously “abort” virus infection so rapidly that they never presented detectable SARS-CoV-2  
683 infection, despite constant exposure to the virus<sup>28, 29, 30, 31</sup>. Similarly, we found the NSP-2, NSP-14,  
684 and Nucleoprotein, which are incorporated in the combined mRNA/LNP vaccine, were also targeted  
685 by enriched lung-resident antigen-specific T follicular helper (T<sub>FH</sub>) cells, cytotoxic T cells (T<sub>CYT</sub>),  
686 effector T cells (T<sub>EFF</sub>) associated with rapid clearance of the virus from the lungs of protected  
687 hamsters<sup>60, 65</sup>. In contrast, the highly conserved, but late expressed T cell antigens, such as the  
688 accessory ORF7a/b protein, the structural Membrane, and Envelope proteins, that do not belong to  
689 the RTC region, although they are targeted by CD4<sup>+</sup> and CD8<sup>+</sup> T-cells from the unvaccinated  
690 asymptomatic COVID-19 patients, did not protect against virus replication in the lungs of vaccinated  
691 hamsters. This suggests that the early expressed conserved antigens that belong to the RTC region  
692 and that are selectively recognized by CD4<sup>+</sup> and CD8<sup>+</sup> T cells from asymptomatic COVID-19 patients  
693 and “SARS-CoV-2 aborters” are ideal targets to be included in future pan-Coronavirus vaccines<sup>28, 29,</sup>  
694 <sup>30, 31</sup>. It is likely that rapid induction of local mucosal antigen-specific CD4<sup>+</sup> and CD8<sup>+</sup> T cells by early  
695 expressed NSP-2, NSP-14, or Nucleoprotein antigens contributed to a rapid control virus replication  
696 and lower lung pathology in the lungs of vaccinated hamsters. Besides, the nucleoprotein is the most  
697 abundant viral protein, and one of the most predominantly targeted antigens by T cells in individuals  
698 with less severe COVID-19 disease<sup>34, 35</sup>. Our results also agree with a previous report showing that  
699 Nucleoprotein-specific T-cell responses were associated with control of SARS-CoV-2 in the upper  
700 airways and improved lung pathology before seroconversion<sup>66</sup>.

701 In the present study, identified five highly conserved regions in the SARS-CoV-2 single-  
702 stranded RNA genome that encodes for 3 structural (Membrane, Envelope, and Nucleoprotein, 11  
703 non-structural (NSP-2, NSP-3, NSP-4, NSP-5-10, NSP-12, NSP-14, and 1 accessory protein  
704 encoded by the open-reading frame, ORF7a/b<sup>33</sup>. The ten selected protein antigens are highly  
705 conserved in all VOCs including in the current highly transmissible and most immune-evasive  
706 Omicron sub-variants ‘Pirola’ BA.2.86 and JN.1 that are currently spreading around the world (Table  
707 1). In contrast, the Spike protein is heavily mutated in these variants with an accumulated 346  
708 mutations, including 60 and 52 new mutations, in BA.2.86 and JN.1 subvariants, respectively. The  
709 omicron variant of SARS-CoV-2 emerged for the first time in South Africa in late 2021. The BA.2  
710 lineage was one of the major omicron descendent lineages that showed significantly higher  
711 transmissibility and infectivity. The BA.2.86 is a notable descendent lineage of BA.2 that emerged in  
712 2023. This variant has higher numbers of spike protein mutations than previously emerged variants.  
713 The most recently emerged JN.1 variant is descendent of BA.2.86 that has gained significantly  
714 higher transmission ability and was designated as a separate variant of interest on 18 December  
715 2023. With an additional substitution mutation (L455S) in the spike protein, the JN.1 variant exhibits  
716 faster circulation than BA.2.86 worldwide. The high number of Spike mutations that occurred in the  
717 recent highly mutated fast-spreading COVID variants BA.2.86 and JN.1, which likely cause more  
718 severe disease<sup>67</sup>, represents a serious evolution of the BA.2.86 and JN.1 that likely warrants the  
719 issuance of new Greek letters, to distinguish them from Omicron. The sequences of the protective T  
720 cell antigens NSP-2, NSP-14, and Nucleoprotein remain relatively conserved in BA.2.86 and JN.1.  
721 This suggests that if our combined Spike, NSP-2, NSP-14, and Nucleoprotein-based mRNA/LNP  
722 vaccine must be implemented today as a pan-Coronavirus it would likely protect against the heavily  
723 Spike-mutated and highly transmissible and likely more pathogenic Omicron sub-variants, BA.2.86  
724 and JN.1<sup>67</sup>. Of importance, the sequence of the T cell antigen NSP-14 is fully conserved (100%) in  
725 all variants and sub-variants, including the BA.2.86 and JN.1, supporting the conserved vital function  
726 of NSP-14 protein in the SARS-CoV-2 life cycle<sup>68, 69, 70, 71, 72, 73</sup>. The NSP-14 (527 aa) is a bifunctional  
727 protein with the N-terminal domain has a methyltransferase function required for virus replication<sup>68,</sup>  
728<sup>69, 70</sup>, while its C-terminal domain has a proofreading exonuclease function, plays a critical role in viral

729 RNA 5' capping and facilitates viral mRNA stability and translation<sup>69, 71, 72, 73</sup>. The NSP-2 (638 aa) is a  
730 multi-subunit RNA-dependent RNA polymerase (RdRp) that is involved in replication and RNA  
731 synthesis<sup>74 75</sup>. The Nucleoprotein (419 aa), the most abundant protein of SARS-CoV-2, plays a vital  
732 role in identifying and facilitating virus RNA packaging and in regulating virus replication and  
733 transcription<sup>76</sup>. Because NSP-2, NSP-14, and Nucleoprotein apparent vital functions in the virus life  
734 cycle, immune targeting of these viral proteins, might result in interfering with virus replication.  
735 Moreover, since the NSP-2, NSP-14, and Nucleoprotein are conserved in SARS-CoV, MERS-CoV,  
736 and animal SL-CoVs from bats, pangolins, civet cats, and camels, the combined mRNA/LNP pan-  
737 CoV vaccine may not only end the current COVID-19 pandemic, but could also prevent future CoV  
738 pandemics.

739 Over the last two decades, it has been technically difficult to perform phenotypic and  
740 functional profiling of CD4<sup>+</sup> and CD8<sup>+</sup> T cells in the hamster model. One major limitation was the  
741 unavailability of monoclonal antibodies (mAbs) and reagents specific to hamsters' T cell subsets,  
742 surface CD, cytokines, and chemokines. Our laboratory is one of the world's leading in hamsters'  
743 immunology, and has recently advanced T cell immunology frontiers in hamsters. We identified,  
744 tested, and validated the specificity of many mAbs and immunological reagents commercially  
745 available to study the phenotype and function of T cell subsets in the hamster model over the last  
746 two years. In the present study, we report on the phenotype and function of CD4<sup>+</sup> and CD8<sup>+</sup> T cells in  
747 the hamster model using validated mAbs. Based on our expertise, function T cell assays, including  
748 IFN- $\gamma$ -ELISpot, surface markers of CD4<sup>+</sup> and CD8<sup>+</sup> T cell subsets, CD69 activation marker, and  
749 GzmB T cell cytotoxic marker, can readily be assessed in the hamster model. Using these markers  
750 we demonstrated the association of lung-resident antigen-specific GzmB<sup>+</sup>CD4<sup>+</sup> T<sub>CYT</sub> and  
751 GzmB<sup>+</sup>CD8<sup>+</sup> T<sub>CYT</sub>, CD69<sup>+</sup>IFN- $\gamma$ <sup>+</sup>TNF $\alpha$ <sup>+</sup>CD4<sup>+</sup> T<sub>EFF</sub> cells and CD69<sup>+</sup>IFN- $\gamma$ <sup>+</sup>TNF $\alpha$ <sup>+</sup>CD8<sup>+</sup> T<sub>EFF</sub> cells, and  
752 CXCR5<sup>+</sup>CD4<sup>+</sup> T<sub>FH</sub> cells with protection induced by combined Spike, NSP-2, NSP-14, and  
753 Nucleoprotein-based mRNA/LNP vaccine.

754 Although the present study demonstrated a cross-protective efficacy of combined mRNA/LNP  
755 vaccine against multiple VOCs, there remain multiple limitations and gaps of knowledge that still

756 need to be addressed. First, the protective efficacy was examined a short time after vaccination (i.e.,  
757 3 to 5 weeks). Ongoing experiments will compare the durability of the protection induced by the  
758 combined Spike, NSP-2, NSP-14, and Nucleoprotein-based mRNA/LNP vaccine vs. Spike  
759 mRNA/LNP vaccine alone at longer intervals (i.e., 3 months, 6 months, and 12 months) after booster  
760 immunization and the results will be the subject of a future report. Since the combined vaccine  
761 induced strong NSP-2, NSP-14, and Nucleoprotein-specific CXCR5<sup>+</sup>CD4<sup>+</sup> T<sub>FH</sub> cell responses,  
762 protection is expected to sustain longer compared to Spike-alone mRNA/LNP vaccine. Second, the  
763 protective efficacy of the combined vaccine was studied in immunologically naïve hamsters.  
764 However, given that the majority of the human population already received one to four doses of the  
765 first generation of Spike-based COVID-19 vaccine and/or already infected at least with one SARS-  
766 CoV-2 variant or subvariant, ongoing animal experiments are modeling these human scenarios, by  
767 studying the protective efficacy of the combined mRNA/LNP vaccine in hamsters with pre-existing  
768 Spike- or SARS-CoV-2-specific immunity<sup>46</sup>. Third, since the highly conserved antigens NSP-2, NSP-  
769 14, and Nucleoprotein contain regions of high homology between SARS-CoV-2 and Common Cold  
770 Coronaviruses, the role of cross-reactive T cells induced by the combined mRNA/LNP vaccine is  
771 also being investigated in animals that are first infected with one of the four major Common Cold  
772 Coronaviruses (i.e., α-CCC-229E, α-CCC-NL63, β-CCC-HKU1 or β-CCC-OC43 strains). Fourth,  
773 since the combined mRNA/LNP vaccine substantially reduced viral load in the upper respiratory  
774 tract, it remains to be determined whether the combined vaccine will also reduce the transmission<sup>11</sup>.  
775 This major gap is being addressed in ongoing experiments in which we will determine whether the  
776 hamsters that received the combined mRNA/LNP vaccine will exhibit a reduction in transmission of  
777 Omicron variants and sub-variants to mock-vaccinated cage mates<sup>11</sup>. Fifth, this report shows that  
778 the combined Spike, NSP-2, NSP-14 and Nucleoprotein-based mRNA/LNP vaccine elicited lung-  
779 resident antigen-specific GzmB<sup>+</sup>CD4<sup>+</sup> T<sub>CYT</sub> and GzmB<sup>+</sup>CD8<sup>+</sup> T<sub>CYT</sub>, CD69<sup>+</sup>IFN-γ<sup>+</sup>TNFα<sup>+</sup>CD4<sup>+</sup> T<sub>EFF</sub> cells  
780 and CD69<sup>+</sup>IFN-γ<sup>+</sup>TNFα<sup>+</sup>CD8<sup>+</sup> T<sub>EFF</sub> cells that may have contributed to eliminating lungs-infected  
781 epithelial cells and interfered locally with virus replication in the lungs. This agrees with reports  
782 showing cross-reactive memory CD4<sup>+</sup> and CD8<sup>+</sup> T cells alone (without antibodies) may have  
783 protected SARS-CoV-2 infected patients with B-cell depletion from severe disease<sup>77,78</sup> and with non-

784 human primates studied that showed that SARS-CoV-2-specific T cells reduced viral loads in  
785 macaques<sup>79</sup>. However, these might not be the only underlying immune mechanisms of the observed  
786 cross-protection. Because immunological reagents and mAbs are limited in the hamster model, a  
787 better understanding of B- and T-cell mechanisms of protection induced by the combined  
788 mRNA/LNP vaccine is underway in the ACE2/HLA triple transgenic mouse model, including  
789 dissection of early protein expression, antigen presentation, and stimulation of the innate and  
790 inflammatory response. T cell depletion.

791

792 Despite these gaps and limitations, this pre-clinical study in the hamster model presents  
793 pathological, virological, and immunological evidence that: (i) Compared to the Spike mRNA/LNP  
794 vaccine alone, a combined Spike, NSP-2, NSP-14, and Nucleoprotein-based mRNA/LNP vaccine  
795 induced stronger and broader protection against infection and disease caused by various VOCs,  
796 including the ancestral wild-type Washington variant, the highly pathogenic Delta variant, and the  
797 highly transmittable and heavily Spike-mutated Omicron sub-variants; and (ii) Observed protection  
798 induced by the combined vaccine was associated with induction of both Spike-specific neutralizing  
799 antibodies and NSP-2, NSP-14, and Nucleoprotein-specific lung-resident NSP-2- NSP-14- and  
800 Nucleoprotein-specific T follicular helper (T<sub>FH</sub>) cells, cytotoxic T cells (T<sub>CYT</sub>), effector T cells (T<sub>EFF</sub>).  
801 Given that the mRNA-LNP platform has been clinically proven in large human populations, we expect  
802 our combined Spike, NSP-2, NSP-14, and Nucleoprotein-based mRNA/LNP pan-Coronavirus  
803 vaccine approach to be rapidly adapted and move to clinical testing against emerging and re-  
804 emerging heavily Spike-mutated variants and sub-variants.

805

## ACKNOWLEDGMENTS

806

807           The authors would like to thank the UC Irvine Center for Clinical Research (CCR) and the  
808 Institute for Clinical & Translational Science (ICTS) for providing human blood samples and  
809 nasopharyngeal swab samples used in this study—a special thanks to Dr. Alessandro Ghigi and Dr.  
810 Kai Zheng for providing patients' clinical information. Dr. Donald N. Forthal, Dr. Garry Landucci,  
811 Izabela Coimbra Ibrahim, Lauren Hitchcock, and Christine Tafoya for support with the BSL3 facility.  
812 We also thank those from TechImmune LLC, Gavin S. Herbert, James H Cavanaugh, Rick Haugen,  
813 Christine Dwight, Scott Whitcup, and Nathan Wheeler who contributed directly or indirectly to this  
814 COVID-19 project and for their continued support for the pan-Coronavirus vaccine project at UC  
815 Irvine. Dr. Steven A. Goldstein, Dr. Michael J. Stamos, Dr. Suzanne B. Sandmeyer, Jim Mazzo, Dr.  
816 Daniela Bota, Janice Briggs, Marge Brannon, Beverley Alberola, Jessica Sheldon, Rosie Magallon,  
817 and Andria Pontello who contributed indirectly to this COVID-19 project.

818           Funding and Conflict of interest: These studies were supported in part by Public Health  
819 Service Research grants AI158060, AI150091, AI143348, AI147499, AI143326, AI138764,  
820 AI124911, and AI110902 from the National Institutes of Allergy and Infectious Diseases (NIAID) to  
821 LBM and by R43AI174383 to TechImmune, LLC. LBM has an equity interest in TechImmune, LLC.,  
822 a company that may potentially benefit from the research results and serves on the company's  
823 Scientific Advisory Board. LBM's relationship with TechImmune, LLC., has been reviewed and  
824 approved by the University of California, Irvine by its conflict-of-interest policies.



825

## MATERIALS & METHODS

826

***Human study population cohort and HLA genotyping:*** Between January 2020 and

827 December 2023, over 1100 unvaccinated patients with mild to severe COVID-19 were enrolled at

828 the University of California Irvine Medical Center, under an approved Institutional Review Board–

829 approved protocol (IRB#-2020-5779). Written informed consent was obtained from all patients

830 before inclusion. SARS-CoV-2 positivity was defined by a positive RT-PCR on a respiratory tract

831 sample. The unvaccinated COVID-19 patients were enrolled throughout the pandemic irrespective

832 of SARS-CoV-2 variants of concern they are exposed to: The ancestral Washington variant

833 (WA1/2020), alpha, beta, gamma, the highly pathogenic Delta variant (B.1.617.2), or the omicron

834 subvariants B.1.1.529, BA.2.86, XBB1.5, EG.5, HV.1, and JN.1. Patients were genotyped by PCR

835 for class I HLA-A\*02:01 and class II HLA-DRB1\*01:01: and ended up with 147 that were HLA-

836 A\*02:01<sup>+</sup> or/and HLA-DRB1\*01:01<sup>+</sup>. The average days between the report of their first symptoms

837 and the blood sample drawing was ~5 days. The 147 patients were from mixed ethnicities (Hispanic

838 (28%), Hispanic Latino (22%), Asian (16%), Caucasian (13%), mixed Afro-American and Hispanic

839 (8%), Afro-American (5%), mixed Afro-American and Caucasian (2%), Native Hawaiian and Other

840 Pacific Islander descent (1%). Six percent of the patients did not reveal their race/ethnicity (**Table**

841 **2**). Following patient discharge, they were divided into groups by medical practitioners depending on

842 the severity of their symptoms and their intensive care unit (ICU) and intubation (mechanical

843 ventilation) status. The following scoring criteria were used: Severity 5: patients who died from

844 COVID-19 complications; Severity 4: infected COVID-19 patients with severe disease who were

845 admitted to the intensive care unit (ICU) and required ventilation support; Severity 3: infected

846 COVID-19 patients with severe disease that required enrollment in ICU, but without ventilation

847 support; Severity 2: infected COVID-19 patients with moderate symptoms that involved a regular

848 hospital admission; Severity 1: infected COVID-19 patients with mild symptoms; and Severity 0:

849 infected individuals with no symptoms. Subsequently, we used 15 liquid-nitrogen frozen PBMCs

850 samples (blood collected pre-COVID-19 in 2018) from HLA-A\*02:01<sup>+</sup>/HLA-DRB1\*01:01<sup>+</sup> unexposed

851 pre-pandemic healthy individuals– 8 males, 7 females; median age: 54 (20-76) as controls.

852 **Peptide synthesis:** Peptide-epitopes from twelve SARS-CoV-2 proteins, including 16 9-mer  
853 long CD8<sup>+</sup> T cell epitopes (ORF1ab<sub>84-92</sub>, ORF1ab<sub>1675-1683</sub>, ORF1ab<sub>2210-2218</sub>, ORF1ab<sub>2363-2371</sub>,  
854 ORF1ab<sub>3013-3021</sub>, ORF1ab<sub>3183-3191</sub>, ORF1ab<sub>3732-3740</sub>, ORF1ab<sub>4283-4291</sub>, ORF1ab<sub>5470-5478</sub>, ORF1ab<sub>6419-6427</sub>,  
855 ORF1ab<sub>6749-6757</sub>, E<sub>20-28</sub>, E<sub>26-34</sub>, M<sub>52-60</sub>, M<sub>89-97</sub>, and ORF7b<sub>26-34</sub>) and 13 13-mer long CD4<sup>+</sup> T cell  
856 epitopes (ORF1a<sub>1350-1365</sub>, ORF1a<sub>1801-1815</sub>, ORF1ab<sub>5019-5033</sub>, ORF1ab<sub>6088-6102</sub>, ORF1ab<sub>6420-6434</sub>, E<sub>20-34</sub>,  
857 E<sub>26-40</sub>, M<sub>176-190</sub>, ORF7a<sub>1-15</sub>, ORF7a<sub>3-17</sub>, ORF7a<sub>98-112</sub>, ORF7b<sub>8-22</sub>, and N<sub>388-403</sub>) that we formerly  
858 identified were selected as described previously<sup>5</sup>. The Epitope Conservancy Analysis tool was used  
859 to compute the degree of identity of CD8<sup>+</sup> T cell and CD4<sup>+</sup> T cell epitopes within a given protein  
860 sequence of SARS-CoV-2 set at 100% identity level<sup>5</sup>. Peptides were synthesized (21<sup>st</sup> Century  
861 Biochemicals, Inc, Marlborough, MA) and the purity of peptides determined by both reversed-phase  
862 high-performance liquid chromatography and mass spectroscopy was over 95%.

863 **Human Peripheral Blood Mononuclear Cells and T cell Stimulation:** Peripheral blood  
864 mononuclear cells (PBMCs) from COVID-19 patients were isolated from the blood using Ficoll (GE  
865 Healthcare) density gradient media and transferred into 96-well plates at a concentration of 2.5 ×  
866 10<sup>6</sup> viable cells per ml in 200µl (0.5 × 10<sup>6</sup> cells per well) of RPMI-1640 media (Hyclone)  
867 supplemented with 10% (v/v) FBS (HyClone), Sodium Pyruvate (Lonza), L-Glutamine, Nonessential  
868 Amino Acids, and antibiotics (Corning). A fraction of the blood was kept separated to perform HLA  
869 genotyping of only the HLA-A\*02:01 and DRB1\*01:01 positive individuals. Subsequently, cells were  
870 stimulated with 10 µg/ml of each one of the 29 individual T cell peptide-epitopes (16 CD8<sup>+</sup> T cell  
871 peptides and 13 CD4<sup>+</sup> T cell peptides) and incubated in a humidified chamber with 5% CO<sub>2</sub> at 37°C.  
872 Post-incubation, cells were stained for flow cytometry, or transferred in IFN-γ ELISpot plates  
873 (**Supplemental Fig. S1A**). The same isolation protocol was followed for HD samples obtained in  
874 2018. Ficoll was kept frozen in liquid nitrogen in FBS DMSO 10%; after thawing, HD PBMCs were  
875 stimulated similarly for the IFN-γ ELISpot technique.

876 **Human ELISpot assay:** We assessed CD4<sup>+</sup> and CD8<sup>+</sup> T-cell response against conserved  
877 SARS-CoV-2-derived class-II restricted epitopes by IFN-γ ELISpot in COVID-19 patients  
878 representing different disease severity categories (**Table 2** and **Supplemental Fig. S1A**). All

879 ELISpot reagents were filtered through a 0.22 µm filter. Wells of 96-well Multiscreen HTS Plates  
880 (Millipore, Billerica, MA) were pre-wet with 30% ethanol for 60 seconds and then coated with 100 µl  
881 primary anti-IFN-γ antibody solution (10 µg/ml of 1-D1K coating antibody from Mabtech, Cincinnati,  
882 OH) OVN at 4°C. After washing, the plate was blocked with 200 µl of RPMI media plus 10% (v/v)  
883 FBS for two hours at room temperature to prevent nonspecific binding. Twenty-four hours following  
884 the blockade, the peptide-stimulated cells from the patient's PBMCs ( $0.5 \times 10^6$  cells/well) were  
885 transferred into the ELISpot-coated plates. PHA-stimulated or non-stimulated cells (DMSO) were  
886 used as positive or negative controls of T cell activation, respectively. Upon incubation in a  
887 humidified chamber with 5% CO<sub>2</sub> at 37°C for an additional 48 hours, cells were washed using PBS  
888 and PBS-Tween 0.02% solution. Next, 100 µl of biotinylated secondary anti-IFN-γ antibody (1 µg/ml,  
889 clone 7-B6-1, Mabtech) in blocking buffer (PBS 0.5% FBS) was added to each well. After a two-hour  
890 incubation and wash, wells were incubated with 100 µl of HRP-conjugated streptavidin (1:1000) for  
891 1 hour at room temperature. Lastly, wells were incubated for 15-30 minutes with 100 µl of TMB  
892 detection reagent at room temperature, and spots were counted both manually and by an  
893 automated ELISpot reader counter (ImmunoSpot Reader, Cellular Technology, Shaker Heights,  
894 OH).

895 **Flow cytometry analysis:** Surface markers detection and flow cytometry analysis were  
896 performed on 147 patients after 72 hours of stimulation with each SARS-CoV-2 class-I or class-II  
897 restricted peptide, and PBMCs ( $0.5 \times 10^6$  cells) were stained. First, the cells were stained with a  
898 live/dead fixable dye (Zombie Red dye, 1/800 dilution – BioLegend, San Diego, CA) for 20 minutes  
899 at room temperature, to exclude dying/apoptotic cells. Cells were then stained for 45 minutes at  
900 room temperature with five different HLA-A\*02\*01 restricted tetramers and/or five HLA-DRB1\*01:01  
901 restricted tetramers (PE-labelled) specific toward the SARS-CoV-2 CD8<sup>+</sup> T cell epitopes Orf1ab<sub>2210-  
902 2218</sub>, and Orf1ab<sub>4283-4291</sub> and the CD4<sup>+</sup> T cell epitopes ORF1a<sub>1350-1365</sub>, E<sub>26-40</sub>, and M<sub>176-190</sub> respectively  
903 (**Supplemental Fig. S1A**). Cells were alternatively stained with the EBV BMLF-1<sub>280-288</sub>-specific  
904 tetramer for control of specificity. We stained HLA-A\*02\*01- HLA-DRB1\*01:01-negative patients  
905 with our 10 tetramers as a negative control aiming to assess tetramers staining specificity.

906 Subsequently, we used anti-human antibodies for surface-marker staining: anti-CD45 (BV785, clone  
907 HI30 – BioLegend), anti-CD3 (Alexa700, clone OKT3 – BioLegend), anti-CD4 (BUV395, clone SK3  
908 – BD), anti-CD8 (BV510, clone SK1 – BioLegend), anti-TIGIT (PercP-Cy5.5, clone A15153G –  
909 BioLegend), anti-TIM-3 (BV 711, clone F38-2E2 – BioLegend), anti-PD1 (PE-Cy7, clone EH12.1 –  
910 BD), anti-CTLA-4 (APC, clone BNI3 – BioLegend), anti-CD137 (APC-Cy-7, clone 4B4-1 –  
911 BioLegend) and anti-CD134 (BV650, clone ACT35 – BD). mAbs against these various cell markers  
912 were added to the cells in phosphate-buffered saline (PBS) containing 1% FBS and 0.1% sodium  
913 azide (fluorescence-activated cell sorter [FACS] buffer) and incubated for 30 minutes at 4°C.  
914 Subsequently, cells were washed twice with FACS buffer and fixed with 4% paraformaldehyde  
915 (PFA, Affymetrix, Santa Clara, CA). A total of ~200,000 lymphocyte-gated PBMCs (140,000 alive  
916 CD45<sup>+</sup>) were acquired by Fortessa X20 (Becton Dickinson, Mountain View, CA) and analyzed using  
917 FlowJo software (TreeStar, Ashland, OR). The gating strategy is detailed in **Supplemental Fig.**  
918 **S1B.**

919 **Viruses:** SARS-CoV-2 viruses specific to six variants, namely (i) SARS-CoV-2-  
920 USA/WA/2020 (Batch Number: G2027B); (v) Delta (B.1.617.2) (isolate h-CoV-19/USA/MA29189;  
921 Batch number: G87167), and Omicron (XBB1.5) (isolate h-CoV-19/USA/FL17829; Batch number:  
922 G76172) were procured from Microbiologics (St. Cloud, MN). The initial batches of viral stocks were  
923 propagated to generate high-titer virus stocks. Vero E6 (ATCC-CRL1586) cells were used for this  
924 purpose. Procedures were completed after appropriate safety training was obtained using an aseptic  
925 technique under BSL-3 containment.

926 **TaqMan quantitative polymerase reaction assay:** We used a laboratory-developed  
927 modification of the CDC SARS-CoV-2 RT-PCR assay for the screening of SARS-CoV-2 Variants in  
928 COVID-19 patients, which received Emergency Use Authorization by the FDA on April 17<sup>th</sup>, 2020.  
929 (<https://www.fda.gov/media/137424/download> [accessed 24 March 2021]).

930 Briefly, 5 ml of the total nucleic acid eluate was added to a 20-ml total-volume reaction  
931 mixture (1x TaqPath 1-Step RT-qPCR Master Mix, CG; Thermo Fisher Scientific, Waltham, MA),  
932 with 0.9 mM each primer and 0.2 mM each probe). RT-PCR was carried out using the ABI

933 StepOnePlus thermocycler (Life Technologies, Grand Island, NY). The S-N501Y, S-E484K, and S-  
934 L452R assays were carried out under the following running conditions: 25°C for 2 minutes, then  
935 50°C for 15 minutes, followed by 10 minutes at 95°C and 45 cycles of 95°C for 15 seconds and  
936 65°C for 1 minute. The  $\Delta_{69-70} / \Delta_{242-244}$  assays were run under the following conditions: 25°C for 2  
937 minutes, then 50°C for 15 minutes, followed by 10 minutes at 95°C and 45 cycles of 95°C for 15  
938 seconds and 60°C for 1 minute. Samples displaying typical amplification curves above the threshold  
939 were considered positive. Samples that yielded a negative result or results in the S- $\Delta_{69-70} / \Delta_{242-}$   
940 244 assays or were positive for S-501Y P2, S-484K P2, and S-452R P2 were considered screen  
941 positive and assigned to VOCs.

942 **Human Enzyme-linked immunosorbent assay (ELISA):** Serum antibodies specific for  
943 epitope peptides and SARS-CoV-2 proteins were detected by ELISA. We used 96-well plates  
944 (Dyner Technologies, Chantilly, VA) and coated them with 0.5  $\mu$ g peptides, 100 ng S or N protein  
945 per well at 4°C overnight, respectively, and then washed three times with PBS and blocked with 3%  
946 BSA (in 0.1% PBST) for 2 hours at 37°C. After blocking, the plates were incubated with serial  
947 dilutions of the sera (100  $\mu$ l/well, in two-fold dilution) for 2 hours at 37°C. The bound serum  
948 antibodies were detected with HRP-conjugated goat anti-mouse IgG and chromogenic substrate  
949 TMB (ThermoFisher, Waltham, MA). The cut-off for seropositivity was set as the mean value plus  
950 three standard deviations (3SD) in HbC-S control sera. The binding of the epitopes to the sera of  
951 SARS-CoV-2 infected samples was detected by ELISA using the same procedure; 96-well plates  
952 were coated with 0.5  $\mu$ g peptides, and sera were diluted at 1:50.

953 **Data and Code Availability:** Human-specific SARS-CoV-2 complete genome sequences  
954 were retrieved from the GISAID database, whereas the SARS-CoV-2 sequences for bats, pangolin,  
955 civet cats, and camels were retrieved from the NCBI GenBank. Genome sequences of previous  
956 strains of SARS-CoV for humans (B.1.177, B.1.160, B.1.1.7, B.1.351, P.1, B.1.427/B.1.429, B.1.258,  
957 B.1.221, B.1.367, B.1.1.277, B.1.1.302, B.1.525, B.1.526, S:677H.Robin1, S:677P.Pelican,  
958 B.1.617.1, B.1.617.2, B.1.1,529) and common cold SARS-CoV strains (SARS-CoV-2-Wuhan-Hu-1  
959 (MN908947.3), SARS-CoV-Urbani (AY278741.1), HKU1-Genotype B (AY884001), CoV-OC43

960 (KF923903), CoV-NL63 (NC\_005831), CoV-229E (KY983587)) and MERS (NC\_019843)), bats  
961 (RATG13 (MN996532.2), ZXC21 (MG772934.1), YN01 (EPI\_ISL\_412976), YN02(EPI\_ISL\_412977),  
962 WIV16 (KT444582.1), WIV1 (KF367457.1), YNLF\_31C (KP886808.1), Rs672 (FJ588686.1)),  
963 pangolin (GX-P2V (MT072864.1), GX-P5E (MT040336.1), GX-P5L (MT040335.1), GX-P1E  
964 (MT040334.1), GX-P4L (MT040333.1), GX-P3B (MT072865.1), MP789 (MT121216.1), Guangdong-  
965 P2S (EPI\_ISL\_410544)), civet cats (Civet007, A022, B039)), and camels (KT368891.1,  
966 MN514967.1, KF917527.1, NC\_028752.1) were retrieved from the NCBI GenBank.

967 ***mRNA synthesis and LNP formulation:*** Sequences of Spike and 10 T cell non-Spike  
968 antigens were derived from the SARS-CoV-2 Omicron sub-variant BA.2 (NCBI GenBank accession  
969 number OM617939) Nucleoside-modified mRNAs expressing SARS-CoV-2 full-length of prefusion-  
970 stabilized Spike protein with two or 6 proline mutations (mRNA-S-2P and mRNA-S-6P (Size: 3804  
971 bp, Nucleotide Range: 21504 bp - 25308 bp)) and part or full-length ten highly conserved non-Spike  
972 T cell antigens (NSP-2 (Size: 1914 bp, Nucleotide Range: 540 bp - 2454 bp), NSP-3 (Size: 4485 bp,  
973 Nucleotide Range: 3804 bp - 8289 bp), NSP-4 (Size: 1500 bp, Nucleotide Range: 8290 bp - 9790  
974 bp), NSP-5-10 (Size: 3378 bp, Nucleotide Range: 9791 bp - 13169 bp), NSP-12 (Size: 2796 bp,  
975 Nucleotide Range: 13170 bp - 15966 bp), NSP-14 (Size: 1581 bp, Nucleotide Range: 17766 bp -  
976 19347 bp), ORF7a/b (Size: 492 bp, Nucleotide Range: 27327 bp - 27819 bp), Membrane (Size: 666  
977 bp, Nucleotide Range: 26455 bp - 27121 bp), Envelope (Size: 225 bp, Nucleotide Range: 26177 bp  
978 - 26402 bp), and Nucleoprotein (Size: 1248 bp, Nucleotide Range: 28206 bp - 29454 bp) were  
979 synthesized by *in vitro* transcription using T7 RNA polymerase (MegaScript, Thermo Fisher  
980 Scientific, Waltham, MA) on linearized plasmid templates, as previously reported<sup>36</sup>. Modified mRNA  
981 transcript with full substitution of Pseudo-U was synthesized by TriLink Biotechnologies using  
982 proprietary CleanCap® technology. The synthesized polyadenylated (80A) mRNAs were subjected  
983 to DNase and phosphatase treatment, followed by Silica membrane purification. Finally, the  
984 synthesized mRNA was packaged as a  $1.00 \pm 6\%$  mg/mL solution in 1 mM Sodium Citrate, pH 6.4.  
985 Purified mRNAs were analyzed by agarose gel electrophoresis and were kept frozen at  $-20^{\circ}\text{C}$ . The  
986 mRNAs were formulated into LNPs using an ethanolic lipid mixture of ionizable cationic lipid and an

987 aqueous buffer system. Formulated mRNA-LNPs were prepared according to RNA concentrations  
988 (1 µg/µl) and were stored at –80°C for animal immunizations.

989 **Confirmation of protein expression by mRNAs.** The expression of target viral protein by  
990 the vaccines was confirmed in HEK293T [American Type Culture Collection (ATCC), CRL-3216]  
991 cells before testing in animal experiments and plated 10<sup>6</sup> cells in 500 µl culture medium in a 6-well  
992 plate on Day 0. Once the cells reached confluency, HEK293T cells in six-well plates were directly  
993 transfected with 2 µg of mRNA-LNP or only transfected with LNP. A transfection mix for mRNA was  
994 prepared and cells were transfected as described by the Lipofectamine™ MessengerMAX™  
995 Transfection Reagent -specific protocol (Thermo Fisher Scientific, Catalog # LMRNA001).

996 **Hamster immunization and SARS-CoV-2 variants challenge:** The mRNA/LNP vaccines  
997 were evaluated in the outbred golden Syrian hamster model for protection against three SARS-CoV-  
998 2 variants and subvariants (Washington, Delta, and Omicron). The Institutional Animal Care and  
999 Use Committee approved animal model usage experiments at the University of California, Irvine  
1000 (Protocol number AUP-22-086). The recommendations in the Guide for the Care and Use of  
1001 Laboratory Animals of the National Institutes of Health performed animal experiments. The sample  
1002 size for each animal study ( $n = 5$  per group) was calculated by power analysis, demonstrating that 5  
1003 hamsters per group were enough to produce significant results with a power > 80%. Animals were  
1004 randomly assigned to each group, and the study design was not blinded to researchers and animal  
1005 facility staff.

1006 For variants and subvariants (Washington, Delta, and Omicron challenge, four groups of 6-  
1007 to 8-week-old female golden Syrian hamsters (5 per group), strain HsdHan: AURA (Envigo, catalog  
1008 no. 8901M), were vaccinated intramuscularly with individual or combined mRNA/LNP (1 µg, 5 µg, or  
1009 10 µg per dose as indicated in Figures) on day 0 (prime) and day 21 (boost). Hamsters that received  
1010 phosphate-buffered saline alone were used as mock-immunized controls (*Saline, Mock, n = 5*). The  
1011 mRNA/LNP vaccines and saline control were administered in 100 µl per injection. Serum samples  
1012 were collected from all hamsters before the viral challenge to measure vaccine-induced neutralizing  
1013 antibodies. Three weeks after booster vaccination (week 6), hamsters were transferred to the ABSL-

1014 3 facility and intranasally challenged with the SARS-CoV-2 Delta variant ( $1 \times 10^5$  pfu) or Washington  
1015 or Omicron strain ( $2 \times 10^5$  pfu; World Reference Center for Emerging Viruses and Arboviruses). At  
1016 the indicated time points, nasal wash samples and equivalent portions of the lung tissues were  
1017 collected for various analyses of vaccine-induced protection. Hamster body weights were monitored  
1018 daily to evaluate vaccine-induced protection from body weight loss.

1019 **Enzyme-linked Immunosorbent Assay (ELISA):** Vaccine-induced Spike IgG was  
1020 measured in serum samples by ELISA. 96-well plates (F8 MAXISORP LOOSE NUNC-IMMUNO  
1021 MODULES, 469949, Thermo Scientific) were coated with 100 ng/well of SARS-CoV-2 (2019-nCoV)  
1022 Spike S1 + S2 ECD-His-Recombinant Protein (40589-V08B1, Sino Biological) overnight at 4°C.  
1023 Plates were washed three times with 1X PBS (5 min each time) and then blocked with blocking  
1024 buffer [3% fetal bovine serum (FBS) in Dulbecco's PBS (DPBS)] for 1 hour at room temperature,  
1025 followed by washing and incubation at 4°C overnight with serially diluted serum samples (initial  
1026 dilution, 1:20; 1:5 serial dilution) in blocking buffer at 100  $\mu$ l per well. The following day, plates were  
1027 rewashed and incubated with HRP-conjugated goat anti-hamster IgG (H+L) secondary antibody  
1028 (HA6007; Invitrogen; 1:1500) for 1 hour at room temperature. After the final wash, plates were  
1029 developed using TMB 1-Component Peroxidase Substrate (Thermo Fisher Scientific), followed by  
1030 reaction termination using the TMB stop solution (Thermo Fisher Scientific). Plates were read at 450  
1031 nm wavelength within 10 minutes using a Microplate Reader (Bio-RAD).

1032 **Neutralizing assay:** Serum neutralizing activity was examined, as previously reported in <sup>51</sup>,  
1033 <sup>80</sup>. Briefly, the assays were performed with Vero E6 cells (ATCC, CRL-1586) using the SARS-CoV-2  
1034 wild-type or Delta strains. Briefly, serum samples were heat-inactivated and three-fold serially  
1035 diluted (initial dilution, 1:10), followed by incubation with 100 pfu of wild-type SARS-CoV-2 (USA-  
1036 WA1/2020) or the Delta strain for 1 hour at 37°C. The serum-virus mixtures were placed onto Vero  
1037 E6 cell monolayer in 96-well plates for incubation for 1 hour at 37°C. The plates were washed with  
1038 DMEM, and the monolayer cells were overlaid with 200  $\mu$ l minimum essential medium (MEM)  
1039 containing 1% (w/v) of methylcellulose, 2% FBS, and 1% penicillin-streptomycin. Cells were then  
1040 incubated for 24 hours at 37°C. Vero E6 monolayers were washed with PBS and fixed with 250  $\mu$ l of



1041 pre-chilled 4% formaldehyde for 30 min at room temperature, followed by aspiration removal of the  
1042 formaldehyde solution and twice PBS wash. The cells were permeabilized using 0.3% (wt/vol)  
1043 hydrogen peroxide in water. The cells were blocked using 5% non-fat dried milk followed by the  
1044 addition of 100  $\mu$ l/well of diluted anti-SARS-CoV-2 antibody (1:1000) to all wells on the microplates  
1045 for 1-2 hours at RT. This was followed by the addition of diluted anti-rabbit IgG conjugate (1/2,000)  
1046 for 1 hour at RT. The plate was washed and developed by the addition of TrueBlue substrate, and  
1047 the foci were counted using an ImmunoSpot analyzer. Each serum sample was tested in duplicates.

1048 ***RNA extraction and RT-PCR quantification of viral RNA copies:*** RNA was extracted from  
1049 the lung tissues (mice and hamsters) and nasal washes (hamsters) using the TRIzol LS Reagent  
1050 (Thermo Fisher Scientific) according to the manufacturer's instructions. The concentration and purity  
1051 of the extracted RNAs were determined using NanoDrop. To quantify SARS-CoV-2 viral RNA  
1052 copies, RT-PCR was performed using the PowerUP SYBR Green Kit (Thermo Fisher) and the  
1053 QuantStudio 5 Real-Time PCR Detection System (Thermo Fisher). The Throat Swab sample was  
1054 analyzed for SARS-CoV-2-specific RNA by quantitative RT-PCR (qRT-PCR). As recommended by  
1055 the Centers for Disease Control and Prevention (CDC), we used ORF1ab-specific primers (forward:  
1056 5'-CCCTG TGGGTTTTACTTAA-3' and reverse: 5'-ACGATTGTGCATCAGCTGA-3') to detect  
1057 the viral RNA level. PCR reactions (10  $\mu$  l) contained primers (10  $\mu$  M), cDNA sample (1.5  $\mu$  l),  
1058 SYBR Green reaction mix (5  $\mu$  l), and molecular grade water (2.5  $\mu$  l). PCR cycling conditions were  
1059 as follows: 95°C for 3 min, 45 cycles of 95°C for 5 s, and 60°C for 30 s. For each RT-PCR, a  
1060 standard curve was included using an RNA standard (Armored RNA Quant<sup>®</sup>) to quantify the  
1061 absolute copies of viral RNA in the throat swabs.

1062 ***Lung histopathology:*** Hamster lungs were preserved in 10% neutral buffered formalin for  
1063 48 hours before being transferred to 70% ethanol. The tissue sections were embedded in paraffin  
1064 blocks and sectioned at 8-mm thickness. Slides were deparaffinized and rehydrated before staining  
1065 for H&E for routine immunopathology.

1066           **Statistical analysis:** Statistical analysis was performed using the GraphPad Prism 10.0  
1067 software (GraphPad Software, La Jolla, CA). Nonparametric tests were used throughout this paper  
1068 for statistical analysis. Data were expressed as the mean  $\pm$  SD. Comparison among groups was  
1069 performed using the Mann-Whitney test (two groups). Two-tailed *P* values were denoted, and *P*  
1070 values <0.05 were considered significant.

1071

## FIGURE LEGENDS

1072

1073 **Figure 1. Highly conserved non-spike, structural, non-structural, and accessory**  
1074 **protein antigens identified in the SARS-CoV-2 genome: (A)** Bioinformatic analysis and alignment  
1075 of the 29903 bp single strand RNA of 8.7 million genome sequences of SARS-CoV-2 strains that  
1076 circulated worldwide over the last 4 years, including 20 VOCs; SARS-CoV; MERS-CoV; common  
1077 cold Coronaviruses; and twenty-five animal's SARS-like Coronaviruses (SL-CoVs) genome  
1078 sequences isolated from bats (*Rhinolophus affinis*, *Rhinolophus malayanus*), pangolins (*Manis*  
1079 *javanica*), civet cats (*Paguma larvata*), and camels (*Camelus dromedaries*). Shown in light green are  
1080 5 highly conserved regions identified from the SARS-CoV-2 genome sequences. **(B)** Depicts 10  
1081 highly conserved non-Spike antigens that comprise 3 structural (Membrane, Envelope, and  
1082 Nucleoprotein), 12 non-structural (NSP-2, NSP-3, NSP-4, NSP-5-10, NSP-12, and NSP-14) and 1  
1083 accessory protein (ORF7a/b) as T cell antigens (*top*) and Spike as the B cell antigen (*bottom*) used  
1084 to construct the individual and combined mRNA/LNP vaccines. **(C)** Illustrates the individual and  
1085 combined mRNA/LNP vaccines that consist of modified mRNAs expressing the B and T cell antigens  
1086 encapsulated in lipid nanoparticles (LNPs), as detailed in *Materials & Methods*, and delivery  
1087 intramuscularly in the outbred golden Syrian hamsters.

1088 **Figure 2. IFN- $\gamma$ -producing CD4<sup>+</sup> and CD8<sup>+</sup> T cell responses to highly conserved**  
1089 **antigens in unvaccinated COVID-19 patients with various degrees of disease severity: (A)**  
1090 Illustrate a positive correlation between the severity of COVID-19 and the magnitude of SARS-CoV-  
1091 2 common antigens -specific CD4<sup>+</sup> and CD8<sup>+</sup> T cell responses in 71 COVID-19 patients. COVID-19  
1092 patients ( $n = 71$ ) are divided into six groups based on disease severity scored 0 to 5, as described  
1093 in *Materials and Methods*, and as identified by six colors on a grayscale (Black = severity 5, to white  
1094 = severity 0). PBMCs from HLA-DR- and HLA-A\*0201-positive COVID-19 patients ( $n = 71$ ) were  
1095 isolated and stimulated for a total of 72 hours with 10 $\mu$ g/ml of each of the previously identified. The  
1096 magnitude of CD4<sup>+</sup> and CD8<sup>+</sup> T cell responses specific to **(B)** CD4<sup>+</sup> and CD8<sup>+</sup> T cell epitopes from  
1097 all the ten selected conserved antigens, **(C)** the 13 individual cross-reactive CD4<sup>+</sup> T cell epitope  
1098 peptides; and **(D)** the 16 individual cross-reactive CD8<sup>+</sup> T cell epitopes that belong to the selected 10

1099 highly conserved antigens (i.e., NSP-2, NSP-3, NSP-4, NSP-5-10, NSP-12, NSP-14, ORF7a/b,  
1100 Membrane, Envelope, and Nucleoprotein) are shown. The number of IFN- $\gamma$ -producing CD8<sup>+</sup> T cells  
1101 was quantified in each of the 71 patients using ELISpot assay. Shown are the average/mean  
1102 numbers ( $\pm$  SD) of IFN- $\gamma$ -spot forming cells (SFCs) after CD4<sup>+</sup> T cell peptide stimulation detected in  
1103 each of the 71 COVID-19 patients divided into six groups based on disease severity scored 0 to 5. A  
1104 mean SFCs between 25 and 50 SFCs corresponds to a medium/intermediate response, whereas a  
1105 strong response is defined for mean SFCs > 50 per  $0.5 \times 10^6$  stimulated PBMCs. PHA was used as  
1106 a positive control of T-cell activation. Unstimulated negative control SFCs (DMSO – no peptide  
1107 stimulation) were subtracted from the SFC counts of peptides-stimulated cells. Shown is the  
1108 correlation between the overall number of (C) IFN- $\gamma$ -producing CD4<sup>+</sup> T cells induced by each of the  
1109 14 cross-reactive CD4<sup>+</sup> T cell epitope peptides; and (D) IFN- $\gamma$ -producing CD8<sup>+</sup> T cells induced by  
1110 each of the 16 cross-reactive CD8<sup>+</sup> T cell epitope peptides in each of the six groups of COVID-19  
1111 patients with various disease severity. For all graphs: the coefficient of determination ( $R^2$ ) is  
1112 calculated from the Pearson correlation coefficients  $\otimes$ . The associated  $P$ -value and the slope ( $S$ ) of  
1113 the best-fitted line (dotted line) are calculated by linear regression analysis is indicated. The gray-  
1114 hatched boxes in the correlation graphs extend from the 25<sup>th</sup> to 75<sup>th</sup> percentiles (hinges of the plots)  
1115 with the median represented as a horizontal line in each box and the extremity of the vertical bars  
1116 showing the minimum and maximum values. Results are representative of two independent  
1117 experiments and were considered statistically significant at  $P \leq 0.05$  using either the Mann-Whitney  
1118 test (two groups) or the Kruskal-Wallis test (more than two groups).

1119 **Figure 3. Screening of 10 highly conserved T cell antigens for protection against the**  
1120 **highly pathogenic Delta variant (B.1.617.2) in golden Syrian hamsters:** (A) Omicron sub-variant  
1121 BA.2.75-based sequences of 10 highly conserved non-Spike T-cell antigens (i.e., NSP-2, NSP-3,  
1122 NSP-4, NSP-5-10, NSP-12, NSP-14, ORF7a/b, Membrane, Envelope, and Nucleoprotein) are used  
1123 to construct methyl-pseudouridine–modified (m<sup>1</sup> $\Psi$ ) mRNA and capped using CleanCap technology  
1124 <sup>81</sup>. Modified mRNAs expressing the prefusion Spike proteins, stabilized by either two (Spike 2P) or  
1125 six (Spike 6P) prolines, were expressed as B cell antigens <sup>37, 38</sup>. The 12 modified mRNAs were then  
1126 encapsulated in lipid nanoparticles (LNPs) as the delivery system. (B) Experimental plan to screen

1127 the vaccine efficacy of the 10 highly conserved T-cell Ags. Female hamsters ( $n = 5$  per group) were  
1128 immunized intramuscularly twice on day 0 (prime) and day 21 (boost) with 1  $\mu\text{g}/\text{dose}$  or 10  $\mu\text{g}/\text{dose}$   
1129 of the mRNA/LNP-based Coronavirus vaccine expressing each of the 10 highly conserved non-  
1130 Spike T-cell antigens. Hamsters that received phosphate-buffered saline alone were used as mock-  
1131 immunized controls (*Saline, Mock, n = 5*). Three weeks after booster vaccination (day 42),  
1132 vaccinated and mock-vaccinated hamsters were intranasally challenged (both nostrils) with  $1 \times 10^5$   
1133 pfu of SARS-CoV-2 highly pathogenic Delta variant (B.1.617.2). Weight losses were assessed for  
1134 14- or 24-days post-challenge. **(C)** Shows percent weight change for 14 days post-challenge  
1135 normalized to the initial body weight on the day of infection in hamsters immunized with mRNA/LNP  
1136 expressing Spike 2P and Spike 6P. **(D)** Shows percent weight change for 14 days post-challenge  
1137 normalized to the initial body weight on the day of infection in hamsters immunized with mRNA/LNP  
1138 expressing individual NSP-2, NSP-3, NSP-4, NSP-5-10, NSP-12, NSP-14, ORF7a/b, Membrane,  
1139 Envelope, and Nucleoprotein at 1  $\mu\text{g}/\text{dose}$  or 10  $\mu\text{g}/\text{dose}$ . The dashed line indicates the 100%  
1140 starting body weight. The arrows indicate the first-day post-challenge when the weight loss is  
1141 reversed in T cell antigen (*back arrow*), Spike (*grey arrow*), and mock (*red arrow*) vaccinated  
1142 hamsters. The data represent two independent experiments; the graphed values and bars represent  
1143 the SD between the two experiments. The Mann-Whitney test (two groups) or the Kruskal-Wallis test  
1144 (more than two groups) were used for statistical analysis. ns  $P > 0.05$ , \*  $P < 0.05$ , \*\*  $P < 0.01$ , \*\*\*  $P <$   
1145 0.001, \*\*\*\*  $P < 0.0001$ .

1146 **Figure 4. Protection against the highly pathogenic Delta variant (B.1.617.2) induced by**  
1147 **individual NSP-2, NSP-14, and Nucleoprotein T cell antigen-based mRNA/LNP vaccines in**  
1148 **golden Syrian hamsters:** **(A)** Illustrates the three mRNA/LNP vaccines that consist of highly  
1149 conserved T-cell Ags, NSP-2, NSP-14, and Nucleoprotein expressed as nucleoside-modified mRNA  
1150 sequences derived from BA.2.75 Omicron sub-variant (BA2) and encapsulated in lipid nanoparticles  
1151 (LNP). **(B)** Experimental plan to screen the vaccine efficacy of the 10 highly conserved T-cell Ags  
1152 (i.e., NSP-2, NSP-3, NSP-4, NSP-5-10, NSP-12, NSP-14, ORF7a/b, Membrane, Envelope, and  
1153 Nucleoprotein). Female hamsters ( $n = 5$  per group) were immunized intramuscularly twice on day 0

1154 (prime) and day 21 (boost) with each mRNA/LNP-based Coronavirus vaccine expressing each of the  
1155 10 highly conserved non-Spike T-cell antigens. Hamsters that received phosphate-buffered saline  
1156 alone were used as mock-immunized controls (*Saline, Mock, n = 5*). Three weeks after booster  
1157 vaccination (day 42), vaccinated and mock-vaccinated hamsters were intranasally challenged (both  
1158 nostrils) with  $1 \times 10^5$  pfu of SARS-CoV-2 highly pathogenic Delta variant (B.1.617.2). COVID-19-like  
1159 symptoms, lung pathology, weight loss, and virus load were assessed for 14 days post-challenge.  
1160 **(C)** Representative H & E staining images of lung pathology at day 14 p.i. of SARS-CoV-2 infected  
1161 hamsters mock vaccinated or vaccinated with three protective NSP-2, NSP-14, and Nucleoprotein-  
1162 based mRNA/LNP vaccines at 4x magnifications. Fourteen days post-challenge, the lung tissues  
1163 were collected and fixed, and 5- $\mu$ m sections were cut from hamsters and stained with hematoxylin  
1164 and eosin. The lung of mock-vaccinated hamsters demonstrates many bronchi with bronchiolitis  
1165 (*arrows*) and adjacent marked interstitial pneumonia (*asteria*). Lungs of hamsters immunized with  
1166 NSP2, NSP-14, or NP mRNA/LNP show few bronchiolitis (*arrow*) and normal bronchial, bronchiolar,  
1167 and alveolar architecture. Scale bars, 1 mm. **(D)** Shows percent weight change for 14 days post-  
1168 challenge normalized to the initial body weight on the day of infection. The dashed line indicates the  
1169 100% starting body weight. The arrows indicate the first-day post-challenge when the weight loss is  
1170 reversed in T cell antigen (*back arrow*) and mock (*red arrow*) vaccinated hamsters. **(E)** Two- and 6  
1171 days post-infection (p.i.), viral loads were analyzed, to evaluate vaccine-induced protection against  
1172 virus replication, by comparing viral RNA copies in the hamster's throats and lungs between mock  
1173 and vaccine groups. Viral RNA copies were quantified by RT-PCR and expressed as  $\log_{10}$  copies  
1174 per milligram of throat or lung tissue. The graphs show a comparison of viral titers in the hamster  
1175 lungs between vaccinated vs. mock-vaccinated hamsters. The data represent two independent  
1176 experiments; the graphed values and bars represent the SD between the two experiments. The  
1177 Mann-Whitney test (two groups) or the Kruskal-Wallis test (more than two groups) were used for  
1178 statistical analysis. ns  $P > 0.05$ , \*  $P < 0.05$ , \*\*  $P < 0.01$ , \*\*\*  $P < 0.001$ , \*\*\*\*  $P < 0.0001$ .

1179 **Figure 5. Protection against multiple SARS-CoV-2 variants and sub-variants of**  
1180 **concern induced by combined NSP-2, NSP-14, and Nucleoprotein-based mRNA/LNP vaccine**  
1181 **in the hamster model:** **(A)** Illustrates the combination of three vaccines that consist of highly

1182 conserved protective T-cell Ags, NSP-2, NSP-14, and Nucleoprotein expressed as nucleoside-  
1183 modified mRNA sequences derived from BA.2.75 Omicron sub-variant (BA2) and encapsulated in  
1184 lipid nanoparticles (LNP). **(B)** Hamster experimental design and timeline to study the vaccine  
1185 efficacy in golden Syrian hamsters of 10 individual T cell antigen-based mRNA/LNP vaccines on  
1186 COVID-19-like symptoms detected. Female hamsters were immunized intramuscularly twice on day  
1187 0 (prime) and day 21 (boost) with the combined NSP-2, NSP-14, and Nucleoprotein-based  
1188 mRNA/LNP vaccine ( $n = 15$  per group) or mock-vaccinated (*Mock*,  $n = 15$  per group). Three weeks  
1189 after booster vaccination (day 42), vaccinated and mock-vaccinated hamsters were intranasally  
1190 challenged (both nostrils) with,  $2 \times 10^5$  pfu of the wild-type Washington variant (WA1/2020),  $1 \times 10^5$   
1191 pfu of the highly pathogenic Delta variant (B.1.617.2) or  $2 \times 10^5$  pfu of the highly transmissible  
1192 Omicron sub-variant (XBB1.5). COVID-19-like symptoms, lung pathology, weight loss, and virus load  
1193 were assessed for 14 days post-challenge. **(C)** Representative H & E staining images of lung  
1194 pathology at day 14 p.i. of SARS-CoV-2 infected hamsters mock vaccinated or vaccinated with the  
1195 combined NSP-2, NSP-14, and Nucleoprotein-based mRNA/LNP vaccines at 4x magnifications.  
1196 Fourteen days post-challenge, the lung tissues were collected and fixed, and 5- $\mu$ m sections were cut  
1197 from hamsters and stained with hematoxylin and eosin. The lung of mock-vaccinated hamsters  
1198 demonstrates many bronchi with bronchiolitis (*arrows*) and adjacent marked interstitial pneumonia  
1199 (*asteria*). Lungs of hamsters that received combined T cell antigens mRNA/LNP vaccine  
1200 demonstrate mostly normal bronchial, bronchiolar, and alveolar architecture. Scale bars, 1 mm. **(D)**  
1201 Shows percent weight change for 14 days post-challenge normalized to the initial body weight on  
1202 the day of infection for each variant and sub-variant. The dashed line indicates the 100% starting  
1203 body weight. The arrows indicate the first-day post-challenge when the weight loss is reversed in T  
1204 cell antigen (*back arrow*), Spike (*grey arrow*), and mock (*red arrow*) vaccinated hamsters. **(E)** Two-  
1205 and 6-days post-infection (p.i.) with the wild-type Washington variant (WA1/2020), the highly  
1206 pathogenic Delta variant (B.1.617.2), or the highly transmissible Omicron sub-variant (XBB1.5), viral  
1207 loads were analyzed, to evaluate vaccine-induced protection against virus replication, by comparing  
1208 viral RNA copies in the hamster's throats and lungs between mock and vaccine groups. Viral RNA  
1209 copies were quantified by RT-PCR and expressed as  $\log_{10}$  copies per milligram of throat or lung

1210 tissue. The graphs show a comparison of viral titers in the hamster lungs between vaccinated vs.  
1211 mock-vaccinated hamsters. Viral titration data showing viral RNA copy number in the throats of  
1212 vaccinated vs. mock-vaccinated hamsters detected at days 2 and 6 post-challenge. The data  
1213 represent two independent experiments; the graphed values and bars represent the SD between the  
1214 two experiments. The Mann-Whitney test (two groups) or the Kruskal-Wallis test (more than two  
1215 groups) were used for statistical analysis. ns  $P > 0.05$ , \*  $P < 0.05$ , \*\*  $P < 0.01$ , \*\*\*  $P < 0.001$ , \*\*\*\*  $P <$   
1216 0.0001.

1217 **Figure 6. Protection induced by combined Spike, NSP-2, NSP-14, and Nucleoprotein-**  
1218 **based mRNA/LNP vaccine against the highly pathogenic Delta variant (B.1.617.2): (A)**  
1219 Illustrates combined Spike, NSP-2, NSP-14, and Nucleoprotein-based mRNA/LNP vaccine that  
1220 consists of Spike mRNA/LNP vaccine combined to highly conserved protective T-cell Ags, NSP-2,  
1221 NSP-14, and Nucleoprotein mRNA/LNP vaccines. All sequences are derived from BA.2.75 Omicron  
1222 sub-variant (BA2). **(B)** Transfection of Spike, NSP-2, NSP-14, and Nucleoprotein mRNA and protein  
1223 expression *in vitro* in the human epithelial HEK293T cells. **(C)** Hamster experimental design and  
1224 timeline to study the beneficial effect in golden Syrian hamsters of adding the Spike mRNA/LNP  
1225 vaccine to the combined NSP-2, NSP-14, and Nucleoprotein-based mRNA/LNP vaccine on the  
1226 protection against the highly pathogenic Delta variant (B.1.617.2). Female hamsters were immunized  
1227 intramuscularly twice on day 0 (prime) and day 21 (boost) with the combined Spike, NSP-2, NSP-14,  
1228 and Nucleoprotein-based mRNA/LNP vaccine (1  $\mu\text{g}/\text{dose}$ ,  $n = 5$  per group), the Spike mRNA/LNP  
1229 vaccine alone (1  $\mu\text{g}/\text{dose}$ ,  $n = 5$  per group), or mock-vaccinated ( $n = 5$  per group). Three weeks after  
1230 booster vaccination (day 42), vaccinated and mock-vaccinated hamsters were intranasally  
1231 challenged (both nostrils) vaccinated and mock-vaccinated hamsters were subsequently intranasally  
1232 challenged (both nostrils) with  $1 \times 10^5$  pfu of the highly pathogenic Delta variant (B.1.617.2). COVID-  
1233 19-like symptoms, lung pathology, weight loss, and virus load were assessed for 14 days post-  
1234 challenge. **(D)** Shows percent weight change for 14 days post-challenge normalized to the initial  
1235 body weight on the day of infection with the highly pathogenic Delta variant (B.1.617.2). The dashed  
1236 line indicates the 100% starting body weight. **(E)** Six days post-infection (p.i.), with the highly



1237 pathogenic Delta variant (B.1.617.2), the viral loads were analyzed, to evaluate vaccine-induced  
1238 protection against virus replication, by comparing viral RNA copies in the hamster's throats and lungs  
1239 between mock and vaccine groups. Viral RNA copies were quantified by RT-PCR and expressed as  
1240  $\log_{10}$  copies per milligram of throat or lung tissue. The graphs show a comparison of viral titers in the  
1241 hamster lungs between vaccinated vs. mock-vaccinated hamsters. The data represent two  
1242 independent experiments; the graphed values and bars represent the SD between the two  
1243 experiments. The Mann-Whitney test (two groups) or the Kruskal-Wallis test (more than two groups)  
1244 were used for statistical analysis. ns  $P > 0.05$ , \*  $P < 0.05$ , \*\*  $P < 0.01$ , \*\*\*  $P < 0.001$ , \*\*\*\*  $P < 0.0001$ .

1245 **Figure 7. Protection induced by the combined Spike, NSP-2, NSP-14, and**  
1246 **Nucleoprotein-based mRNA/LNP vaccine against the wild-type Washington variant**  
1247 **(WA1/2020) and the highly transmissible Omicron sub-variant (XBB1.5). (A)** Illustrates  
1248 combined Spike, NSP-2, NSP-14, and Nucleoprotein-based mRNA/LNP vaccine. **(B and C)** Shows  
1249 percent weight change for 14 days post-challenge normalized to the initial body weight on the day of  
1250 challenge with the wild-type Washington variant (WA1/2020) at  $2 \times 10^5$  pfu/hamster and the highly  
1251 transmissible Omicron sub-variant (XBB1.5) at  $2 \times 10^5$  pfu/hamster, respectively. The dashed line  
1252 indicates the 100% starting body weight. The arrows indicate the first-day post-challenge when the  
1253 weight loss is reversed in T cell antigen (*back arrow*), Spike (*grey arrow*), and mock (*red arrow*)  
1254 vaccinated hamsters. **(D)** Representative H & E staining images of lung pathology at day 14 p.i. of  
1255 SARS-CoV-2 infected hamsters mock vaccinated or vaccinated with the combined Spike, NSP-2,  
1256 NSP-14, and Nucleoprotein-based mRNA/LNP vaccine (1  $\mu\text{g}/\text{dose}$ ), or the Spike mRNA/LNP  
1257 vaccine alone (1  $\mu\text{g}/\text{dose}$ ) at 4x magnifications. Hamster lung histopathology is shown. Fourteen  
1258 days post-challenge, the lung tissues were collected and fixed, and 5- $\mu\text{m}$  sections were cut from  
1259 hamsters and stained with hematoxylin and eosin. The lung of mock-immunized hamsters  
1260 demonstrates many bronchi with bronchiolitis (*arrows*) and adjacent marked interstitial pneumonia  
1261 (*asteria*). Lungs of hamsters immunized with Spike mRNA/LNP alone show peri bronchiolitis (*arrow*),  
1262 perivascularitis (*asterisk*), and multifocal interstitial pneumonia. Lungs of hamsters that received a  
1263 combination Spike mRNA/LNP vaccine and combined T cell antigens mRNA/LNP vaccine  
1264 demonstrate mostly normal bronchial, bronchiolar (*arrows*), and alveolar architecture. Scale bars, 1

1265 mm. **(E and F)** Viral titration data showing viral RNA copy number in the throats of vaccinated vs.  
1266 mock-vaccinated hamsters detected at days 2 and 6 post-challenge with the wild-type Washington  
1267 variant (WA1/2020) and the highly transmissible Omicron sub-variant (XBB1.5), respectively. The  
1268 data represent two independent experiments; the graphed values and bars represent the SD  
1269 between the two experiments. The Mann-Whitney test (two groups) or the Kruskal-Wallis test (more  
1270 than two groups) were used for statistical analysis. ns  $P > 0.05$ , \*  $P < 0.05$ , \*\*  $P < 0.01$ , \*\*\*  $P < 0.001$ ,  
1271 \*\*\*\*  $P < 0.0001$ .

1272 **Figure 8. Lungs-resident antigen-specific functional CD4<sup>+</sup> T and CD8<sup>+</sup> T cells induced**  
1273 **by the combined NSP-2, NSP-14, and Nucleoprotein-based mRNA/LNP vaccines in the**  
1274 **hamsters:** The panel shows average frequencies of functional CD4<sup>+</sup> and CD8<sup>+</sup> T cells in the lungs  
1275 of hamsters vaccinated with the combined NSP-2, NSP-14, and Nucleoprotein-based mRNA/LNP  
1276 vaccines. The graphs depict the differences in the percentage of **(A)** NSP-2-specific, **(B)** NSP-14-  
1277 specific, **(C)** nucleoprotein- and **(D)** Spike-specific CD4<sup>+</sup> and CD8<sup>+</sup> cells present in the lungs of non-  
1278 protected mock-vaccinated hamsters and lungs of protected spike-alone-mRNA/LNP and combined  
1279 Spike, NSP-2, NSP-14, and Nucleoprotein-based mRNA/LNP vaccinated hamsters. Bars represent  
1280 the means  $\pm$  SEM. ANOVA test was used to analyze the data. **(E) Top Panel:** Graph showing the  
1281 IgG level among hamsters vaccinated with a combination of NSP-2, NSP-14, and Nucleoprotein-  
1282 based mRNA/LNP vaccines, spike alone vaccine, and mock vaccination. **Bottom Panel:**  
1283 Neutralization assay data among the vaccinated and mock-vaccinated groups showing vaccine-  
1284 induced serum-neutralizing activities. Comparison of the neutralizing antibodies induced by the  
1285 combination of Spike mRNA/LNP vaccine and highly conserved protective T-cell Ags, NSP-2, NSP-  
1286 14, and Nucleoprotein expressed as nucleoside-modified mRNA sequences derived from BA.2.75  
1287 Omicron sub-variant (BA2) and encapsulated in lipid nanoparticles (LNP). The data represent two  
1288 independent experiments; the graphed values and bars represent the SD between the two  
1289 experiments. Data are presented as median and IQR where appropriate. Data were analyzed by  
1290 multiple t-tests. Results were considered statistically significant at  $P < 0.05$ . The Mann-Whitney test  
1291 (two groups) or the Kruskal-Wallis test (more than two groups) were used for statistical analysis. ns  
1292  $P > 0.05$ , \*  $P < 0.05$ , \*\*  $P < 0.01$ , \*\*\*  $P < 0.001$ , \*\*\*\*  $P < 0.0001$ .

1293            **Supplemental Figure S1: Experimental plan and gating strategy:** (A) shows the  
1294 experimental plan followed for the flow-cytometry experiments and the ELISpot experiments  
1295 presented in **Fig. 2**, starting with the COVID-19 blood samples collection, patient genotyping,  
1296 PBMCs extraction, and peptide stimulation. (B) shows the gating strategy applied when analyzing  
1297 the flow cytometry data presented in **Fig. 8**.

## REFERENCES

1298

1299

- 1300 1. Prakash, S. *et al.* Cross-Protection Induced by Highly Conserved Human B, CD4 (+,) and  
1301 CD8 (+) T Cell Epitopes-Based Coronavirus Vaccine Against Severe Infection, Disease, and  
1302 Death Caused by Multiple SARS-CoV-2 Variants of Concern. *Frontiers In Immunology* **29**,  
1303 45-56 (2024).
- 1304 2. Dhanushkodi, N.R. *et al.* Anti-Viral and Anti-Inflammatory Therapeutic Effect of RAGE-Ig  
1305 Protein Against Multiple SARS-CoV-2 Variants of Concern Demonstrated in K18-hACE2  
1306 Mouse and Syrian Golden Hamster Models. *J Immunol* **212**, 1-10 (2024).
- 1307  
1308 3. Zayou, L. *et al.* A multi-epitope/CXCL11 prime/pull coronavirus mucosal vaccine boosts the  
1309 frequency and the function of lung-resident memory CD4(+) and CD8(+) T cells and  
1310 enhanced protection against COVID-19-like symptoms and death caused by SARS-CoV-2  
1311 infection. *J Virol* **97**, 1-13 (2023).
- 1312  
1313 4. Evans, J.P. & Liu, S.L. Challenges and Prospects in Developing Future SARS-CoV-2  
1314 Vaccines: Overcoming Original Antigenic Sin and Inducing Broadly Neutralizing Antibodies. *J*  
1315 *Immunol* **211**, 1459-1467 (2023).
- 1316  
1317 5. Prakash, S. *et al.* Genome-Wide B Cell, CD4(+), and CD8(+) T Cell Epitopes That Are Highly  
1318 Conserved between Human and Animal Coronaviruses, Identified from SARS-CoV-2 as  
1319 Targets for Preemptive Pan-Coronavirus Vaccines. *J Immunol* **206**, 2566-2582 (2021).
- 1320  
1321 6. Pedersen, S.F. & Ho, Y.C. SARS-CoV-2: A Storm is Raging. *J Clin Invest* (2020).
- 1322  
1323 7. Bellocchi, M.C. *et al.* Frequency of Atypical Mutations in the Spike Glycoprotein in SARS-  
1324 CoV-2 Circulating from July 2020 to July 2022 in Central Italy: A Refined Analysis by Next  
1325 Generation Sequencing. *Viruses* **15** (2023).
- 1326  
1327 8. Washington, N.L. *et al.* Emergence and rapid transmission of SARS-CoV-2 B.1.1.7 in the  
1328 United States. *Cell* **184**, 2587-2594 e2587 (2021).
- 1329  
1330 9. Konings, F. *et al.* SARS-CoV-2 Variants of Interest and Concern naming scheme conducive  
1331 for global discourse. *Nat Microbiol* **6**, 821-823 (2021).
- 1332  
1333 10. The, L. The COVID-19 pandemic in 2023: far from over. *Lancet* **401**, 79 (2023).
- 1334  
1335 11. Sharma, S. *et al.* Updated vaccine protects against SARS-CoV-2 variants including Omicron  
1336 (B.1.1.529) and prevents transmission in hamsters. *Nat Commun* **13**, 6644 (2022).
- 1337  
1338 12. Kumar, S., Thambiraja, T.S., Karuppanan, K. & Subramaniam, G. Omicron and Delta variant  
1339 of SARS-CoV-2: A comparative computational study of spike protein. *J Med Virol* **94**, 1641-  
1340 1649 (2022).
- 1341

- 1342  
1343 13. Cevik, M., Grubaugh, N.D., Iwasaki, A. & Openshaw, P. COVID-19 vaccines: Keeping pace  
1344 with SARS-CoV-2 variants. *Cell* **184**, 5077-5081 (2021).
- 1345  
1346 14. Yisimayi, A. *et al.* Repeated Omicron exposures override ancestral SARS-CoV-2 immune  
1347 imprinting. *Nature* (2023).
- 1348  
1349 15. Renner, T.M. *et al.* Tuning the immune response: sulfated archaeal glycolipid archaeosomes  
1350 as an effective vaccine adjuvant for induction of humoral and cell-mediated immunity towards  
1351 the SARS-CoV-2 Omicron variant of concern. *Front Immunol* **14**, 1182556 (2023).
- 1352  
1353 16. Ma, Q. *et al.* SARS-CoV-2 bivalent mRNA vaccine with broad protection against variants of  
1354 concern. *Front Immunol* **14**, 1195299 (2023).
- 1355  
1356 17. Rubin, E.J., Baden, L.R., Marks, P. & Morrissey, S. Audio Interview: The FDA and Covid-19  
1357 Vaccines. *The New England journal of medicine* **387**, e60 (2022).
- 1358  
1359 18. Chowell, G. & Mizumoto, K. The COVID-19 pandemic in the USA: what might we expect?  
1360 *Lancet* **395**, 1093-1094 (2020).
- 1361  
1362 19. Park, T. *et al.* Vaccines against SARS-CoV-2 variants and future pandemics. *Expert Rev*  
1363 *Vaccines* **21**, 1363-1376 (2022).
- 1364  
1365 20. Nelde, A. *et al.* SARS-CoV-2-derived peptides define heterologous and COVID-19-induced T  
1366 cell recognition. *Nat Immunol* **22**, 74-85 (2021).
- 1367  
1368 21. Peng, Y. *et al.* Broad and strong memory CD4(+) and CD8(+) T cells induced by SARS-CoV-  
1369 2 in UK convalescent individuals following COVID-19. *Nat Immunol* **21**, 1336-1345 (2020).
- 1370  
1371 22. Schub, D. *et al.* High levels of SARS-CoV-2-specific T cells with restricted functionality in  
1372 severe courses of COVID-19. *JCI insight* **5**, e142167 (2020).
- 1373  
1374 23. Sette, A. & Crotty, S. Adaptive immunity to SARS-CoV-2 and COVID-19. *Cell* **184**, 861-880  
1375 (2021).
- 1376  
1377 24. Rydzynski Moderbacher, C. *et al.* Antigen-Specific Adaptive Immunity to SARS-CoV-2 in  
1378 Acute COVID-19 and Associations with Age and Disease Severity. *Cell* **183**, 996-1012 e1019  
1379 (2020).
- 1380  
1381 25. Brand, I. *et al.* Broad T Cell Targeting of Structural Proteins After SARS-CoV-2 Infection:  
1382 High Throughput Assessment of T Cell Reactivity Using an Automated Interferon Gamma  
1383 Release Assay. *Front Immunol* **12**, 688436 (2021).
- 1384  
1385 26. Bange, E.M. *et al.* CD8(+) T cells contribute to survival in patients with COVID-19 and  
1386 hematologic cancer. *Nat Med* **27**, 1280-1289 (2021).

- 1387  
1388 27. Zhao, J. *et al.* Airway Memory CD4(+) T Cells Mediate Protective Immunity against Emerging  
1389 Respiratory Coronaviruses. *Immunity* **44**, 1379-1391 (2016).
- 1390  
1391 28. Swadling, L. *et al.* Pre-existing polymerase-specific T cells expand in abortive seronegative  
1392 SARS-CoV-2. *Nature* **601**, 110-117 (2022).
- 1393  
1394 29. Diniz, M.O. *et al.* Airway-resident T cells from unexposed individuals cross-recognize SARS-  
1395 CoV-2. *Nat Immunol* **23**, 1324-1329 (2022).
- 1396  
1397 30. Kundu, R. *et al.* Cross-reactive memory T cells associate with protection against SARS-CoV-  
1398 2 infection in COVID-19 contacts. *Nat Commun* **13**, 80 (2022).
- 1399  
1400 31. Mitsi, E. *et al.* Respiratory mucosal immune memory to SARS-CoV-2 after infection and  
1401 vaccination. *Nat Commun* **14**, 6815 (2023).
- 1402  
1403 32. Yan, L. *et al.* Architecture of a SARS-CoV-2 mini replication and transcription complex. *Nat*  
1404 *Commun* **11**, 5874 (2020).
- 1405  
1406 33. Finkel, Y. *et al.* The coding capacity of SARS-CoV-2. *Nature* **589**, 125-130 (2021).
- 1407  
1408 34. Mateus, J. *et al.* Selective and cross-reactive SARS-CoV-2 T cell epitopes in unexposed  
1409 humans. *Science* **370**, 89-94 (2020).
- 1410  
1411 35. Primard, C. *et al.* OVX033, a nucleocapsid-based vaccine candidate, provides broad-  
1412 spectrum protection against SARS-CoV-2 variants in a hamster challenge model. *Front*  
1413 *Immunol* **14**, 1188605 (2023).
- 1414  
1415 36. Pardi, N., Muramatsu, H., Weissman, D. & Kariko, K. In vitro transcription of long RNA  
1416 containing modified nucleosides. *Methods Mol Biol* **969**, 29-42 (2013).
- 1417  
1418 37. Zhang, Y. *et al.* A highly efficacious live attenuated mumps virus-based SARS-CoV-2  
1419 vaccine candidate expressing a six-proline stabilized prefusion spike. *Proc Natl Acad Sci U S*  
1420 *A* **119**, e2201616119 (2022).
- 1421  
1422 38. Lu, M. *et al.* SARS-CoV-2 prefusion spike protein stabilized by six rather than two prolines is  
1423 more potent for inducing antibodies that neutralize viral variants of concern. *Proc Natl Acad*  
1424 *Sci U S A* **119**, e2110105119 (2022).
- 1425  
1426 39. Maier, M.A. *et al.* Biodegradable lipids enabling rapidly eliminated lipid nanoparticles for  
1427 systemic delivery of RNAi therapeutics. *Mol Ther* **21**, 1570-1578 (2013).
- 1428  
1429 40. Sia, S.F. *et al.* Pathogenesis and transmission of SARS-CoV-2 in golden hamsters. *Nature*  
1430 **583**, 834-838 (2020).

- 1431  
1432 41. Imai, M. *et al.* Syrian hamsters as a small animal model for SARS-CoV-2 infection and  
1433 countermeasure development. *Proc Natl Acad Sci U S A* **117**, 16587-16595 (2020).
- 1434  
1435 42. Dowall, S. *et al.* Development of a Hamster Natural Transmission Model of SARS-CoV-2  
1436 Infection. *Viruses* **13** (2021).
- 1437  
1438 43. Monchatre-Leroy, E. *et al.* Hamster and ferret experimental infection with intranasal low dose  
1439 of a single strain of SARS-CoV-2. *J Gen Virol* **102** (2021).
- 1440  
1441 44. Chu, H., Chan, J.F. & Yuen, K.Y. Animal models in SARS-CoV-2 research. *Nat Methods* **19**,  
1442 392-394 (2022).
- 1443  
1444 45. Hajnik, R.L. *et al.* Dual spike and nucleocapsid mRNA vaccination confer protection against  
1445 SARS-CoV-2 Omicron and Delta variants in preclinical models. *Science translational*  
1446 *medicine* **14**, eabq1945 (2022).
- 1447  
1448 46. Murray, S.M. *et al.* The impact of pre-existing cross-reactive immunity on SARS-CoV-2  
1449 infection and vaccine responses. *Nat Rev Immunol* **23**, 304-316 (2023).
- 1450  
1451 47. Desmecht, S. *et al.* Kinetics and Persistence of the Cellular and Humoral Immune  
1452 Responses to BNT162b2 mRNA Vaccine in SARS-CoV-2-Naive and -Experienced Subjects:  
1453 Impact of Booster Dose and Breakthrough Infections. *Front Immunol* **13**, 863554 (2022).
- 1454  
1455 48. Liu, H. *et al.* Development of optimized drug-like small molecule inhibitors of the SARS-CoV-  
1456 2 3CL protease for treatment of COVID-19. *Nat Commun* **13**, 1891 (2022).
- 1457  
1458 49. Vabret, N. *et al.* Immunology of COVID-19: Current State of the Science. *Immunity* **52**, 910-  
1459 941 (2020).
- 1460  
1461 50. Weisblum, Y. *et al.* Escape from neutralizing antibodies by SARS-CoV-2 spike protein  
1462 variants. *Elife* **9** (2020).
- 1463  
1464 51. Xie, X. *et al.* Neutralization of SARS-CoV-2 spike 69/70 deletion, E484K and N501Y variants  
1465 by BNT162b2 vaccine-elicited sera. *Nat Med* **27**, 620-621 (2021).
- 1466  
1467 52. Matchett, W.E. *et al.* Cutting Edge: Nucleocapsid Vaccine Elicits Spike-Independent SARS-  
1468 CoV-2 Protective Immunity. *J Immunol* **207**, 376-379 (2021).
- 1469  
1470 53. Mooij, P. *et al.* Poxvirus MVA Expressing SARS-CoV-2 S Protein Induces Robust Immunity  
1471 and Protects Rhesus Macaques From SARS-CoV-2. *Front Immunol* **13**, 845887 (2022).
- 1472  
1473 54. Boudewijns, R. *et al.* MVA-CoV2-S Vaccine Candidate Neutralizes Distinct Variants of  
1474 Concern and Protects Against SARS-CoV-2 Infection in Hamsters. *Front Immunol* **13**,  
1475 845969 (2022).

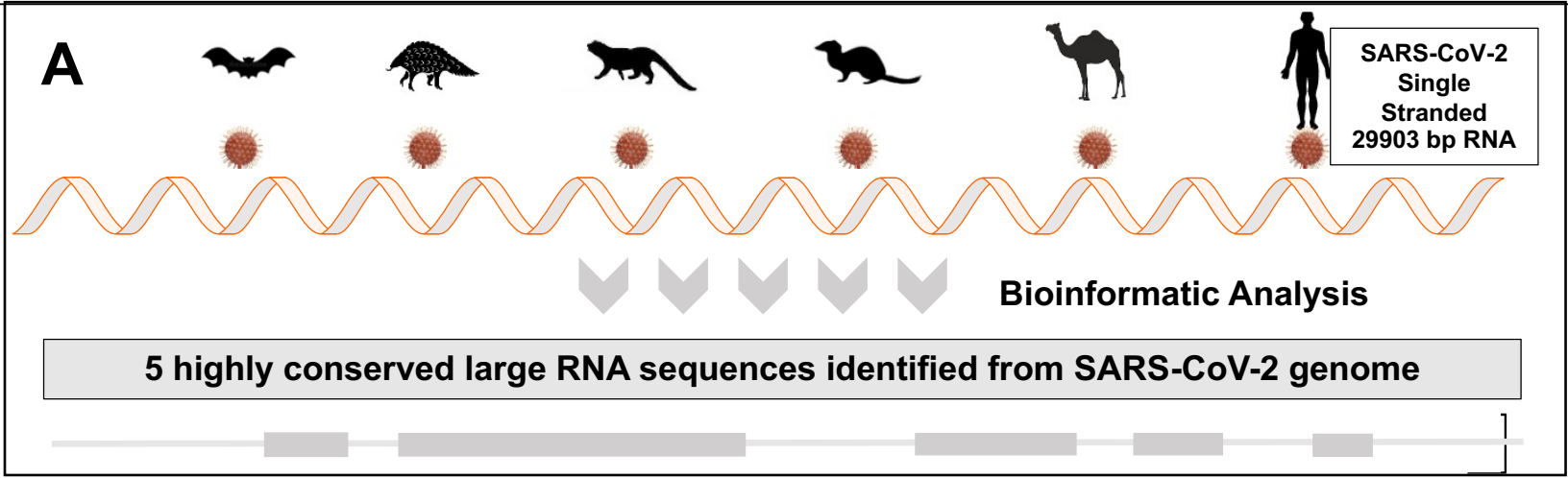
- 1476  
1477 55. Americo, J.L., Cotter, C.A., Earl, P.L., Liu, R. & Moss, B. Intranasal inoculation of an MVA-  
1478 based vaccine induces IgA and protects the respiratory tract of hACE2 mice from SARS-  
1479 CoV-2 infection. *Proc Natl Acad Sci U S A* **119**, e2202069119 (2022).
- 1480  
1481 56. Abdelnabi, R. *et al.* Optimized vaccine candidate MVA-S(3P) fully protects against SARS-  
1482 CoV-2 infection in hamsters. *Front Immunol* **14**, 1163159 (2023).
- 1483  
1484 57. Doll, T.A. *et al.* Optimizing the design of protein nanoparticles as carriers for vaccine  
1485 applications. *Nanomedicine* **11**, 1705-1713 (2015).
- 1486  
1487 58. Breitfeld, D. *et al.* Follicular B helper T cells express CXC chemokine receptor 5, localize to B  
1488 cell follicles, and support immunoglobulin production. *J Exp Med* **192**, 1545-1552 (2000).
- 1489  
1490 59. Noto, A. *et al.* CXCL12 and CXCL13 Cytokine Serum Levels Are Associated with the  
1491 Magnitude and the Quality of SARS-CoV-2 Humoral Responses. *Viruses* **14** (2022).
- 1492  
1493 60. Yuzefpolskiy, Y. *et al.* Cutting Edge: Effect of Disease-Modifying Therapies on SARS-CoV-2  
1494 Vaccine-Induced Immune Responses in Multiple Sclerosis Patients. *J Immunol* **208**, 1519-  
1495 1524 (2022).
- 1496  
1497 61. Almendro-Vazquez, P., Laguna-Goya, R. & Paz-Artal, E. Defending against SARS-CoV-2:  
1498 The T cell perspective. *Front Immunol* **14**, 1107803 (2023).
- 1499  
1500 62. Vanderheiden, A. *et al.* Type I and Type III Interferons Restrict SARS-CoV-2 Infection of  
1501 Human Airway Epithelial Cultures. *J Virol* **94** (2020).
- 1502  
1503 63. Ruby, J., Bluethmann, H. & Peschon, J.J. Antiviral activity of tumor necrosis factor (TNF) is  
1504 mediated via p55 and p75 TNF receptors. *J Exp Med* **186**, 1591-1596 (1997).
- 1505  
1506 64. Lin, J. *et al.* Longitudinal Assessment of SARS-CoV-2-Specific T Cell Cytokine-Producing  
1507 Responses for 1 Year Reveals Persistence of Multicytokine Proliferative Responses, with  
1508 Greater Immunity Associated with Disease Severity. *J Virol* **96**, e0050922 (2022).
- 1509  
1510 65. Boppana, S. *et al.* SARS-CoV-2-specific circulating T follicular helper cells correlate with  
1511 neutralizing antibodies and increase during early convalescence. *PLoS Pathog* **17**, e1009761  
1512 (2021).
- 1513  
1514 66. Eser, T.M. *et al.* Nucleocapsid-specific T cell responses associate with control of SARS-CoV-  
1515 2 in the upper airways before seroconversion. *Nat Commun* **14**, 2952 (2023).
- 1516  
1517 67. Hoffmann, M. *et al.* Omicron subvariant BA.5 efficiently infects lung cells. *Nat Commun* **14**,  
1518 3500 (2023).
- 1519



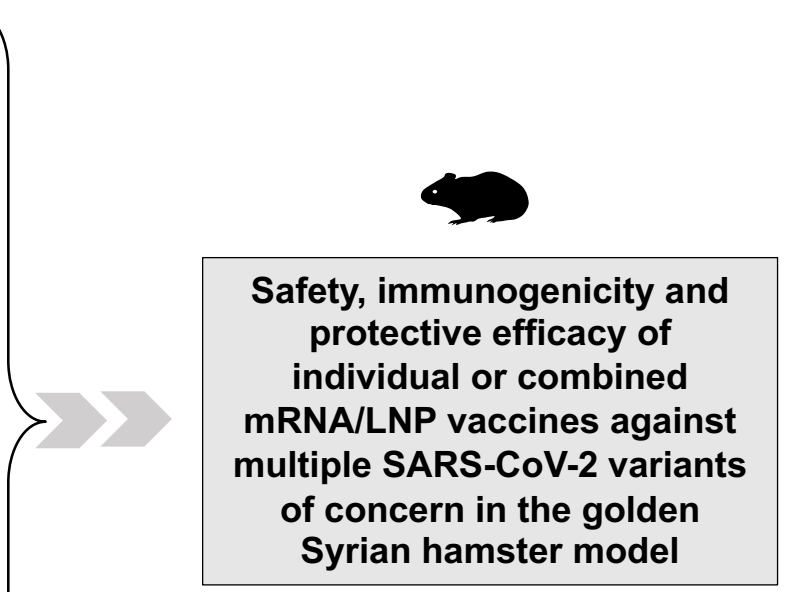
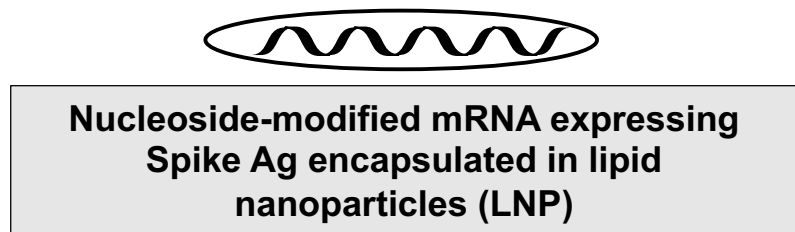
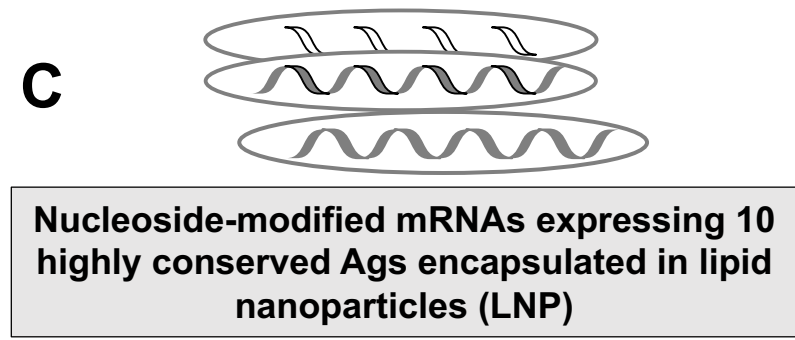
- 1520 68. Bouvet, M. *et al.* RNA 3'-end mismatch excision by the severe acute respiratory syndrome  
1521 coronavirus nonstructural protein nsp10/nsp14 exoribonuclease complex. *Proc Natl Acad Sci*  
1522 *U S A* **109**, 9372-9377 (2012).
- 1523  
1524 69. Hsu, J.C., Laurent-Rolle, M., Pawlak, J.B., Wilen, C.B. & Cresswell, P. Translational  
1525 shutdown and evasion of the innate immune response by SARS-CoV-2 NSP14 protein. *Proc*  
1526 *Natl Acad Sci U S A* **118** (2021).
- 1527  
1528 70. Ferron, F. *et al.* Structural and molecular basis of mismatch correction and ribavirin excision  
1529 from coronavirus RNA. *Proc Natl Acad Sci U S A* **115**, E162-E171 (2018).
- 1530  
1531 71. Le Bert, N. *et al.* Highly functional virus-specific cellular immune response in asymptomatic  
1532 SARS-CoV-2 infection. *J Exp Med* **218** (2021).
- 1533  
1534 72. Chen, Y. *et al.* Functional screen reveals SARS coronavirus nonstructural protein nsp14 as a  
1535 novel cap N7 methyltransferase. *Proc Natl Acad Sci U S A* **106**, 3484-3489 (2009).
- 1536  
1537 73. Zhao, Y. *et al.* Structural basis for replicase polyprotein cleavage and substrate specificity of  
1538 main protease from SARS-CoV-2. *Proc Natl Acad Sci U S A* **119**, e2117142119 (2022).
- 1539  
1540 74. van Hemert, M.J. *et al.* SARS-coronavirus replication/transcription complexes are  
1541 membrane-protected and need a host factor for activity in vitro. *PLoS Pathog* **4**, e1000054  
1542 (2008).
- 1543  
1544 75. Hagemeijer, M.C. & de Haan, C.A. Studying the dynamics of coronavirus replicative  
1545 structures. *Methods Mol Biol* **1282**, 261-269 (2015).
- 1546  
1547 76. Becerra-Artiles, A. *et al.* Immunopeptidome profiling of human coronavirus OC43-infected  
1548 cells identifies CD4 T-cell epitopes specific to seasonal coronaviruses or cross-reactive with  
1549 SARS-CoV-2. *PLoS Pathog* **19**, e1011032 (2023).
- 1550  
1551 77. Morita, R. *et al.* COVID-19 relapse associated with SARS-CoV-2 evasion from CD4(+) T-cell  
1552 recognition in an agammaglobulinemia patient. *iScience* **26**, 106685 (2023).
- 1553  
1554 78. Sabatino, J.J., Jr. *et al.* Multiple sclerosis therapies differentially affect SARS-CoV-2 vaccine-  
1555 induced antibody and T cell immunity and function. *JCI Insight* **7** (2022).
- 1556  
1557 79. Munoz-Fontela, C. *et al.* Animal models for COVID-19. *Nature* **586**, 509-515 (2020).
- 1558  
1559 80. Muruato, A.E. *et al.* A high-throughput neutralizing antibody assay for COVID-19 diagnosis  
1560 and vaccine evaluation. *Nat Commun* **11**, 4059 (2020).
- 1561  
1562 81. Pascolo, S. Nonreplicating synthetic mRNA vaccines: A journey through the European  
1563 (Journal of Immunology) history. *Eur J Immunol* **53**, e2249941 (2023).

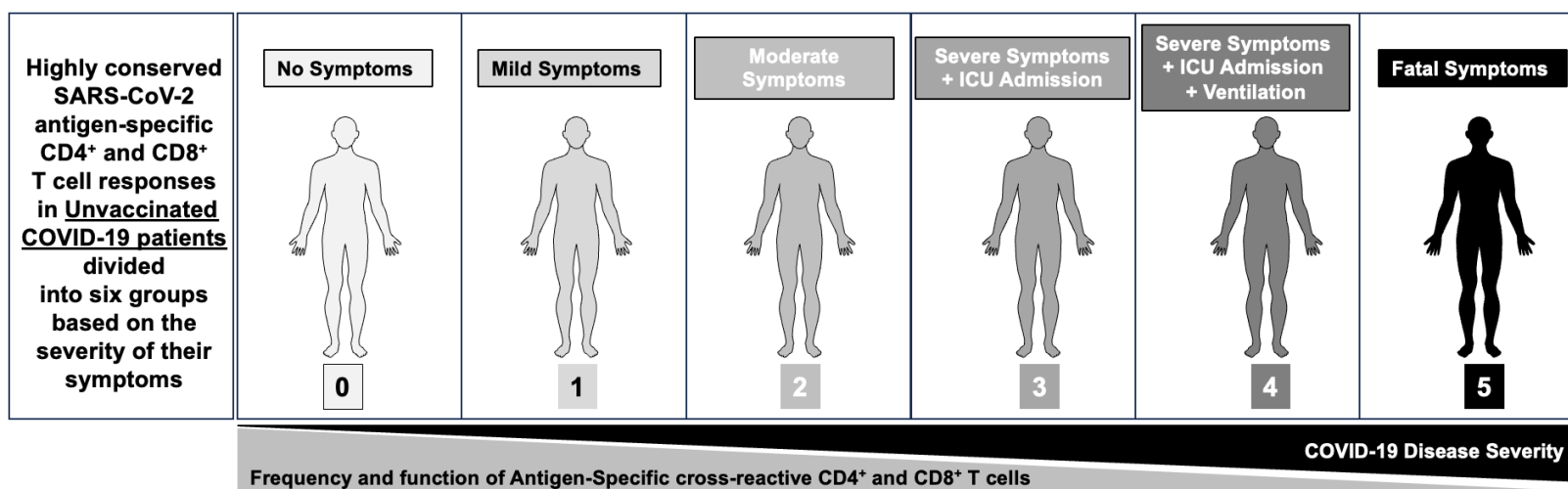
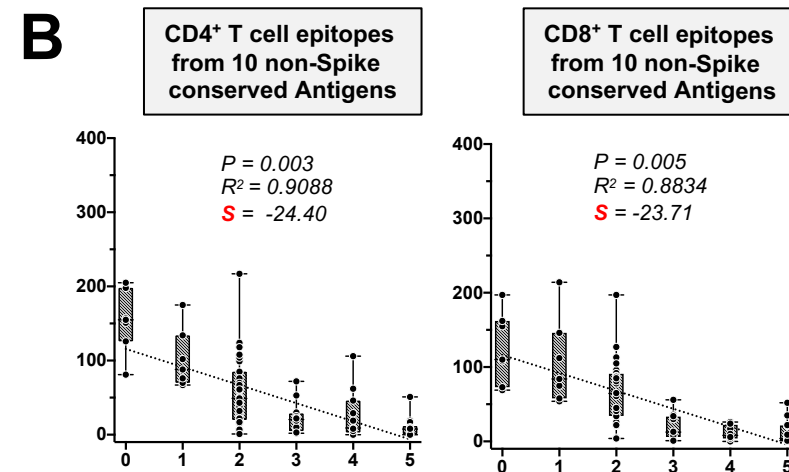
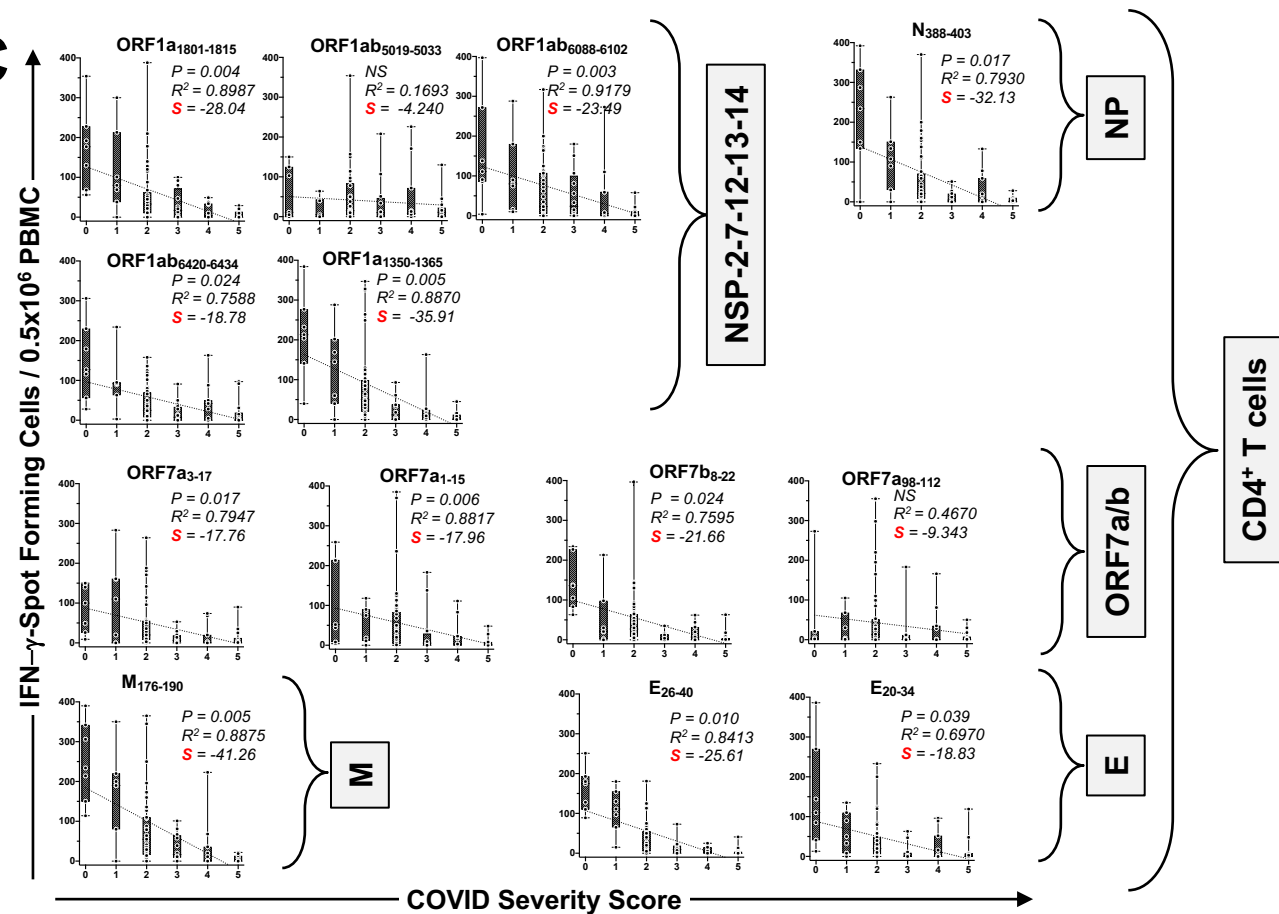
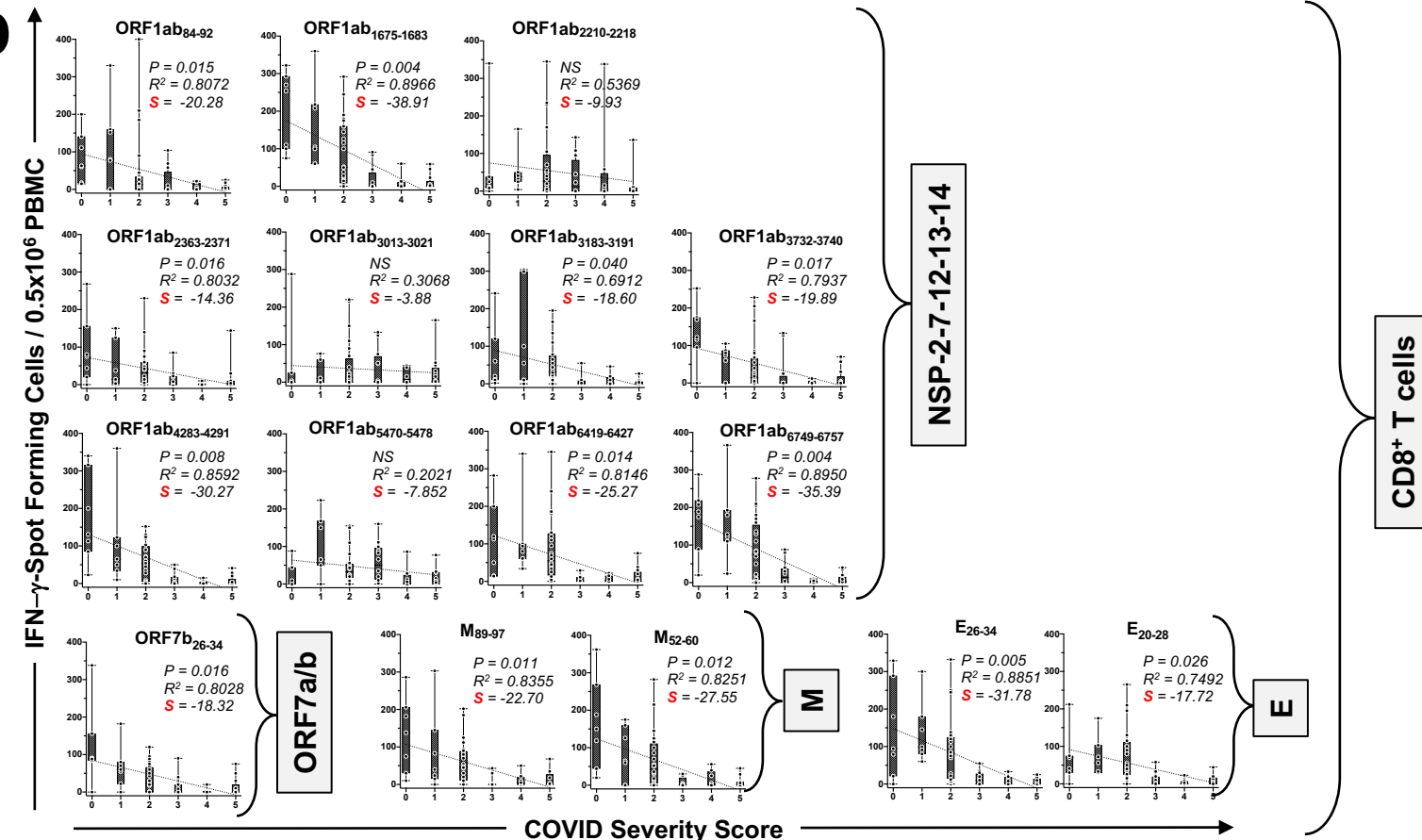
1564

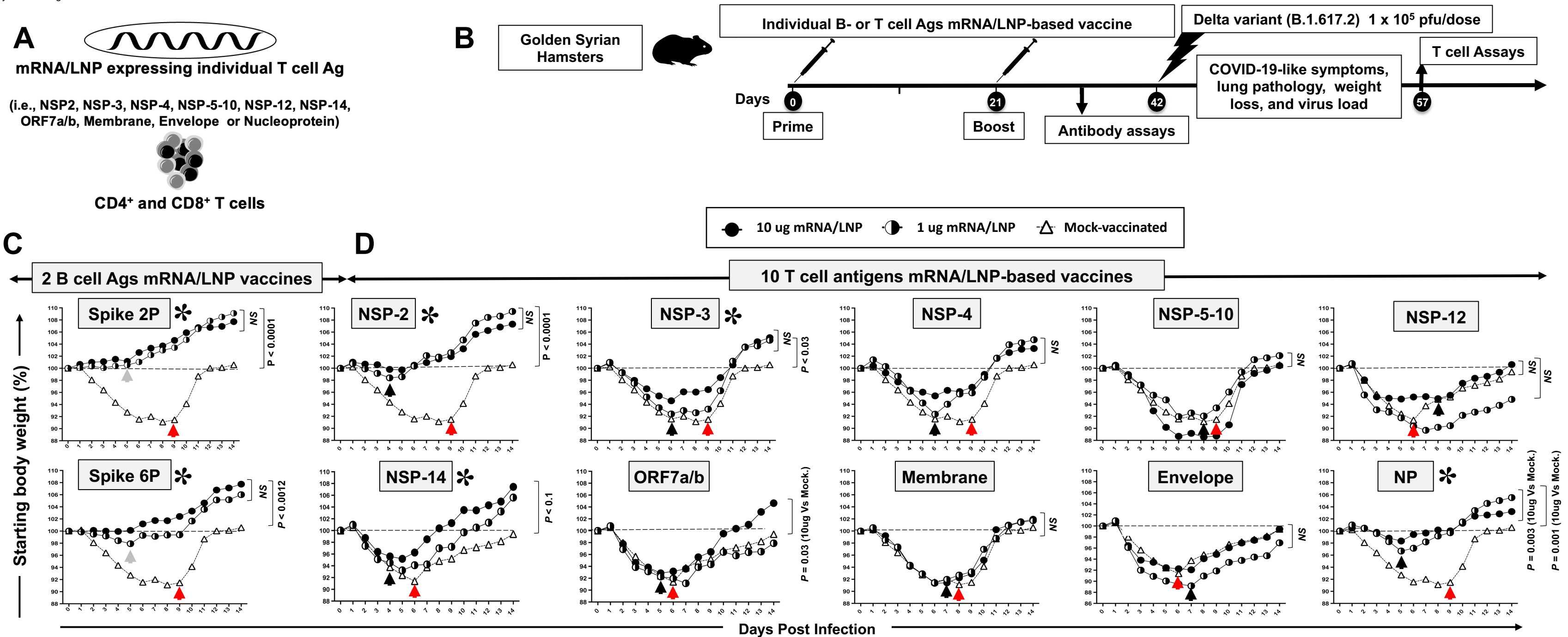
1565



NSP-2	1914 bp
NSP-3	4485 bp
NSP-4	1500 bp
NSP-5-10	3378 bp
NSP-12	2796 bp
NSP-14	1581 bp
ORF7a-7b	492 bp
Membrane	666 bp
Envelope	225 bp
Nucleoprotein	1248 bp
Spike	3804 bp



**A****B****C****D**

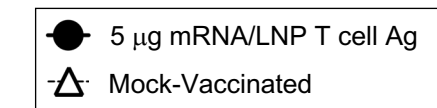


**A**

mRNA/LNP expressing 1 T cell Ag  
(i.e., NSP2, NSP-14 or Nucleoprotein)



CD4<sup>+</sup> and CD8<sup>+</sup> T cells

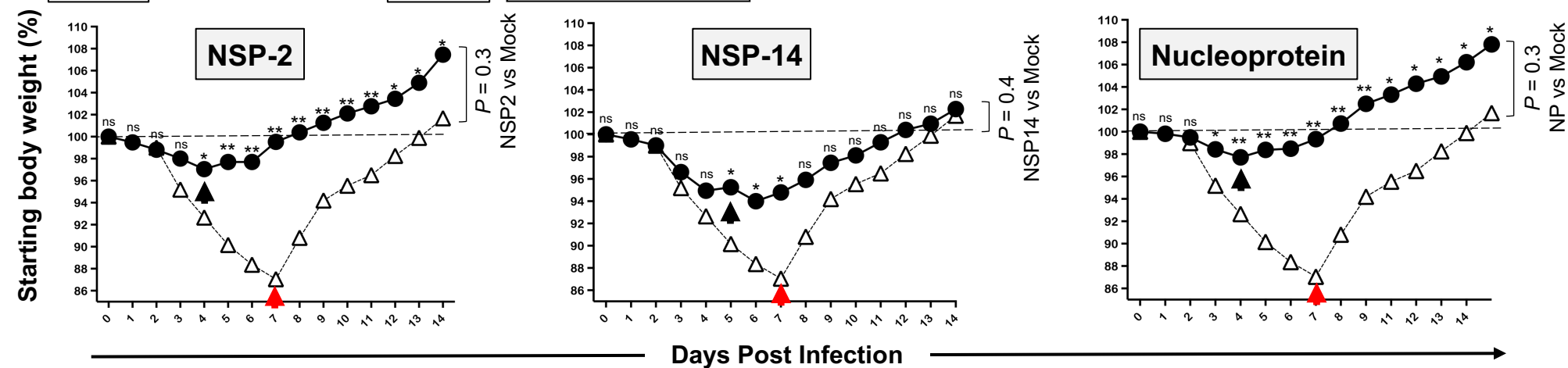
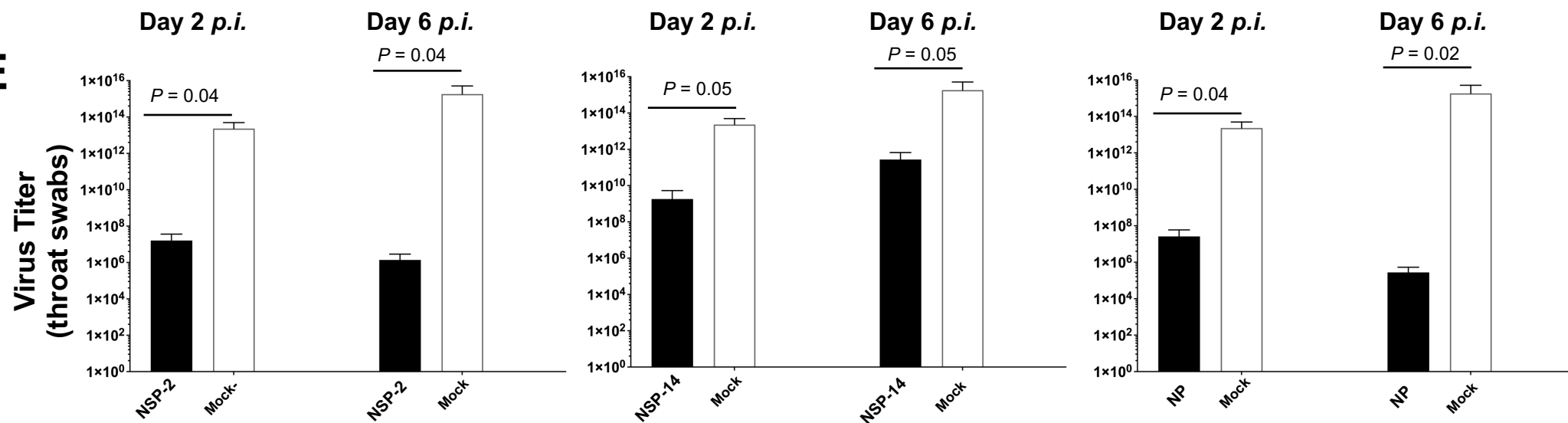
**B**

Golden Syrian Hamsters



Individual T cell Ags mRNA/LNP-based vaccine

Delta variant (B.1.617.2) 1 x 10<sup>5</sup> pfu/dose

**D****C****E**

**B**

Golden Syrian Hamsters



Combined NSP-2, NSP-14, and Nucleoprotein mRNA/LNP-based vaccine

SARS-CoV-2 Variants and Sub-Variants

T cell Assays

Days 0

Prime

21

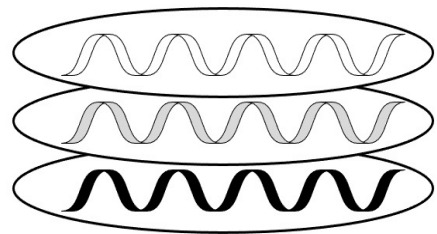
Boost

Antibody assays

42

COVID-19-like symptoms, lung pathology, weight loss, and virus load

57

**A**

Combination of mRNA/LNP expressing 3 T cell Ags (i.e., NSP2, NSP-14 and Nucleoprotein)

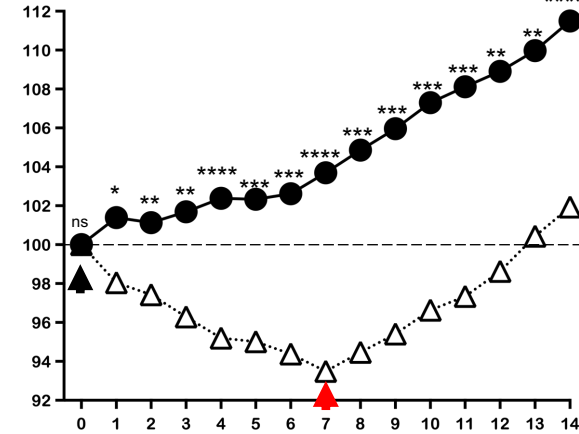
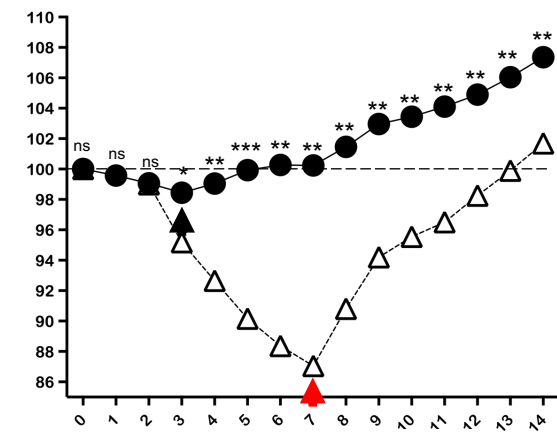
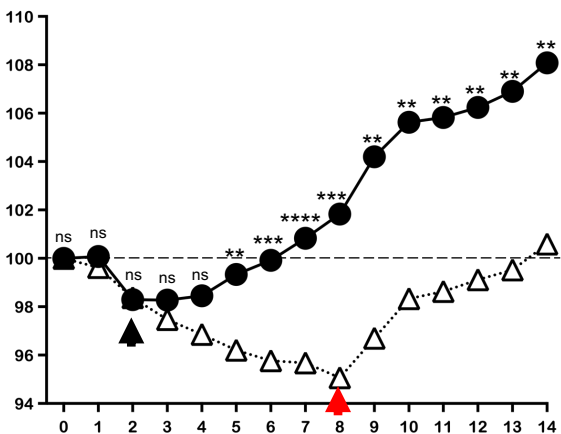
CD4<sup>+</sup> & CD8<sup>+</sup> T cells**C****D**

Wild-type Washington variant (WA1/2020)

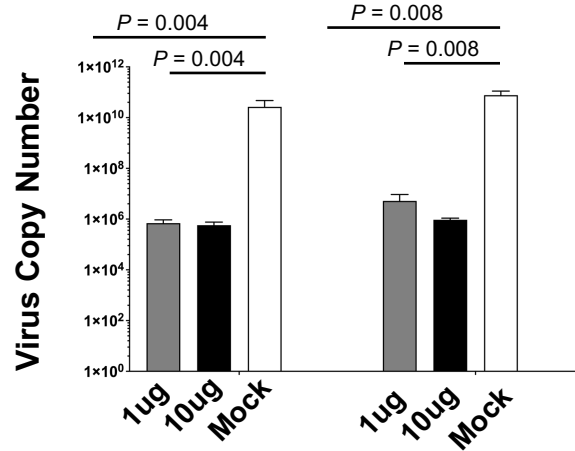
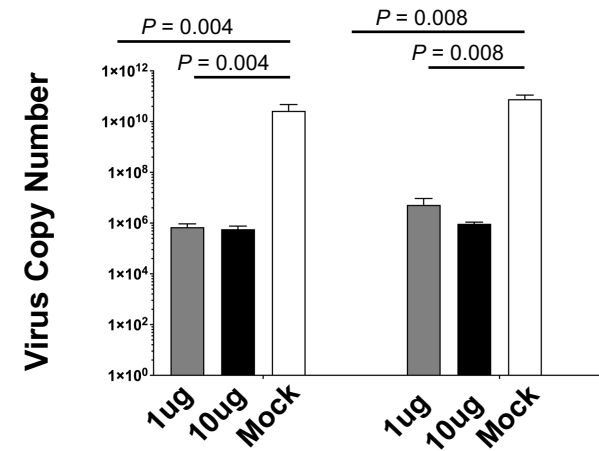
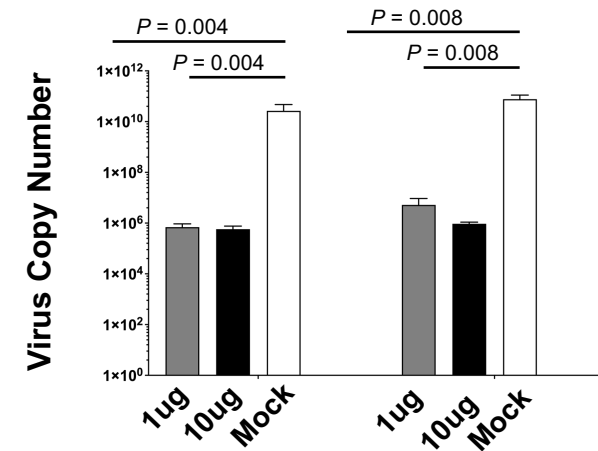
Delta variant (B.1.617.2)

Omicron sub-variant (XBB1.5)

Starting body weight (%)

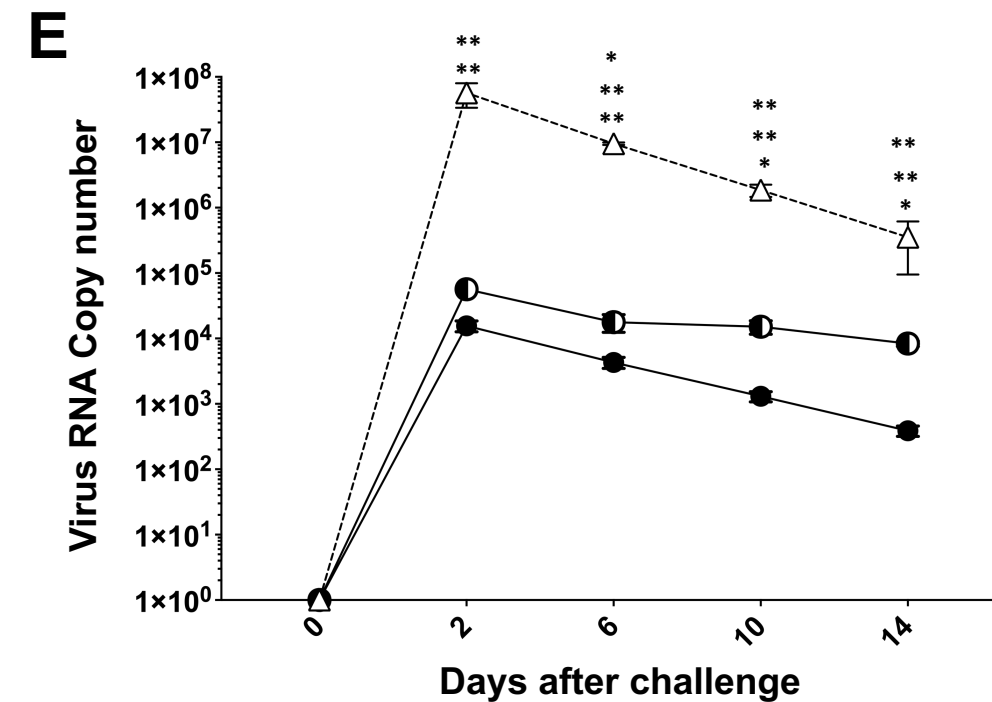
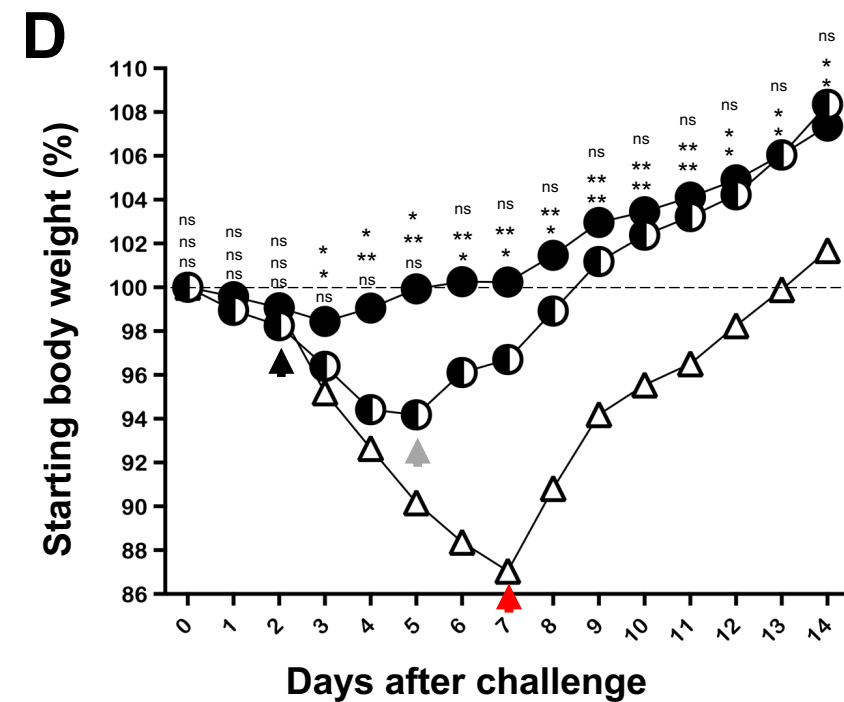
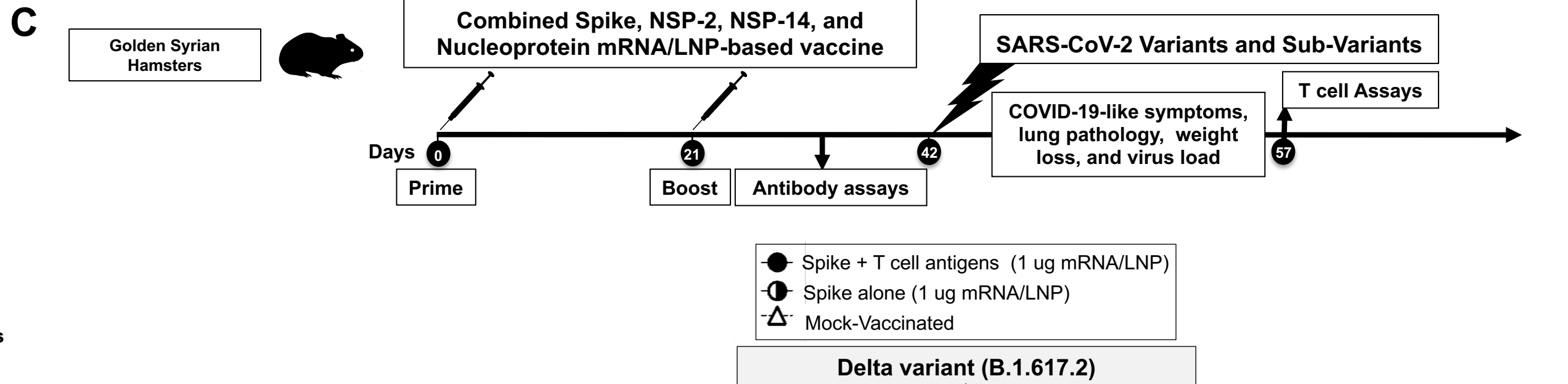
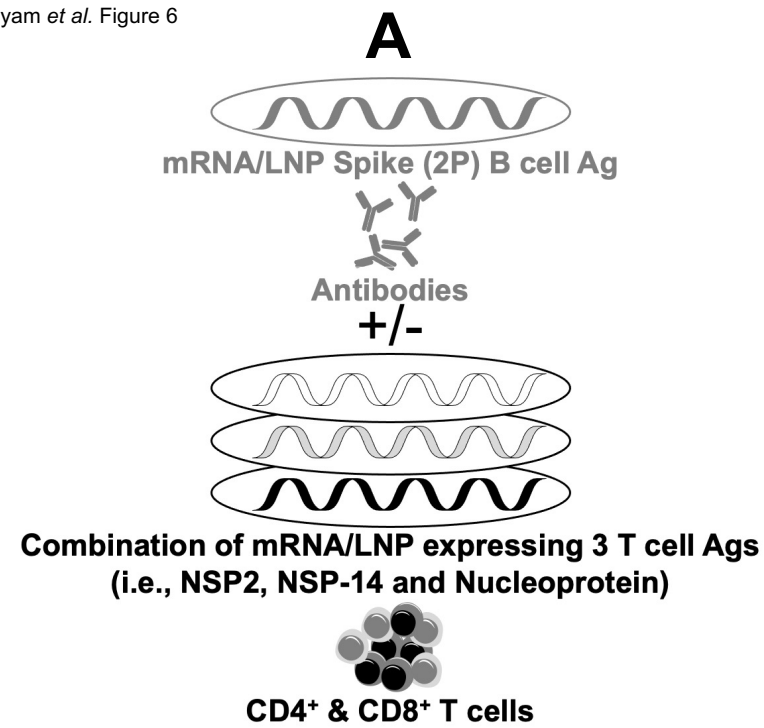


Days after challenge

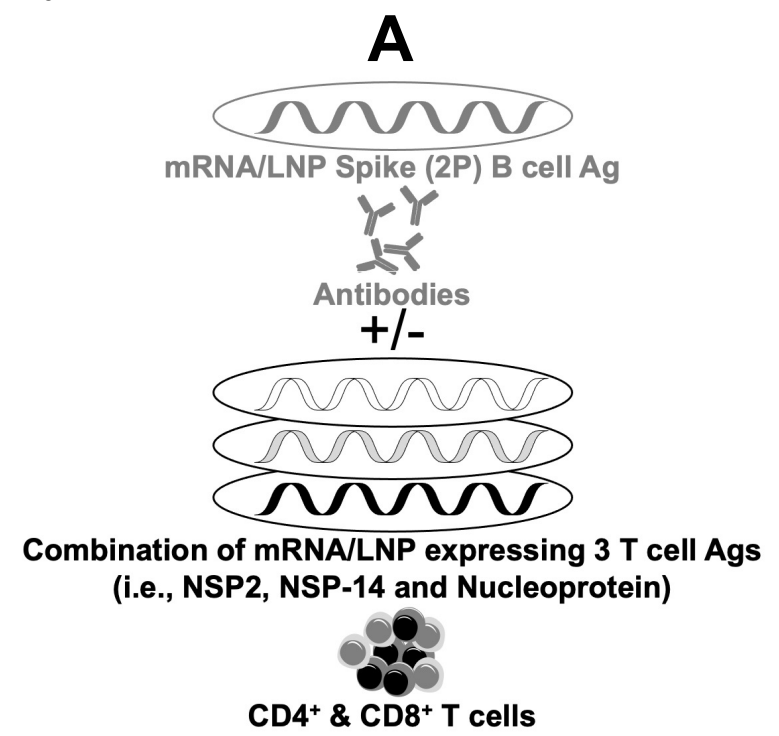
**E**Day 2 *p.i.*Day 6 *p.i.*Day 2 *p.i.*Day 6 *p.i.*Day 2 *p.i.*Day 6 *p.i.*

● 3 T cell Antigens Ag (10 μg)  
 △ Mock-Vaccinated (Mock)

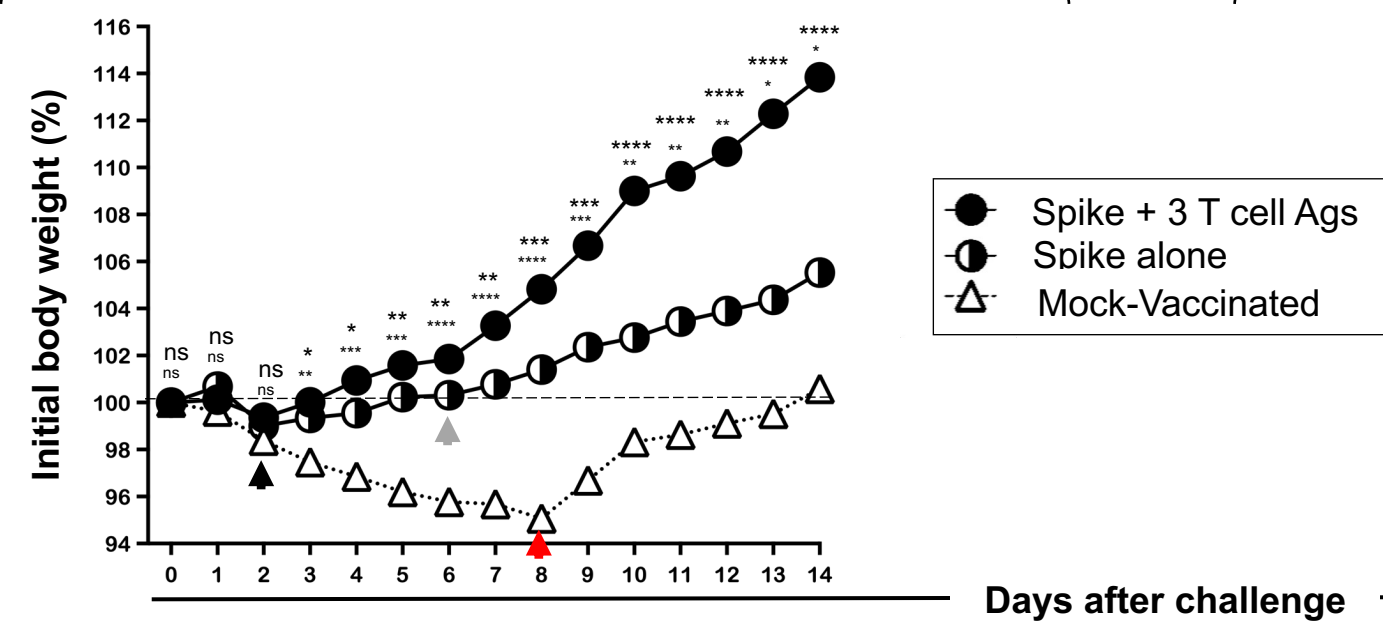
P < 0.0001  
3 T cell Ags vs Mock.P = 0.03  
3 T cell Ags vs Mock.P < 0.0001  
3 T cell Ags vs Mock.

**B**

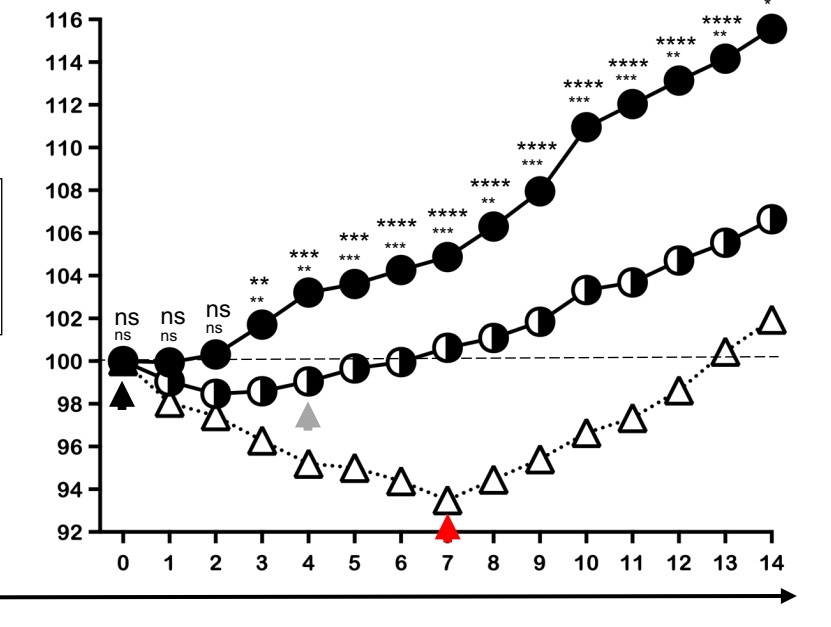




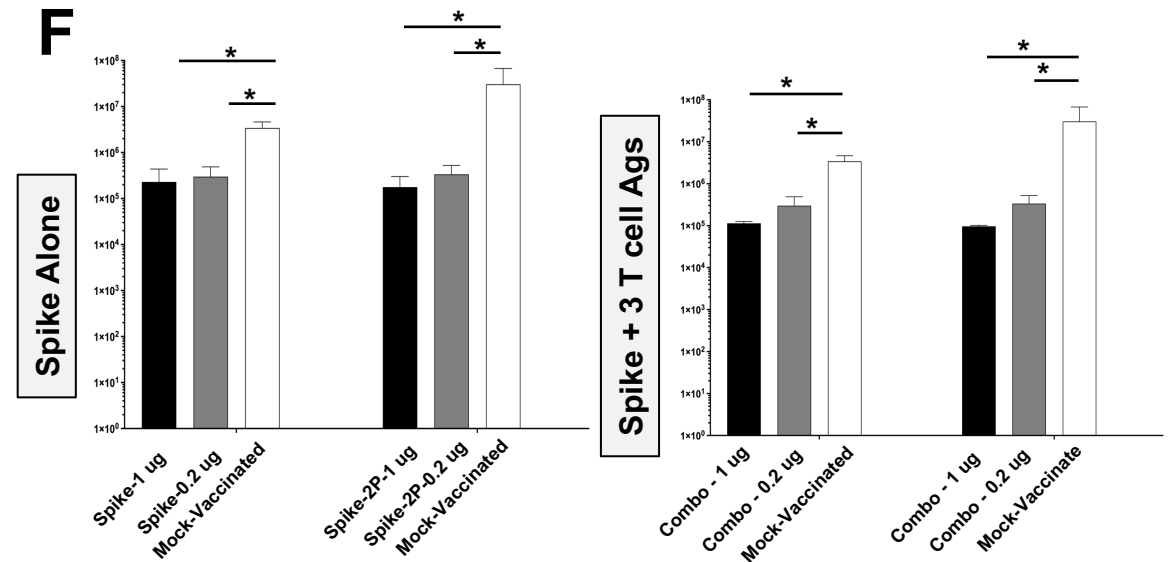
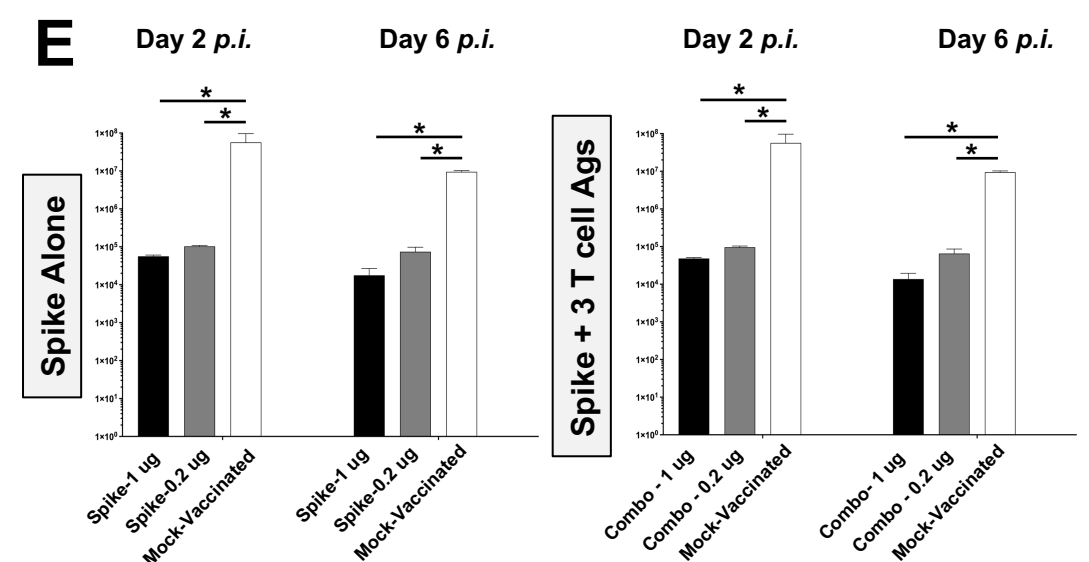
**B** Wild-type Washington variant (WA1/2020)



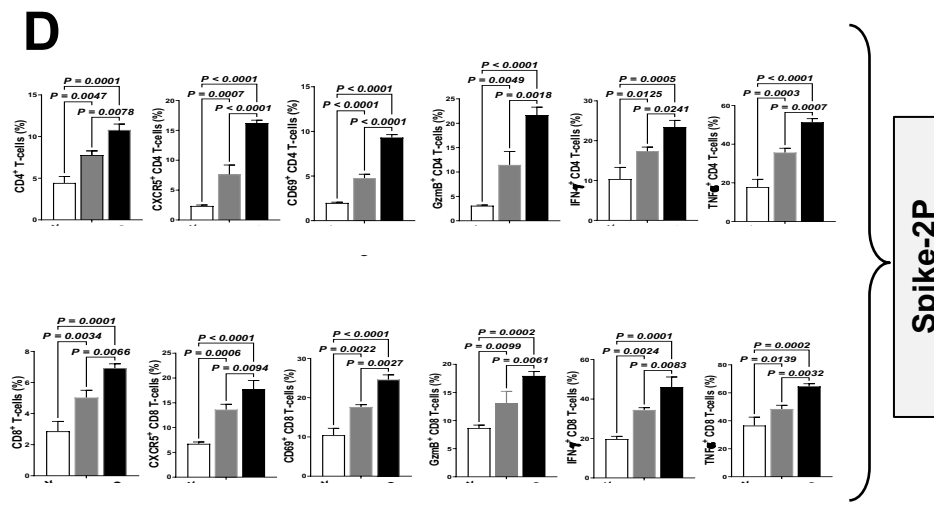
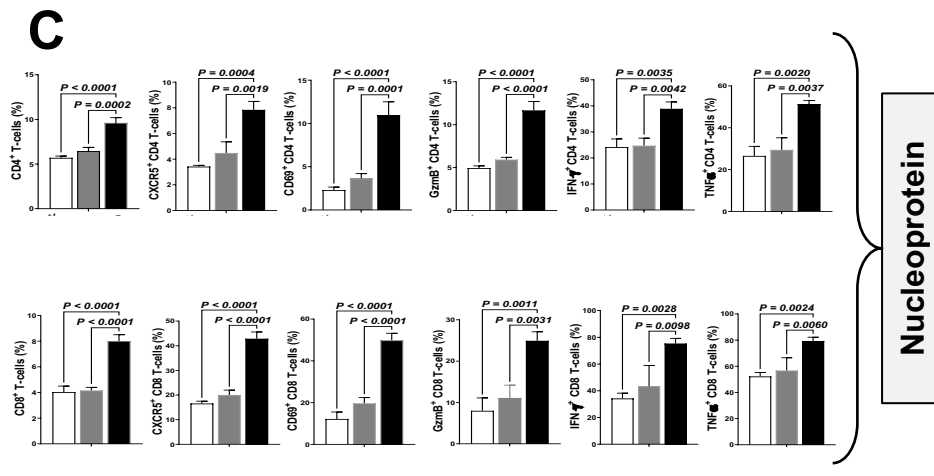
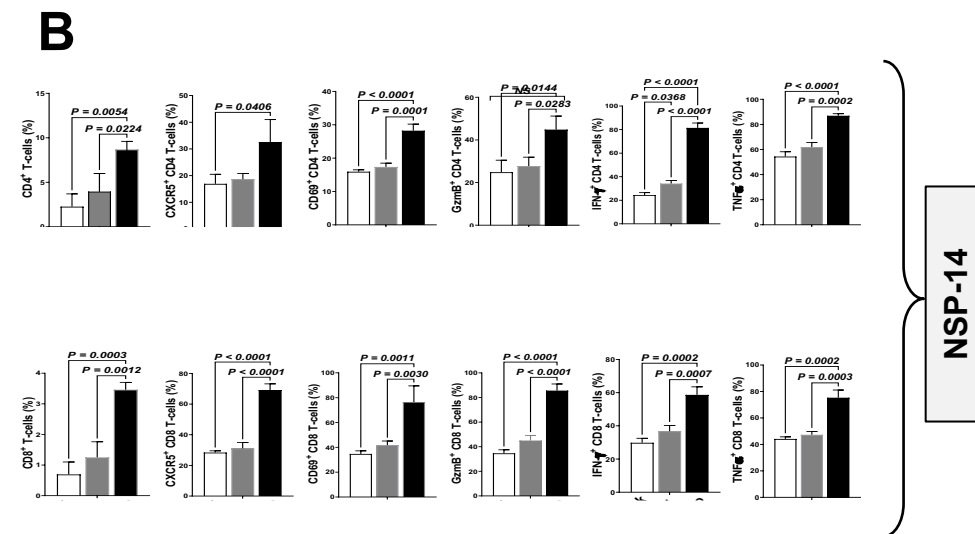
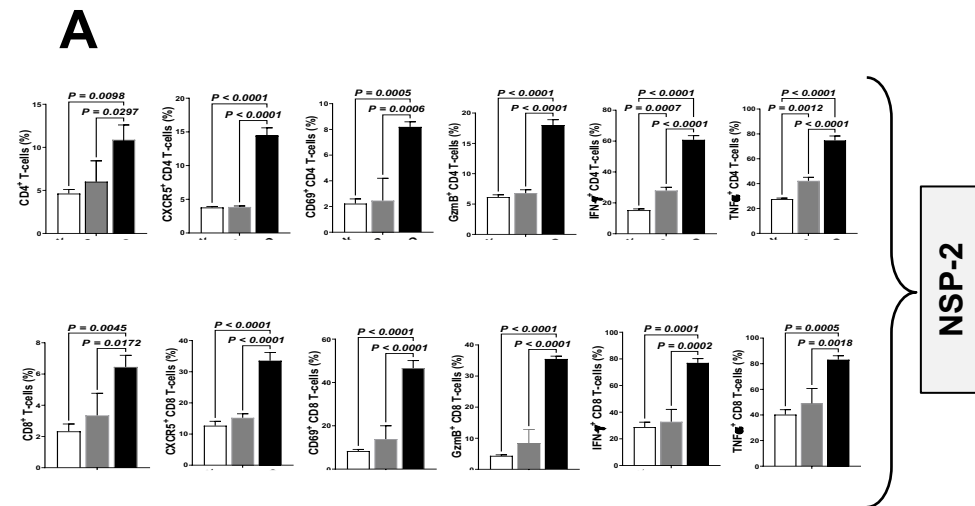
**C** Omicron sub-variant (XBB.1.5)



**D**

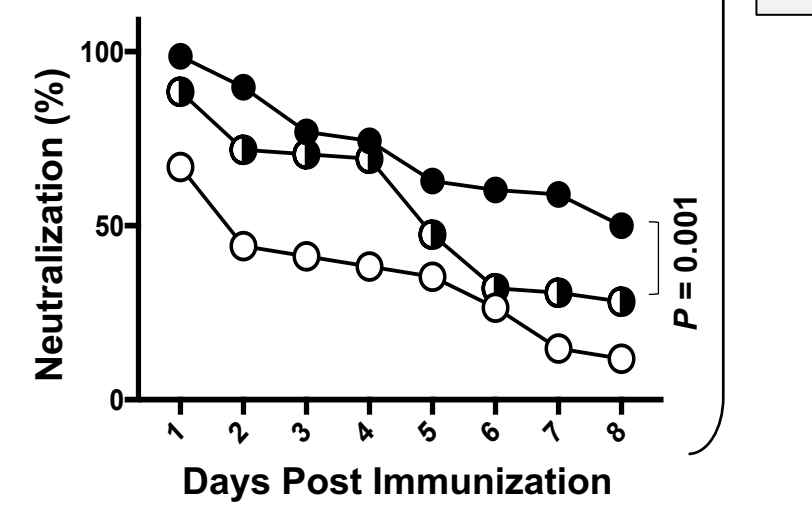
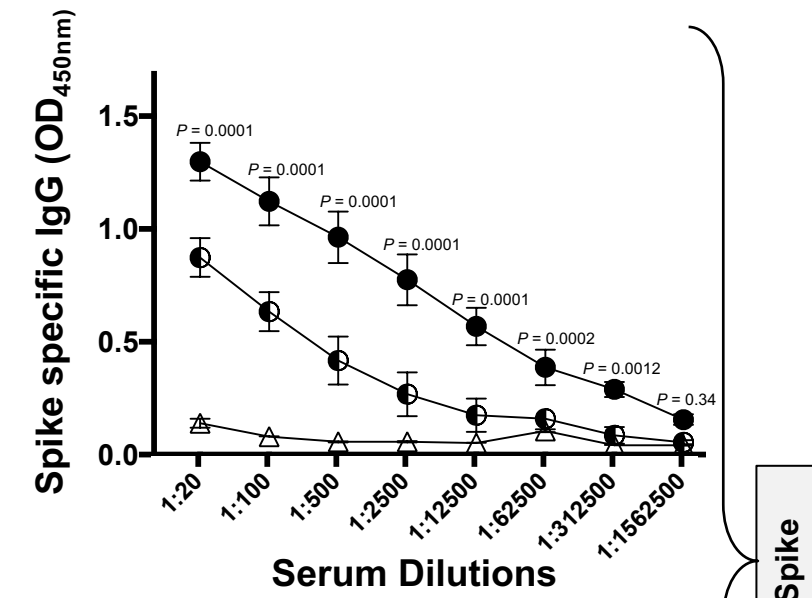


Spike + T cell antigens (1 ug mRNA/LNP)  
 Spike alone (1 ug mRNA/LNP)  
 Mock-Vaccinated



**E**

Spike + 3 T cell Ags  
 Spike alone  
 Mock-Vaccinated



SARS-CoV-2 Antigen	Heavily Spike-Mutated Omicron Sub-Variants												Total Mutations
	Wuhan	Alpha	Beta	Gamma	Delta	BA.2	BA.5	XBB.1.5	BA2.86	EG.5	HV.1	JN.1	
Spike	0	10	10	12	10	42	34	31	60	43	42	52	346
Membrane	0	0	0	0	1	2	3	2	5	2	2	5	22
Envelope	0	0	0	0	1	1	1	2	1	2	2	1	11
Nucleocapsid	0	4	1	3	3	7	7	7	9	7	4	5	57
NSP-2	0	1	2	1	2	1	1	2	2	3	3	3	21
NSP-3	0	3	1	3	1	5	5	5	8	10	8	9	58
NSP-4	0	0	0	0	0	3	0	3	4	5	5	3	18
NSP-5-10	0	3	4	3	0	4	4	4	6	6	3	4	41
NSP-12	0	0	0	0	0	0	0	0	0	0	0	0	0
NSP-14	0	0	0	0	0	0	0	0	0	0	0	0	0
ORF7a/b	0	0	0	0	2	0	0	0	0	1	0	0	3

**Table 1:** Comparison of cumulative mutation frequencies between Spike B cell antigen and 10 conserved non-Spike T cell antigens among 12 SARS-CoV-2 variants and sub-variants of concern, including the recent highly mutated COVID variants ‘Pirola’ BA.2.86 and JN.1 that may cause more severe disease.

Patients' characteristics classified by Severity of COVID-19 (n=147)		Severity 5 (SYMP) (Patients died) (n = 26)	Severity 4 (SYMP) (ICU + vent.) (n = 15)	Severity 3 (SYMP) (ICU) (n = 21)	Severity 2 (SYMP) (Inpatients, Reg. Adm.) (n = 64)	Severity 1 (SYMP) (ED) (n = 12)	Severity 0 (ASYMP) (n = 9)
<b>Demographic features</b>	Age median	65 (39-90)	52 (33-85)	53 (26-86)	57 (23-85)	51 (27-91)	27 (19-51)
	Gender (Male/Female)	19/7 (73%/27%)	9/6 (60%/40%)	13/8 (62%/38%)	37/27 (58%/42%)	5/7 (42%/58%)	5/4 (56%/44%)
	Race (% White/non-White)	6/20 (23%/77%)	8/7 (53%/47%)	13/8 (62%/38%)	25/39 (39%/61%)	7/5 (58%/42%)	2/7 (29%/71%)
<b>Class I &amp; II HLA status</b>	HLA-A*0201 <sup>+</sup>	13 (50%)	8 (53%)	12 (57%)	24 (38%)	7 (58%)	7 (78%)
	HLA-DRB1*01:01 <sup>+</sup>	14 (54%)	11 (73%)	12 (57%)	41 (64%)	7 (58%)	7 (78%)
<b>Clinical parameters</b>	<i>(4.8 days average for all 147 patients)</i>						
	Days between onset of symptoms and blood draw (mean)	5.9	5.7	4.6	4.5	4.1	-
	Fever (>38°C)	21 (81%)	11 (73%)	10 (48%)	30 (47%)	4 (33%)	0 (0%)
	Cough	23 (88%)	13 (87%)	16 (76%)	22 (34%)	4 (33%)	0 (0%)
	Shortness of Breath/Dyspnea	28 (100%)	15 (100%)	6 (29%)	11 (17%)	1 (8%)	0 (0%)
	Fatigue/Myalgia	9 (35%)	5 (33%)	6 (29%)	3 (5%)	3 (25%)	0 (0%)
	Headache	5 (19%)	1 (%)	4 (19%)	12 (19%)	4 (33%)	0 (0%)
	Nausea	3 (12%)	3 (20%)	3 (14%)	3 (5%)	0 (0%)	0 (0%)
	Diarrhea	7 (27%)	2 (13%)	2 (10%)	8 (13%)	0 (0%)	0 (0%)
	Anosmia/Ageusia	6 (23%)	4 (27%)	6 (29%)	17 (27%)	1 (8%)	0 (0%)
	Sore Throat	4 (15%)	1 (7%)	1 (5%)	3 (5%)	1 (8%)	0 (0%)
	ICU Admission	26 (100%)	15 (100%)	21 (100%)	0 (0%)	0 (0%)	0 (0%)
	Ventilator Support	26 (100%)	15 (100%)	0 (0%)	0 (0%)	0 (0%)	0 (0%)
	White Blood Cells – (count: 10 <sup>3</sup> cells /μL of blood) (average)	14.3	10.8	10.1	8.4	6.2	8.0
	Lymphocytes – (10 <sup>3</sup> cells /μL of blood and %) (average)	0.7 (6%)	0.9 (10%)	1.0 (13%)	1.4 (16%)	1.6 (27%)	2.4 (29.3%)
<b>Comorbidities</b>	Average number of all comorbidities	3.5	2.9	2.8	1.9	1.6	0.7
	Diabetes	14 (54%)	9 (60%)	13 (62%)	29 (45%)	4 (33%)	0 (0%)
	Hypertension (HTN)	16 (62%)	6 (40%)	9 (43%)	18 (28%)	4 (33%)	1 (11%)
	Cardiovascular disease (CVD)	17 (65%)	6 (40%)	6 (29%)	13 (20%)	3 (25%)	0 (0%)
	Coronary Artery disease (CAD)	12 (46%)	5 (33%)	7 (33%)	12 (19%)	2 (17%)	0 (0%)
	Kidney diseases (CKD/ESRD)	7 (27%)	4 (27%)	6 (29%)	7 (11%)	1 (8%)	0 (0%)
	Asthma/COPD	9 (35%)	1 (7%)	3 (14%)	12 (19%)	0 (0%)	1 (11%)
	Obesity	12 (46%)	12 (80%)	7 (33%)	29 (45%)	4 (33%)	4 (44%)
	Cancer	4(15%)	0(0%)	2(10%)	6(9%)	1(8%)	0 (0%)

